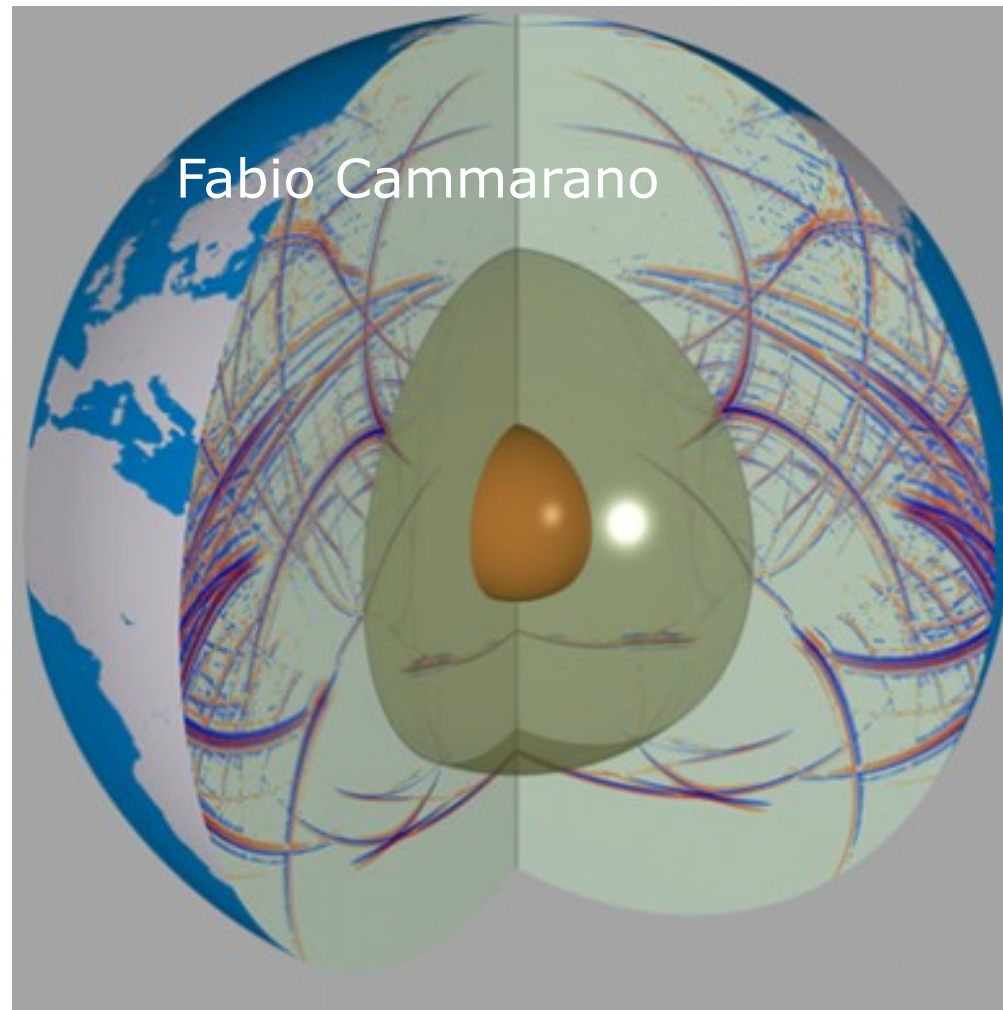


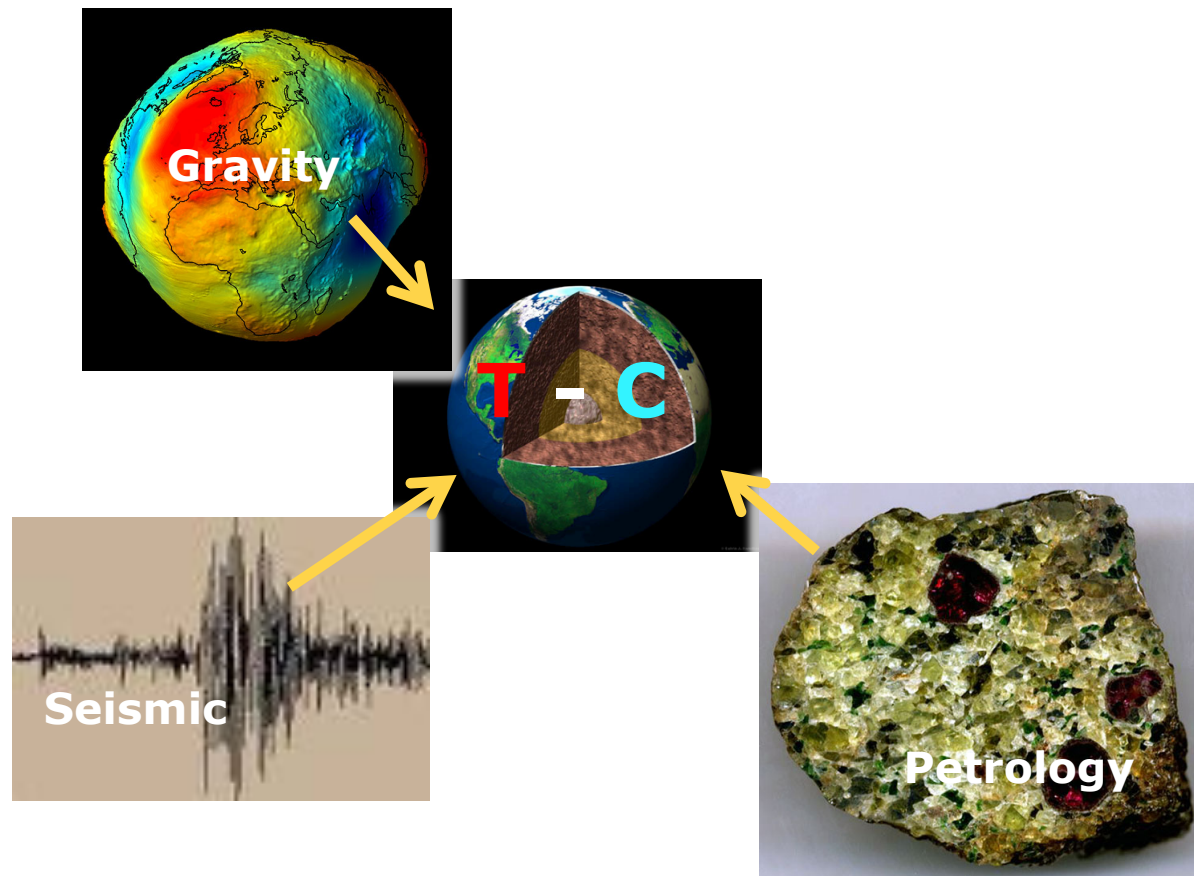
Basics of Seismology and Earth Structure



Fabio Cammarano

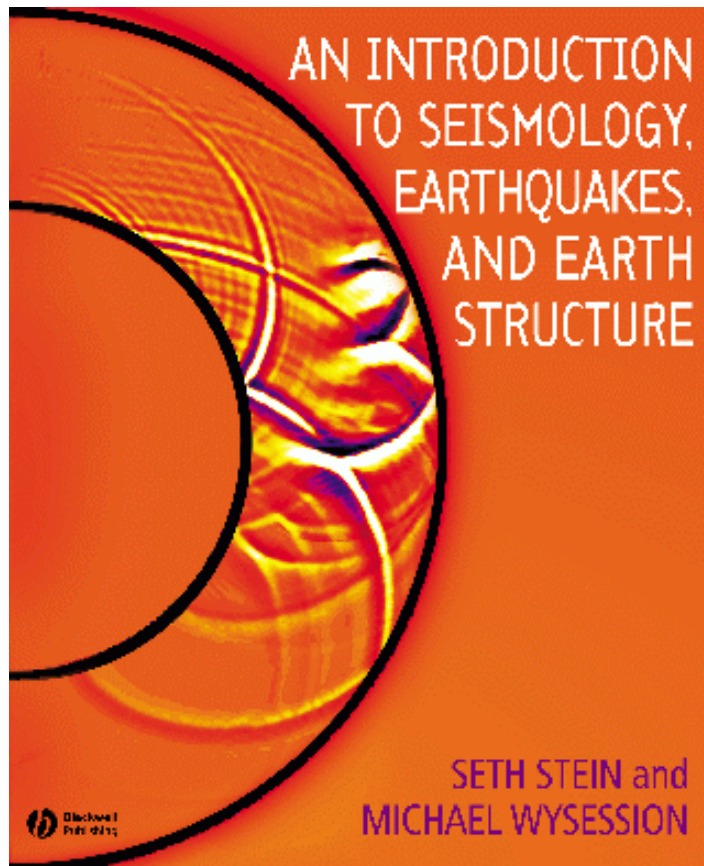
mail: fabio.cammarano@uniroma3.it

<http://jupiter.ethz.ch/~fabioca/research.html>



Online materials and books

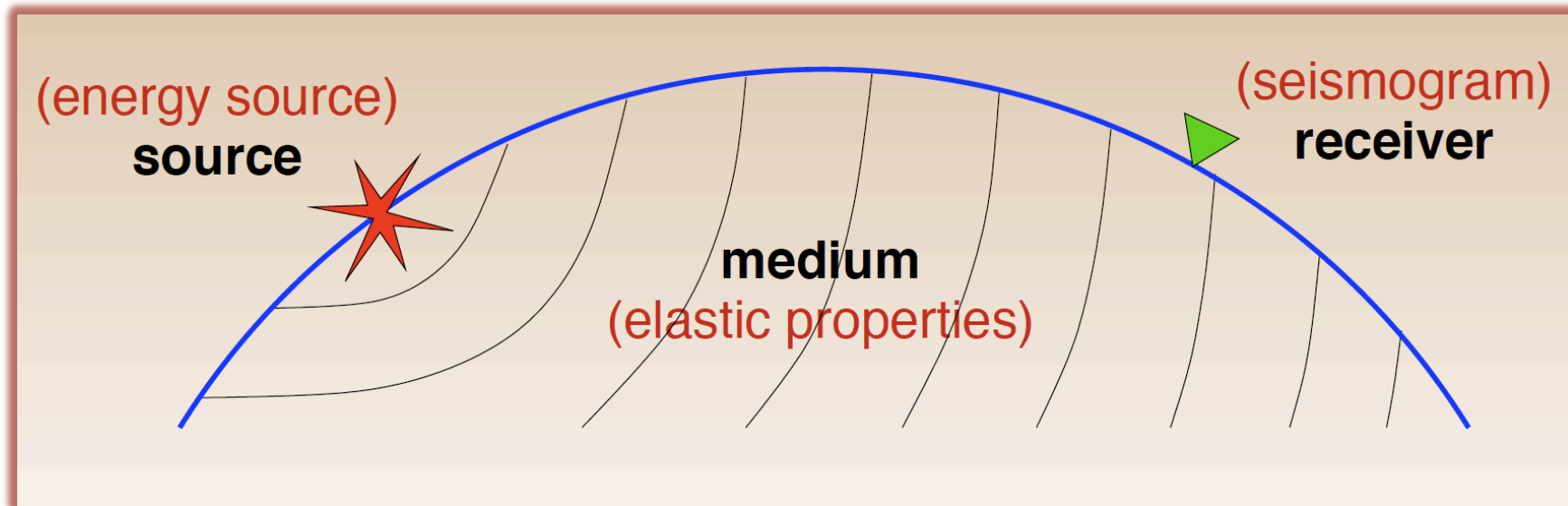
Stein, S. and M. Wyssession, Introduction to Seismology, Earthquakes, and Earth Structure, Blackwell Publishing, 2003.



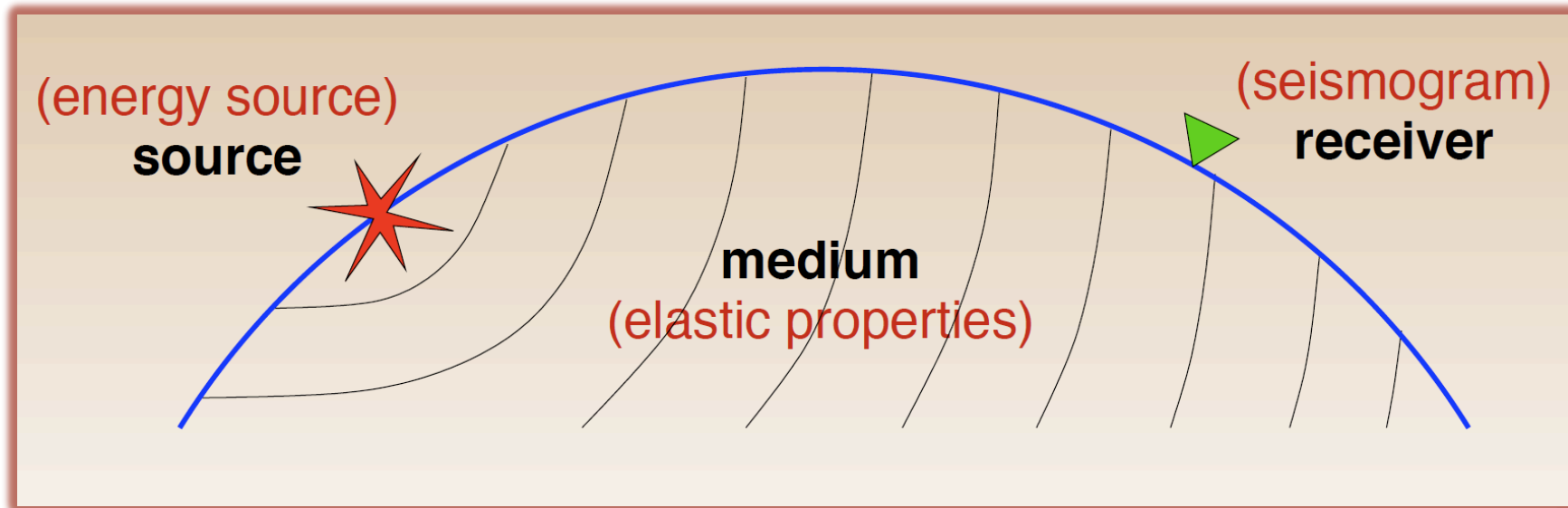
- IRIS: Incorporated Research Institutions for Seismology
<https://www.iris.edu/hq/>
- CIDER: Cooperative Institute for Dynamic Earth Research
http://www.deep-earth.org/wiki_cider/Seismology
- INGV: Istituto Nazionale di Geofisica e Vulcanologia
<http://www.ingv.it/it/>

What seismology is?

- ✧ Seismology is the study of elastic waves in the earth.
- ✧ Seismic wave **theory**, **observations** and **interpretation** are the key components of modern seismology.
- ✧ Seismology is motivated by our ability to record ground motion caused by the passage of seismic waves.



✧ Seismograms depend on the source and on elastic properties of the medium → seismology is useful to know more about **Earthquakes** and **Earth's interior structure**



- ✧ **Earthquake seismology** : is all about the source
 - ➔ location, mechanism, intensity.
 - ✓ Understanding how stresses accumulate and are released in the crust
 - ✓ Mitigate seismic hazard
 - ✓ Measuring plate-tectonics processes
 - ✓ Monitor nuclear explosions
 - ✓ Even global warming => glacial Earthquakes
-

- ✧ **Seismic structure**: is all about the medium
 - ✓ Seismic structure (from global to local scale) ➔ seismic tomography
 - ✓ Physical properties (elasticity depends on physical parameters as temperature and composition)

(**controlled source seismology** is used, mostly, for local studies ➔ location of economic resources like hydrocarbon, mineral deposits)

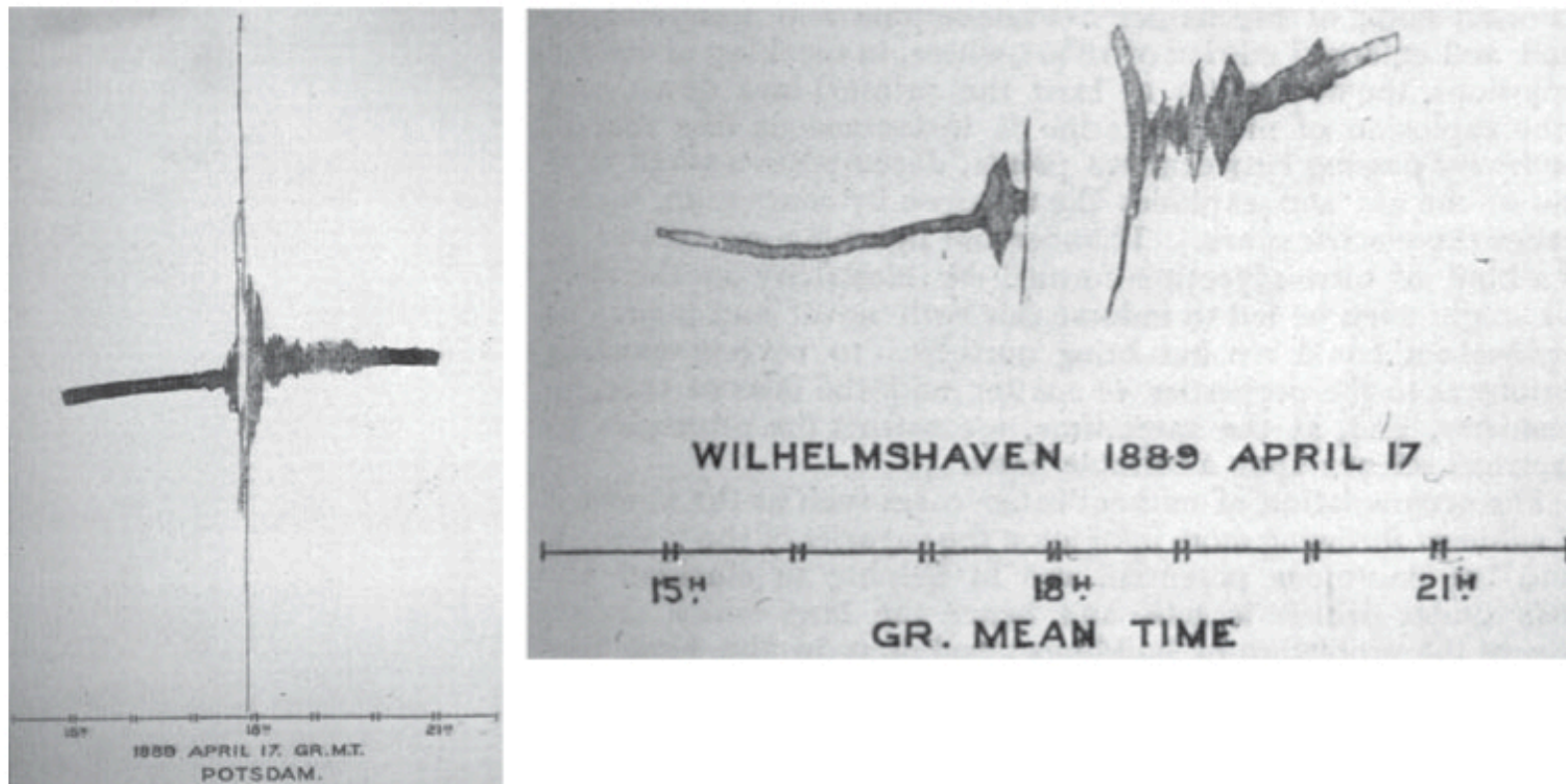


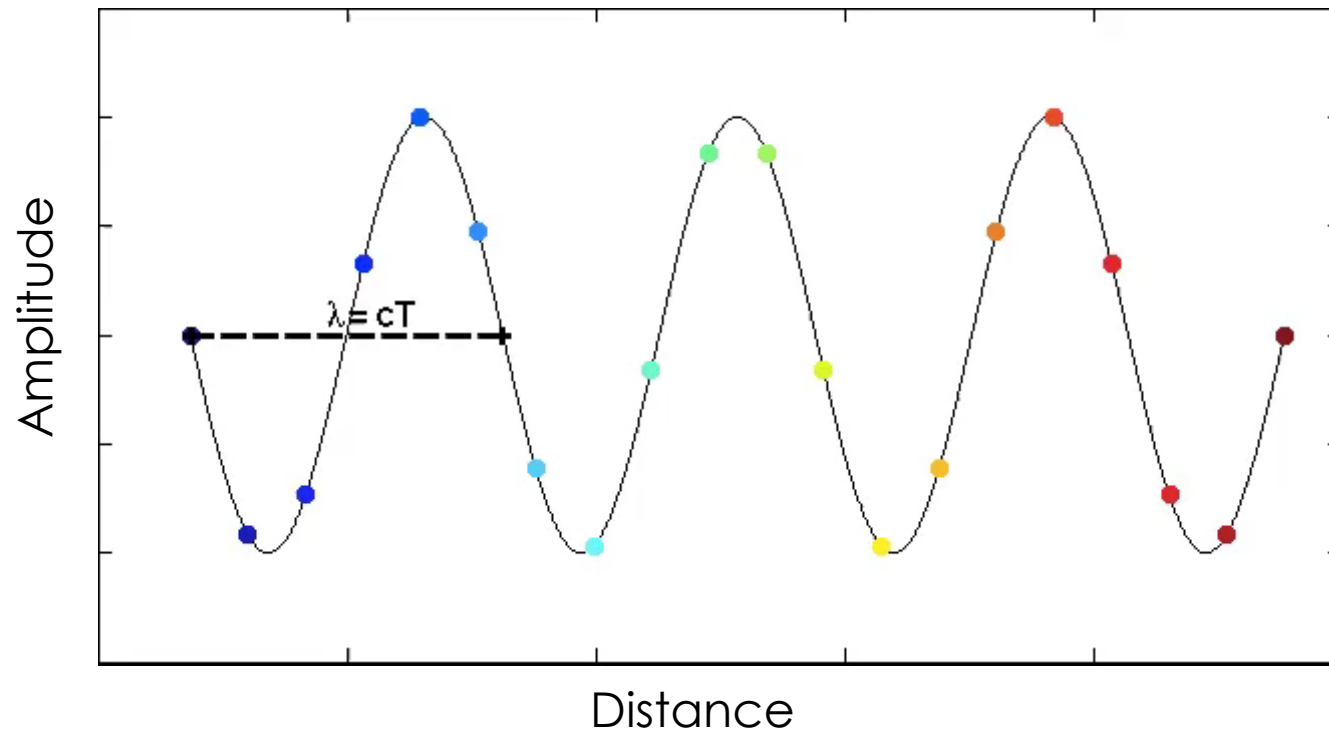
Figure 6. The two records of an earthquake in Japan made on 17 April 1889 by Rebeur-Paschwitz in parallel in Potsdam and in Wilhelmshaven, Germany. These two records are the oldest known observations of an earthquake at teleseismic distance (Rebeur-Paschwitz 1889).

First teleseismic (i.e. far distance) record of an Earthquake

Theory – Basics

(slides from Ved Lekic)

- Elasticity – stress-strain
- Eq. of motion => seismic wave equation => P, S waves
- Ray parameter, Travel times
- Earth structure first constraints => shadow zones, triplications and mantle discontinuities
- Surface waves, dispersion, surface-waves studies
- Wave Amplitudes and their use



Period =
Frequency⁻¹
 $T = 1/f$

Wavelength =
Wavenumber⁻¹
 $\lambda = 1/k$

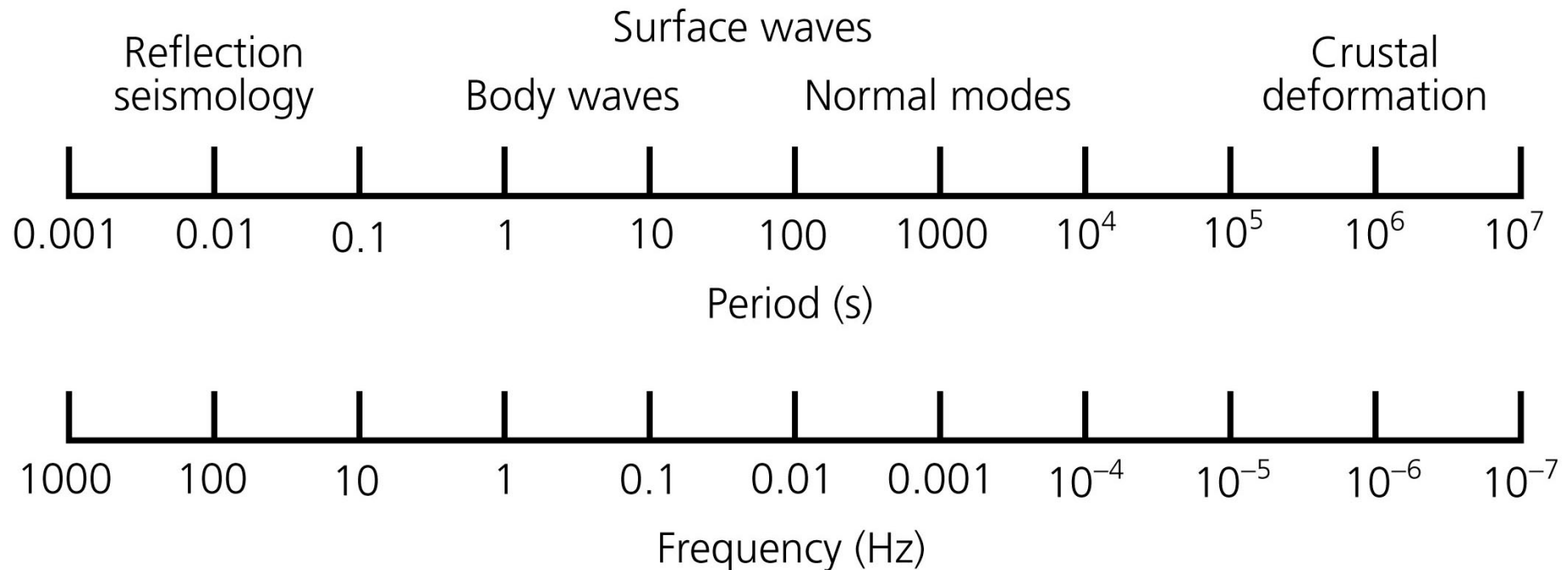
Speed (c):
 $c = \lambda f = f/k$

What are **elastic** waves?

In an elastic continuum, perturbing the position of one particle will result in a restoring force that will accelerate that particle back and past the equilibrium position

Perturbation in position of one particle will accelerate its neighbors

Figure 2.4-7: Seismic spectrum for various studies.



From Stein and Wyssession, 2003

Frequencies / Periods of motion

Seismology spans ~6 orders of magnitude in frequency, from waves that oscillate >1000 times in a second, to those that take >1000 seconds to oscillate once

Tractions and the stress tensor



Pressure:
direction
depends
on surface

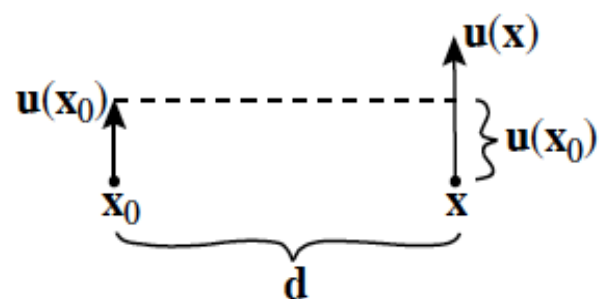
Gravity:
direction
always down

- The stress tensor describes forces acting across infinitesimal planes within a continuum (i.e. tractions)
- Its units are: N/m^2 a.k.a. Pa
- Can vary with position, describes both compression / extension and shearing
- Stress tensor is symmetric, in 3D has 6 independent components

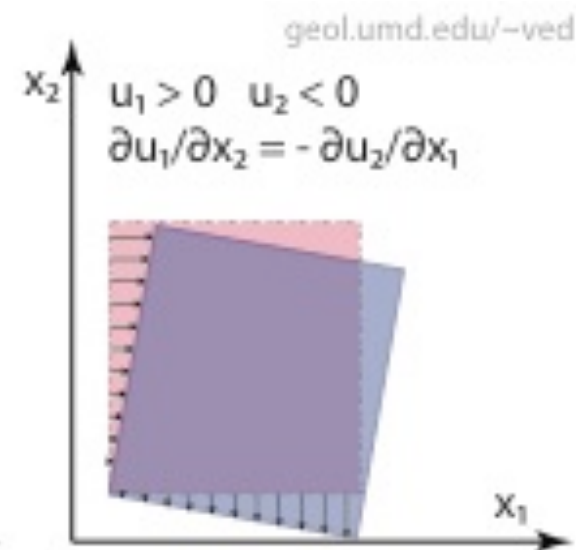
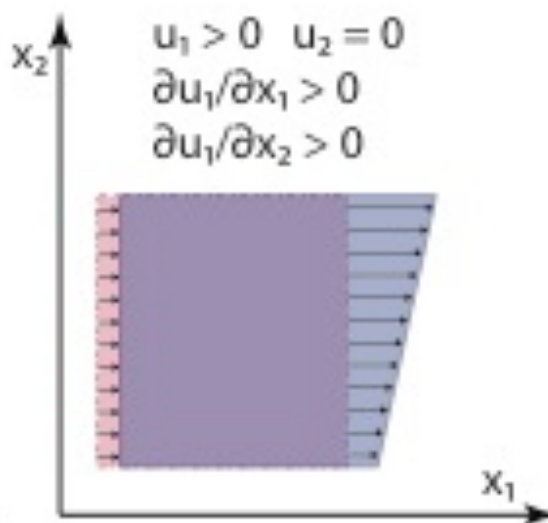
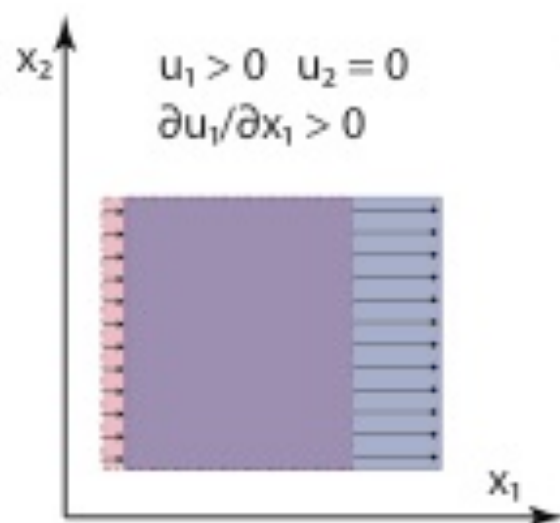
$$\mathbf{t}(\hat{\mathbf{n}}) = \boldsymbol{\tau} \hat{\mathbf{n}} = \begin{bmatrix} t_x(\hat{\mathbf{n}}) \\ t_y(\hat{\mathbf{n}}) \\ t_z(\hat{\mathbf{n}}) \end{bmatrix} = \begin{bmatrix} \tau_{xx} & \tau_{xy} & \tau_{xz} \\ \tau_{xy} & \tau_{yy} & \tau_{yz} \\ \tau_{xz} & \tau_{yz} & \tau_{zz} \end{bmatrix} \begin{bmatrix} \hat{n}_x \\ \hat{n}_y \\ \hat{n}_z \end{bmatrix}$$

Internal deformation

■ How do we describe (small) internal deformations?



$$\mathbf{u}(\mathbf{x}) = \begin{bmatrix} u_x \\ u_y \\ u_z \end{bmatrix} = \mathbf{u}(\mathbf{x}_0) + \begin{bmatrix} \frac{\partial u_x}{\partial x} & \frac{\partial u_x}{\partial y} & \frac{\partial u_x}{\partial z} \\ \frac{\partial u_y}{\partial x} & \frac{\partial u_y}{\partial y} & \frac{\partial u_y}{\partial z} \\ \frac{\partial u_z}{\partial x} & \frac{\partial u_z}{\partial y} & \frac{\partial u_z}{\partial z} \end{bmatrix} \begin{bmatrix} d_x \\ d_y \\ d_z \end{bmatrix}$$



Strain and Rotation tensors

- No net rotation only if $\partial u_i / \partial x_j - \partial u_j / \partial x_i = 0$
- Decompose deformation into **Strain** and **Rotation** matrices:

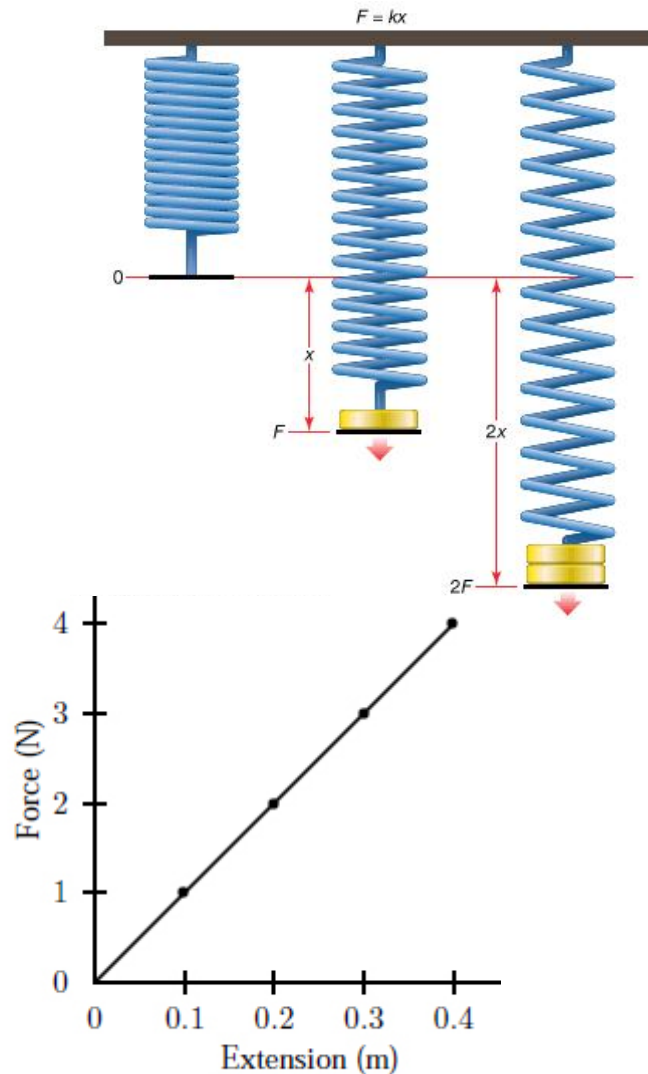
Strain tensor is symmetric

Rotation tensor is anti-symmetric

$$\begin{bmatrix} \frac{\partial u_x}{\partial x} & \frac{1}{2} \left(\frac{\partial u_x}{\partial y} + \frac{\partial u_y}{\partial x} \right) & \frac{1}{2} \left(\frac{\partial u_x}{\partial z} + \frac{\partial u_z}{\partial x} \right) \\ \frac{1}{2} \left(\frac{\partial u_y}{\partial x} + \frac{\partial u_x}{\partial y} \right) & \frac{\partial u_y}{\partial y} & \frac{1}{2} \left(\frac{\partial u_y}{\partial z} + \frac{\partial u_z}{\partial y} \right) \\ \frac{1}{2} \left(\frac{\partial u_z}{\partial x} + \frac{\partial u_x}{\partial z} \right) & \frac{1}{2} \left(\frac{\partial u_z}{\partial y} + \frac{\partial u_y}{\partial z} \right) & \frac{\partial u_z}{\partial z} \end{bmatrix} + \begin{bmatrix} 0 & \frac{1}{2} \left(\frac{\partial u_x}{\partial y} - \frac{\partial u_y}{\partial x} \right) & \frac{1}{2} \left(\frac{\partial u_x}{\partial z} - \frac{\partial u_z}{\partial x} \right) \\ -\frac{1}{2} \left(\frac{\partial u_x}{\partial y} - \frac{\partial u_y}{\partial x} \right) & 0 & \frac{1}{2} \left(\frac{\partial u_y}{\partial z} - \frac{\partial u_z}{\partial y} \right) \\ -\frac{1}{2} \left(\frac{\partial u_x}{\partial z} - \frac{\partial u_z}{\partial x} \right) & -\frac{1}{2} \left(\frac{\partial u_y}{\partial z} - \frac{\partial u_z}{\partial y} \right) & 0 \end{bmatrix}$$

- Strain is a dimensionless quantity ($\Delta L/L$)
- Strain due to passage of seismic waves are typically $<10^{-5}$

Constitutive relationship



- In an elastic medium, stress and strain are linearly related (for small strains, and assuming perfect elasticity)

- In 1D, this is the familiar Hooke's Law:

$$\mathbf{F} = -k \mathbf{x}$$

- The constant k is the spring stiffness

- In 3D, \mathbf{x} becomes the strain tensor, and \mathbf{F} becomes the stress tensor:

$$\tau_{ij} = c_{ijkl} e_{kl} \equiv \sum_{k=1}^3 \sum_{l=1}^3 c_{ijkl} e_{kl}$$

Elastic tensor and anisotropy

- The 4-th order tensor relating stress to strain has 81 components ($3 \times 3 \times 3 \times 3 = 81$) with units of pressure (GPa)
- Because of symmetry of stress and strain tensors internal deformation energy considerations, $c_{ijkl} = c_{klij} = c_{ikjl} = c_{jkl i} \rightarrow 21$ independent components
- Specifying all 21 at every point is needed in a medium with **general anisotropy**
- To zeroth order, Earth is isotropic at large scales: only 2 independent components (Lamé parameters):

$$c_{ijkl} = \lambda \delta_{ij} \delta_{kl} + \mu (\delta_{il} \delta_{jk} + \delta_{ik} \delta_{jl})$$

Kronecker delta ($\delta_{ij} = 1$ for $i = j$, $\delta_{ij} = 0$ for $i \neq j$)

Isotropic medium representations

- In an isotropic medium, wave speed depends on NEITHER the direction of propagation NOR polarization direction

- Relationship between stress and strain is simple:

$$\tau_{ij} = 2\mu e_{ij} + \lambda \delta_{ij} \sum_{k=1}^3 e_{kk}$$

$$\mu = \tau_{xy} / 2e_{xy}.$$

- **Shear modulus**: measure of the resistance of material to shear.

$$\kappa = \lambda + \frac{2}{3}\mu$$

- **Bulk modulus**: measure of incompressibility of a material. Given by hydrostatic stress divided by fractional volume change.

$$\sigma = \frac{\lambda}{2(\lambda + \mu)}$$

- **Poisson's ratio**: lateral contraction of a cylinder divided by longitudinal extension.

Momentum \rightarrow Seismic Equation

✧ The equation of motion expresses $\mathbf{F} = m\mathbf{a}$ in terms of surface and body forces (for a continuum)

$$\nabla \cdot \boldsymbol{\sigma} + \rho \mathbf{g} = \rho \frac{\partial^2 \mathbf{u}}{\partial t^2}$$

In the absence of body forces (not valid for very low frequencies, e.g., normal modes) and away from the source:

Homogeneous eq. of motion

$$\nabla \cdot \boldsymbol{\sigma} = \rho \frac{\partial^2 \mathbf{u}}{\partial t^2}$$

The seismic wave-equation

Stress-strain relationship
(isotropic, elastic medium)



$$\sigma_{ij} = \lambda \theta \delta_{ij} + 2\mu e_{ij}$$

Homogeneous eq. of motion



$$\nabla \cdot \boldsymbol{\sigma} = \rho \frac{\partial^2 \mathbf{u}}{\partial t^2}$$

The seismic wave-equation

Stress-strain relationship
(isotropic, elastic medium)



$$\sigma_{ij} = \lambda \theta \delta_{ij} + 2\mu e_{ij}$$

Homogeneous eq. of motion



$$\nabla \cdot \boldsymbol{\sigma} = \rho \frac{\partial^2 \mathbf{u}}{\partial t^2}$$

- ✧ Eq. of motion relates spatial stress derivatives to time derivative of \mathbf{u}
- ✧ The solution of equation of motion can be done numerically, using finite-difference computations => i.e. 1st order approximations of the derivatives.
- ✧ Exploiting the stress-strain relationship, the homogeneous equation of motion can be solved in terms of displacements

The seismic wave-equation

Stress-strain relationship
(isotropic, elastic medium)



$$\sigma_{ij} = \lambda \theta \delta_{ij} + 2\mu e_{ij}$$

Homogeneous eq. of motion →

$$\nabla \cdot \boldsymbol{\sigma} = \rho \frac{\partial^2 \mathbf{u}}{\partial t^2}$$

After some algebra... and a vector identity:

$$\nabla^2 \mathbf{u} = \nabla \nabla \cdot \mathbf{u} - \nabla \times \nabla \times \mathbf{u}$$

Seismic Wave Equation for an isotropic medium

$$\rho \ddot{\mathbf{u}} = \nabla \lambda (\nabla \cdot \mathbf{u}) + \nabla \mu \cdot [\nabla \mathbf{u} + (\nabla \mathbf{u})^T] + (\lambda + 2\mu) \nabla \nabla \cdot \mathbf{u} - \mu \nabla \times \nabla \times \mathbf{u}$$

Momentum \rightarrow Seismic Equation

$$\rho \frac{\partial^2 u_i}{\partial t^2} = \partial_j \tau_{ij}$$

□ **Homogeneous momentum equation** governs seismic waves outside of source regions

□ **Summation convention**: repeated index \rightarrow summation, e.g. $e_{kk} = e_{11} + e_{22} + e_{33}$.

$$\tau_{ij} = \lambda \delta_{ij} \partial_k u_k + \mu (\partial_i u_j + \partial_j u_i)$$

□ **Constitutive relation** for isotropic medium, where we used $2e_{jk} = (\partial u_k / \partial x_j + \partial u_j / \partial x_k)$

+ manipulation and a vector identity:

$$\nabla^2 \mathbf{u} = \nabla \nabla \cdot \mathbf{u} - \nabla \times \nabla \times \mathbf{u}$$

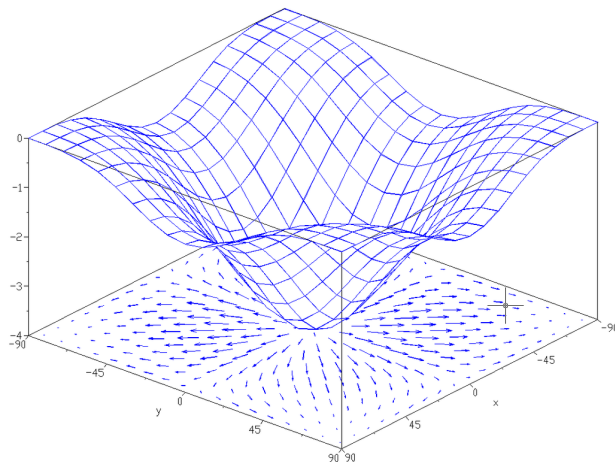
□ **Seismic Wave Equation** for an isotropic medium

$$\rho \ddot{\mathbf{u}} = \nabla \lambda (\nabla \cdot \mathbf{u}) + \nabla \mu \cdot [\nabla \mathbf{u} + (\nabla \mathbf{u})^T] + (\lambda + 2\mu) \nabla \nabla \cdot \mathbf{u} - \mu \nabla \times \nabla \times \mathbf{u}$$

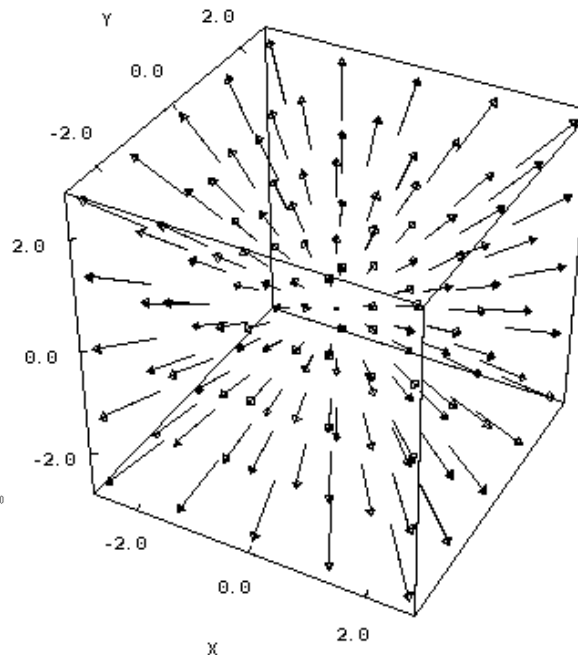
Seismic Wave Equation

$$\rho \ddot{\mathbf{u}} = \underbrace{\nabla \lambda (\nabla \cdot \mathbf{u})}_{\text{Divergence}} + \underbrace{\nabla \mu \cdot [\nabla \mathbf{u} + (\nabla \mathbf{u})^T]}_{\text{Divergence}} + \underbrace{(\lambda + 2\mu) \nabla \nabla \cdot \mathbf{u}}_{\text{Divergence}} - \underbrace{\mu \nabla \times \nabla \times \mathbf{u}}_{\text{Curl}}$$

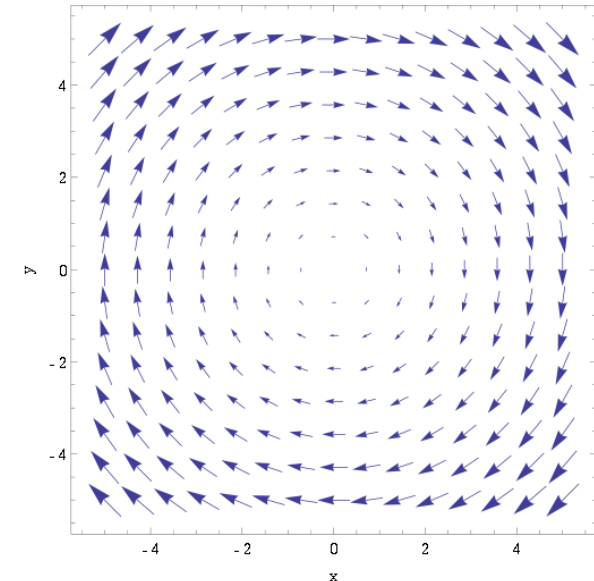
Gradient: Vector describing the direction and magnitude of change in a quantity



Divergence: Scalar describing volume change



Curl: Vector describing infinitesimal rotation (think paddle wheel)



The seismic wave-equation

- Rather than directly solve the wave equation derived on the previous slide, we can express the displacement field in terms of two other functions, a scalar $\Phi(\mathbf{x}, t)$ and a vector $\Psi(\mathbf{x}, t)$, via Helmholtz' theorem

$$\mathbf{u} = \nabla \Phi + \nabla \times \Psi$$

- In this representation, the displacement is the sum of the gradient of a scalar potential and the curl of a vector potential.
- Although this representation of the displacement field would at first appear to introduce complexity, it actually clarifies the problem because of the following two vector identities

$$\nabla \times (\nabla \Phi) = 0$$

$$\nabla \cdot (\nabla \times \Psi) = 0$$

The seismic wave-equation

- $\nabla\phi$: No curl or rotation and gives rise to compressional waves.
- $\nabla \times \psi$: Zero divergence; causes no volume change and corresponds to shear waves.

$$\nabla \times (\nabla \phi) = 0$$

$$\nabla \cdot (\nabla \times \mathbf{r}) = 0$$

What does it mean?

That we can separate the displacement field into two parts:

A first that does not have any rotational component, but divergence is not zero \Rightarrow volume change \Rightarrow give rise to compressional waves.

A second does not produce change in volume (divergence is zero), but only has a rotational component \Rightarrow shear-disturbance \Rightarrow S-wave

The seismic wave-equation

$$\rho \ddot{\mathbf{u}} = (\lambda + 2\mu) \nabla \nabla \cdot \mathbf{u} - \mu \nabla \times \nabla \times \mathbf{u}.$$

$$\nabla^2(\nabla \cdot \mathbf{u}) - \frac{1}{\alpha^2} \frac{\partial^2(\nabla \cdot \mathbf{u})}{\partial t^2} = 0$$

P-wave equation

$$\nabla^2(\nabla \times \mathbf{u}) - \frac{1}{\beta^2} \frac{\partial^2(\nabla \times \mathbf{u})}{\partial t^2} = 0$$

S-wave equation

The seismic wave-equation

$$\rho \ddot{\mathbf{u}} = (\lambda + 2\mu) \nabla \nabla \cdot \mathbf{u} - \mu \nabla \times \nabla \times \mathbf{u}.$$

$$\nabla^2(\nabla \cdot \mathbf{u}) - \frac{1}{\alpha^2} \frac{\partial^2(\nabla \cdot \mathbf{u})}{\partial t^2} = 0$$

P-wave equation

$$\nabla^2(\nabla \times \mathbf{u}) - \frac{1}{\beta^2} \frac{\partial^2(\nabla \times \mathbf{u})}{\partial t^2} = 0$$

S-wave equation

where

$$\alpha = \sqrt{\frac{\lambda + 2\mu}{\rho}}$$

P-wave velocity

$$\beta = \sqrt{\frac{\mu}{\rho}}$$

S-wave velocity

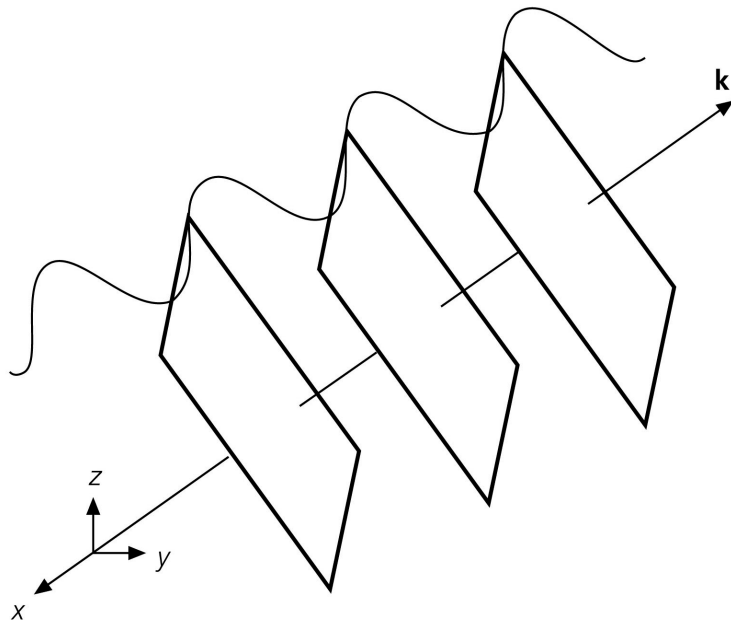
The seismic wave-equation

Solution of P-wave and S-wave equations can be done assuming plane waves (Cartesian coordinates) or spherical waves.

Harmonic solution of wave equation

$$u(x, t) = Ae^{i(\omega t \pm kx)}$$

Figure 2.4-1: Plane wave fronts.



Same for vector wave equation in 3D:

$$\nabla^2 \Upsilon(\mathbf{x}, t) = \frac{1}{v^2} \frac{\partial^2 \Upsilon(\mathbf{x}, t)}{\partial t^2}$$

The harmonic plane wave solution to the vector wave equation is:

$$\Upsilon(\mathbf{x}, t) = \mathbf{A} \exp(i(\omega t - \mathbf{k} \cdot \mathbf{x}))$$

Note that $\Upsilon(\mathbf{x}, t)$ and the constant \mathbf{A} are now vectors.

Homogeneous medium

- In a homogeneous medium, or in the high-frequency approximation, the gradients of λ and μ can be neglected:

$$\rho \ddot{\mathbf{u}} = (\lambda + 2\mu) \nabla \nabla \cdot \mathbf{u} - \mu \nabla \times \nabla \times \mathbf{u}$$

- Taking the divergence of the equation (remember $\nabla \cdot (\nabla \times \Psi) = 0$):

$$\nabla^2 (\nabla \cdot \mathbf{u}) - \frac{1}{\alpha^2} \frac{\partial^2 (\nabla \cdot \mathbf{u})}{\partial t^2} = 0$$

Compressional wave (P-wave) propagating at speed α

$$\alpha^2 = \frac{\lambda + 2\mu}{\rho}$$

- Taking the curl of the equation (remember $\nabla \cdot (\nabla \times \mathbf{u}) = 0$, and $\nabla \times (\nabla \phi) = 0$):

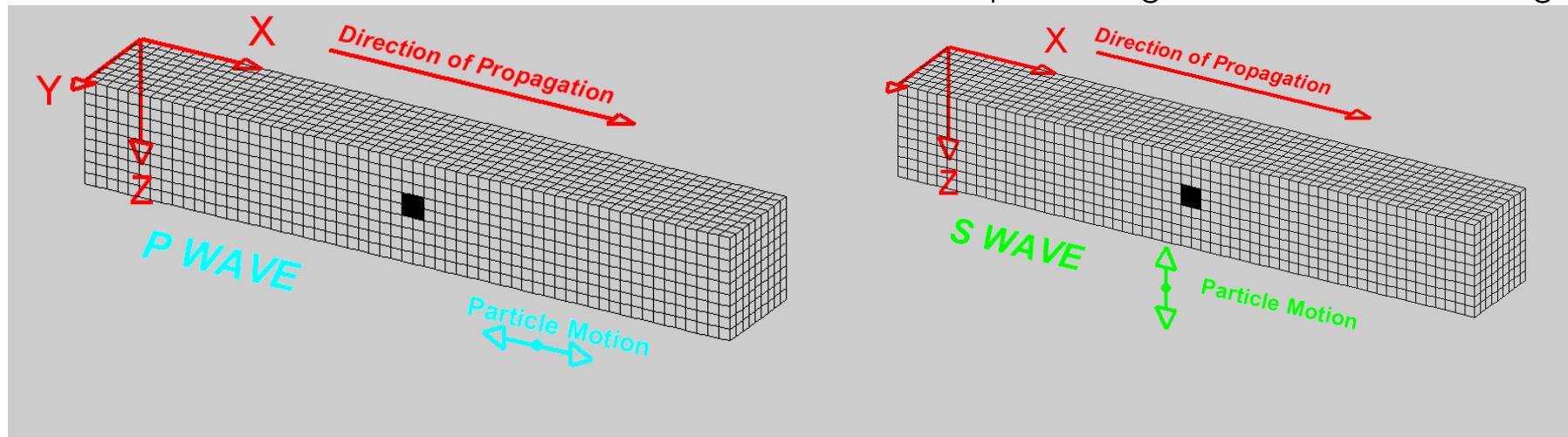
$$\nabla^2 (\nabla \times \mathbf{u}) - \frac{1}{\beta^2} \frac{\partial^2 (\nabla \times \mathbf{u})}{\partial t^2} = 0$$

Shear wave (S-wave) involving no volume change propagating at speed β

$$\beta^2 = \frac{\mu}{\rho}$$

P and S waves

<http://www.geo.mtu.edu/UPSeis/images/>



- P waves: volume & shape change, particle motion in the direction of propagation
- S waves: only shape change (no volume change), particle motion perpendicular to direction of propagation
 - SH – particle motion in the horizontal plane
 - SV – particle motion in the vertical plane

Plane waves

- Solutions to the P and S equations are waves: $u(\mathbf{x}, t) = f(\mathbf{x} \pm \mathbf{v}t)$,
 \mathbf{v} = velocity

- Plane waves: $\mathbf{u}(\mathbf{x}, t) = \mathbf{f}(t - \hat{\mathbf{s}} \cdot \mathbf{x}/c)$
 $= \mathbf{f}(t - \mathbf{s} \cdot \mathbf{x}),$

\mathbf{s} is the **slowness vector**

- Particle displacement at a frequency ω :

$$\begin{aligned}\mathbf{u}(\mathbf{x}, t) &= \mathbf{A}(\omega)e^{-i\omega(t-\mathbf{s}\cdot\mathbf{x})} \\ &= \mathbf{A}(\omega)e^{-i(\omega t - \mathbf{k}\cdot\mathbf{x})}\end{aligned}$$

\mathbf{k} is the **wavenumber vector**

(Figure from Stein and Wysession, 2003)

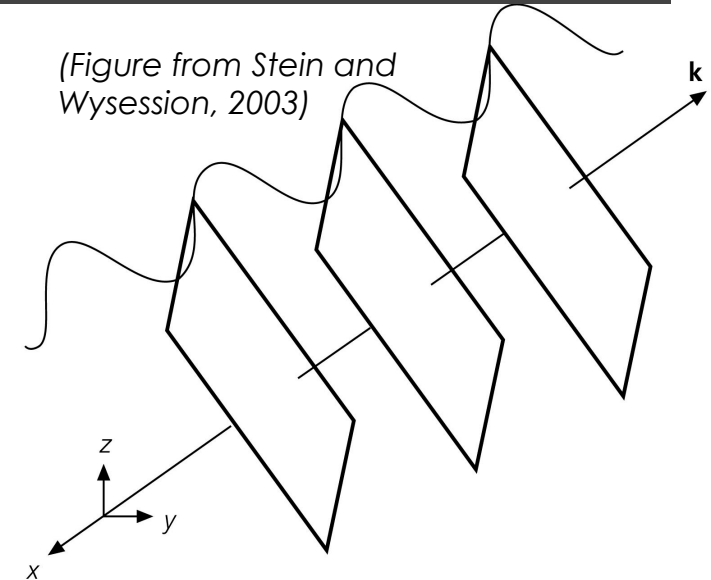
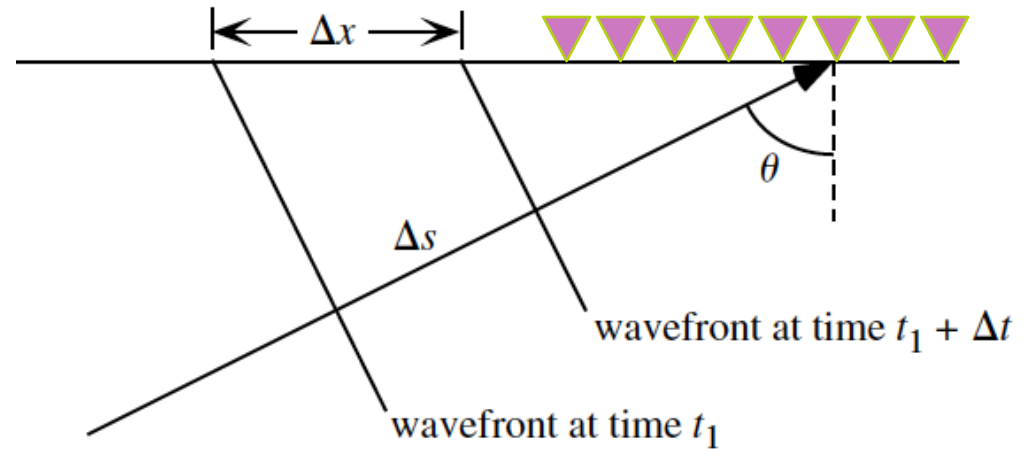
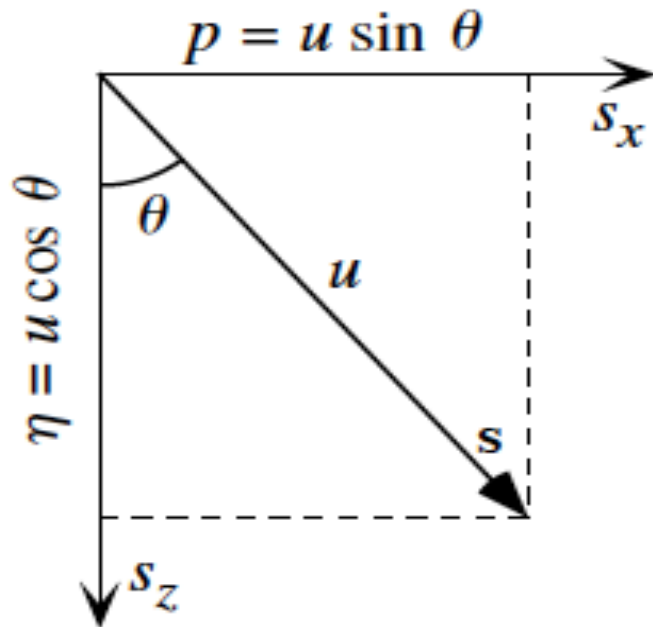


Table 3.1: Harmonic wave parameters.

Angular frequency	ω	time ⁻¹	$\omega = 2\pi f = \frac{2\pi}{T} = ck$
Frequency	f	time ⁻¹	$f = \frac{\omega}{2\pi} = \frac{1}{T} = \frac{c}{\Lambda}$
Period	T	time	$T = \frac{1}{f} = \frac{2\pi}{\omega} = \frac{\Lambda}{c}$
Velocity	c	distance time ⁻¹	$c = \frac{\Lambda}{T} = f\Lambda = \frac{\omega}{k}$
Wavelength	Λ	distance	$\Lambda = \frac{c}{f} = cT = \frac{2\pi}{k}$
Wavenumber	k	distance ⁻¹	$k = \frac{\omega}{c} = \frac{2\pi}{\Lambda} = \frac{2\pi f}{c} = \frac{2\pi}{cT}$

Horizontal & vertical slownesses



- Slowness: $u = 1 / c$
- Horizontal slowness: $p = \Delta T / \Delta X$
- Vertical slowness: $\eta = (u^2 - p^2)^{1/2}$

- We can measure how quickly a wave sweeps across a small, dense array of seismometers

figures from Shearer, 2009

Snell's Law – the ray parameter

For wavefield to remain continuous along interface between regions with different velocities, waves will change direction in addition to their speed.

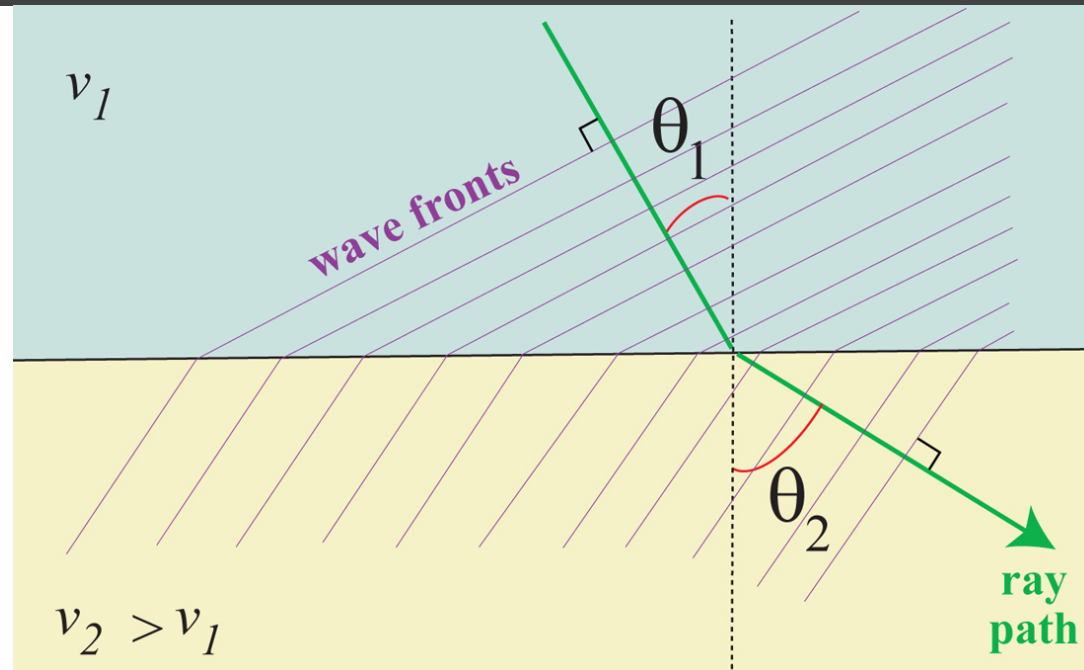
Snell's Law I

Velocity 1: 6 km/s
Velocity 2: 8 km/s

<http://web.utah.edu/thorne>

Snell's Law – the ray parameter

For wavefield to remain continuous along interface between regions with different velocities, waves will change direction in addition to their speed.



□ Snell's Law:
$$\frac{\sin \theta_1}{v_1} = \frac{\sin \theta_2}{v_2} = p$$

- Ray parameter (horizontal slowness) remains the same along the ray path

figure from garnero.asu.edu

Layered / shell medium

By specifying a ray parameter and a starting location, we fix the ray-path through a layered or spherically-symmetric Earth

The deepest depth the ray can reach is one where:

$$\frac{\sin 90}{v_1} = \frac{1}{v_1} = p$$

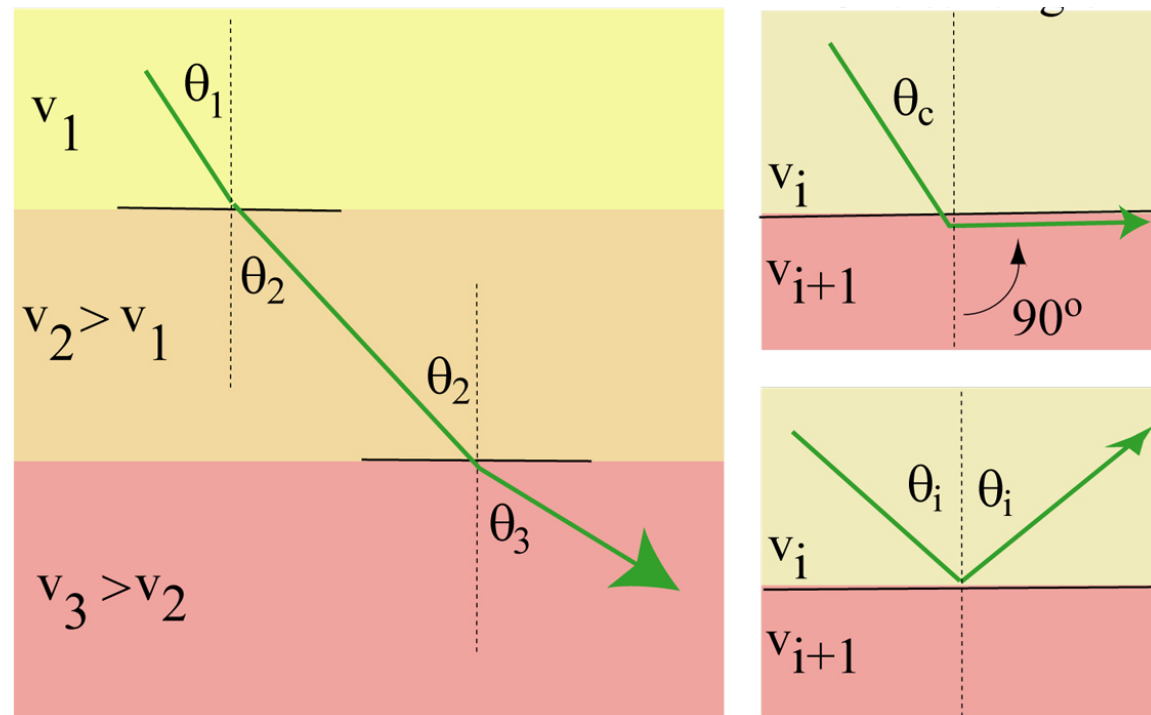
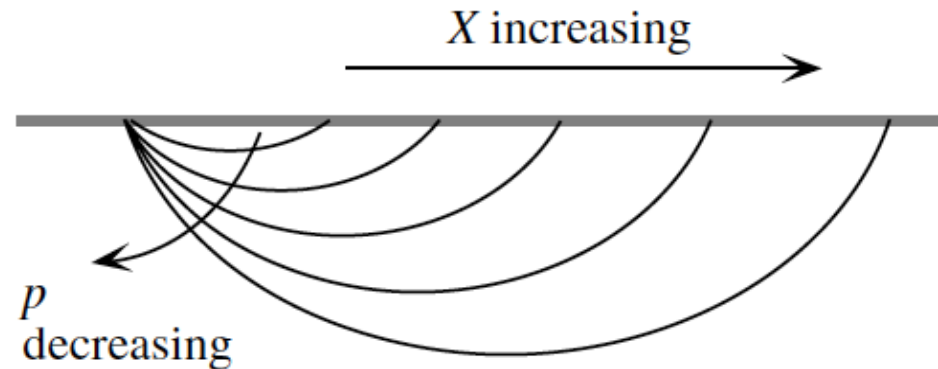
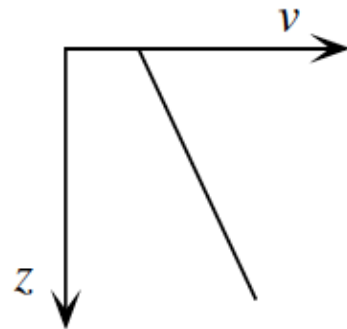


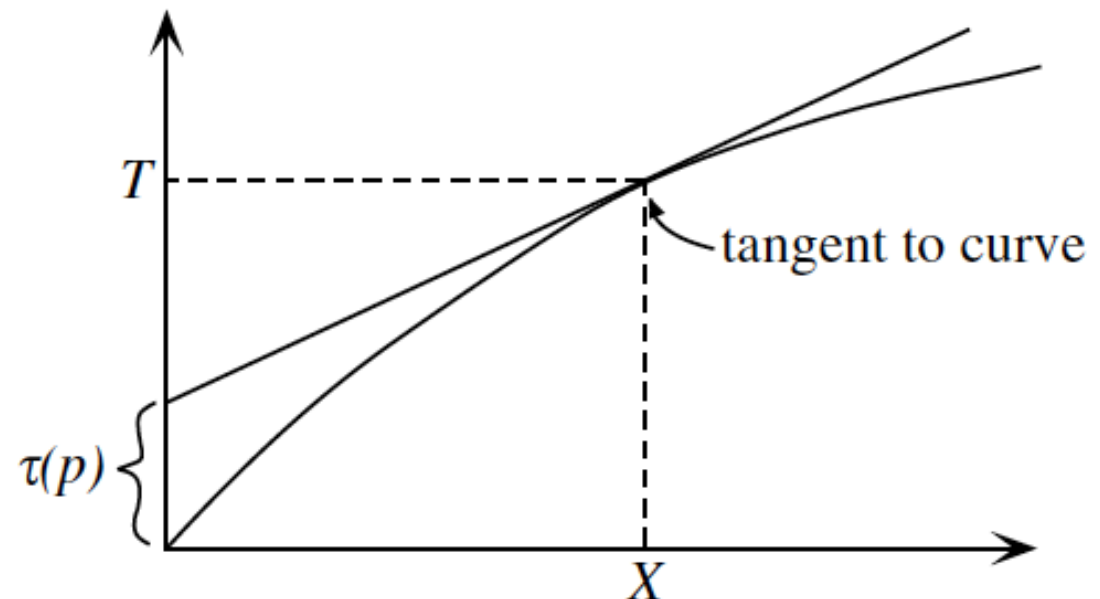
figure from garnero.asu.edu

Travel-time curves

figures from Shearer, 2009



- $T(X) = \tau(p) + pX$
- Ray parameter (horizontal slowness) is the slope of the travel-time curve
- Different rays observed at different distances
- Shallowing of slope dT/dX with distance \rightarrow slowness decreases with depth



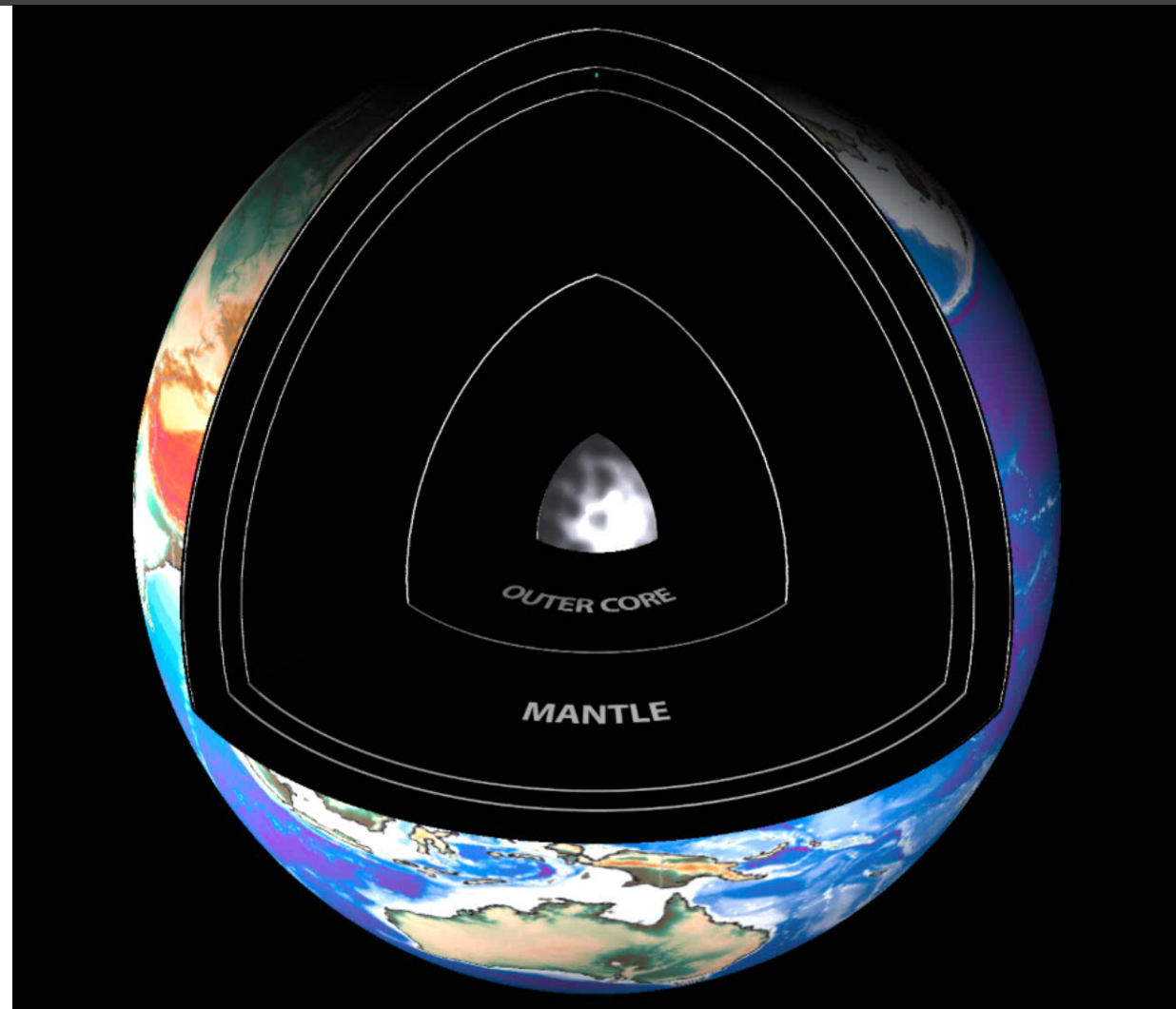
Seismic wavefield

P waves

S waves

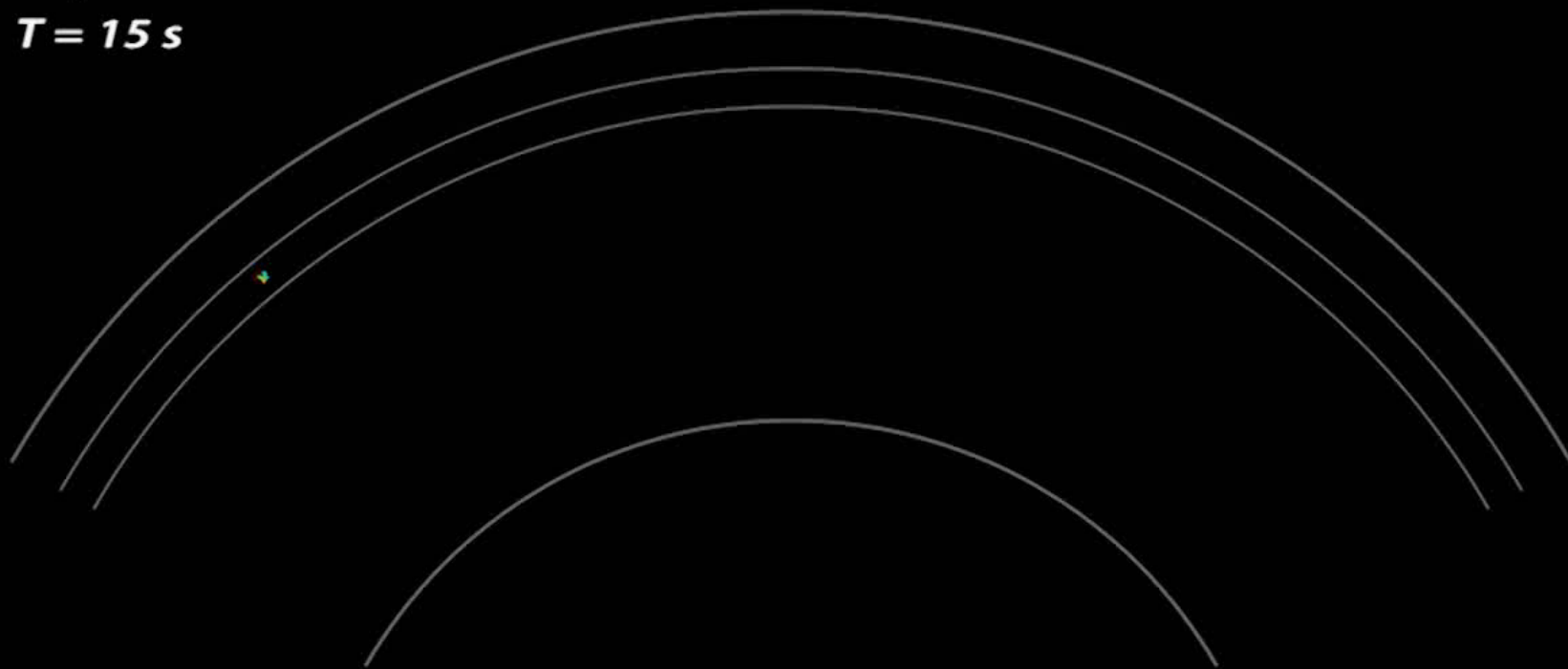
Seismic waves take a variety of paths and sample all parts of the Earth

They provide most complete and direct information on present-day state of the deep interior

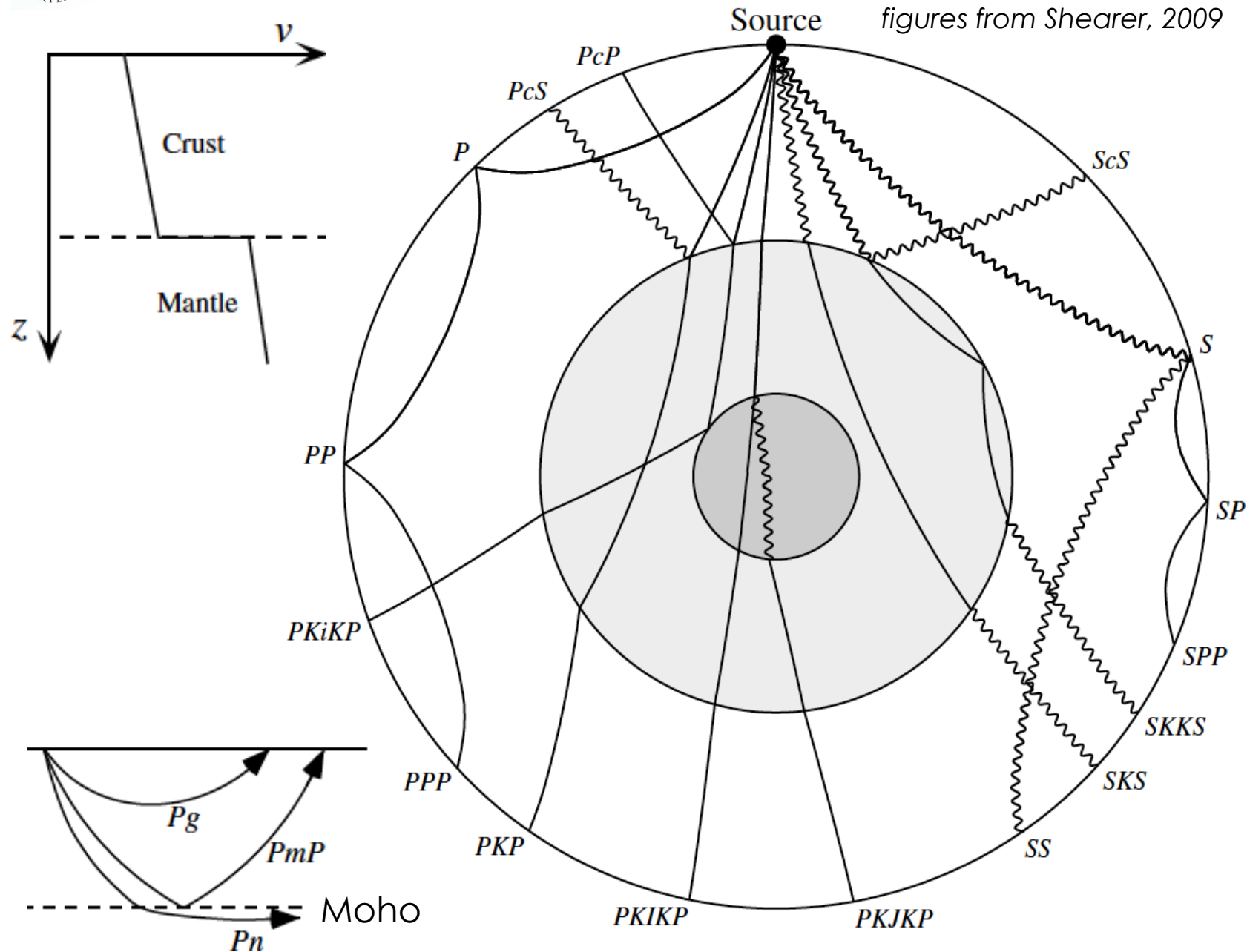


Wavefronts and raypaths

Phases: S , ScS (60°)
Depth: 500 km
 $T = 15$ s



<http://web.utah.edu/thorne>

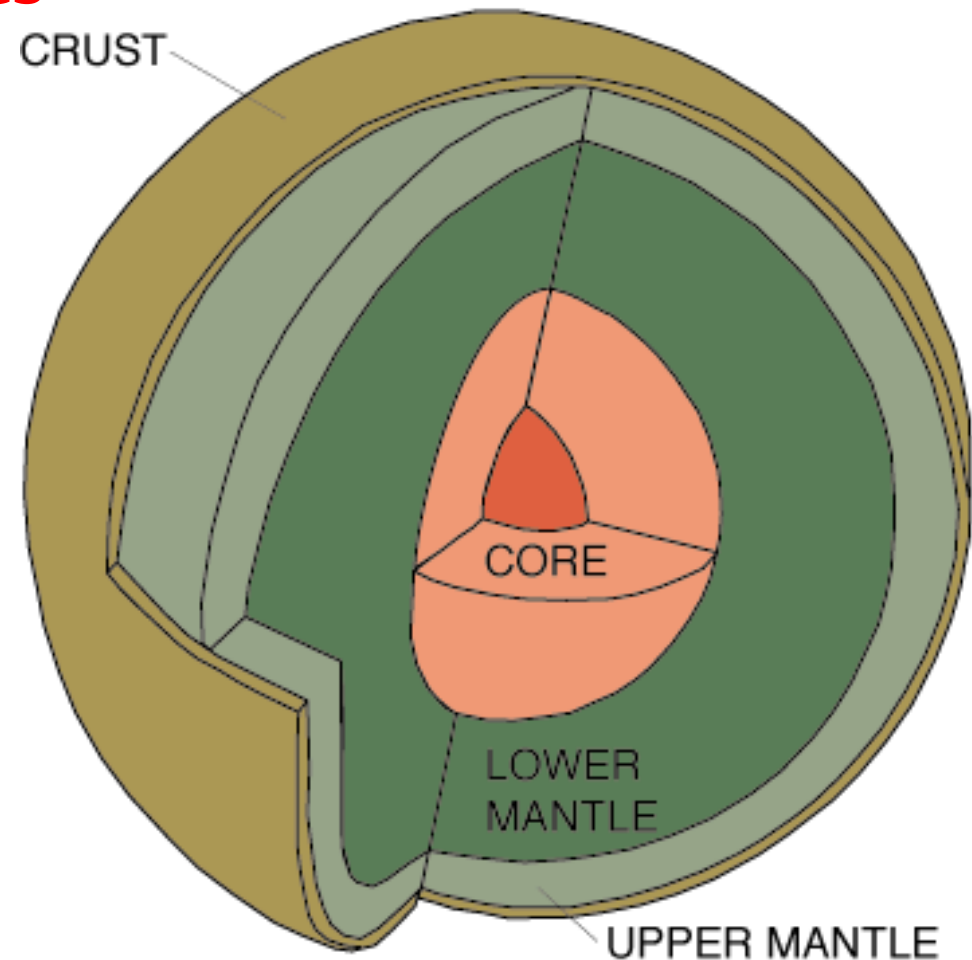
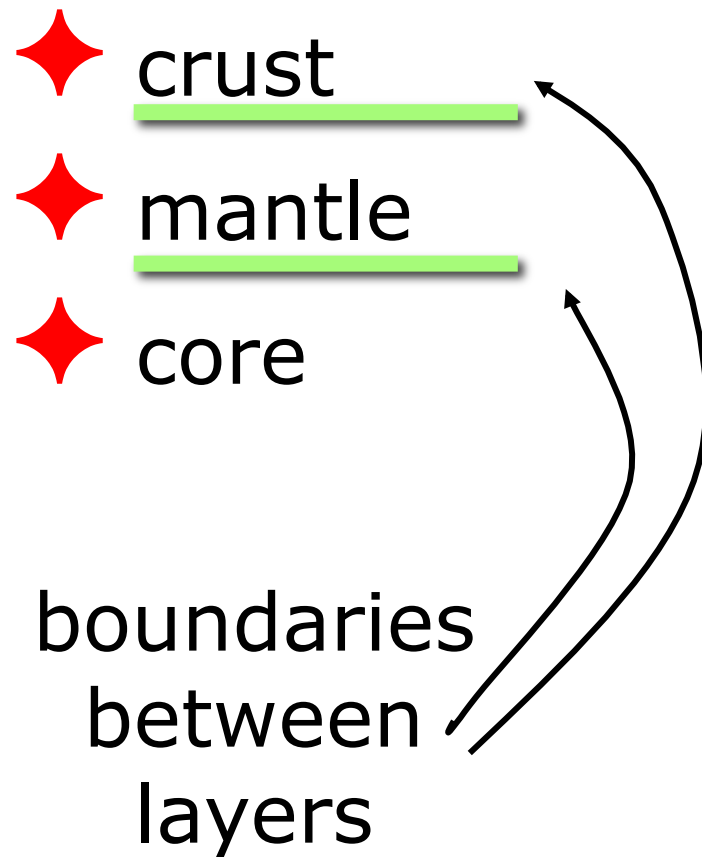


Ray nomenclature

The Earth as a planet

First-order Seismic constraints on Earth's structure

Discovering Major boundaries



Discovering Major boundaries

◆ The Crust

Thickness: ~ 30 km (continents)
3-15 km (oceanic)

Composition:

similar to granodiorite (continents)



predominantly basalt (oceanic)

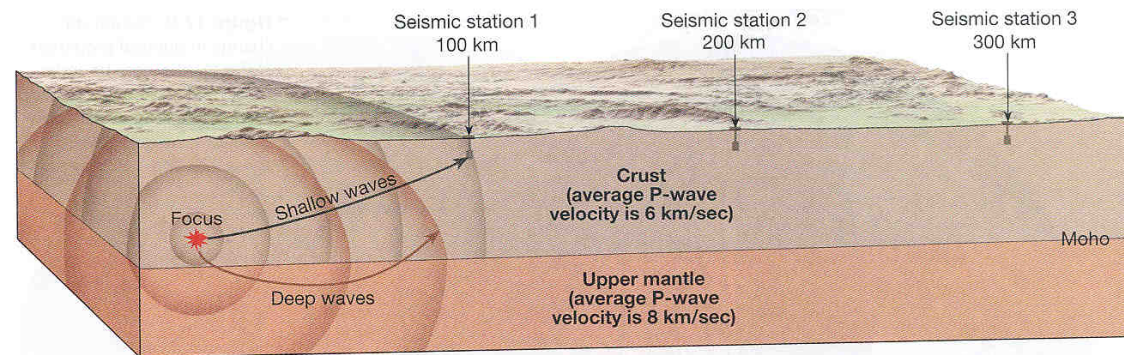
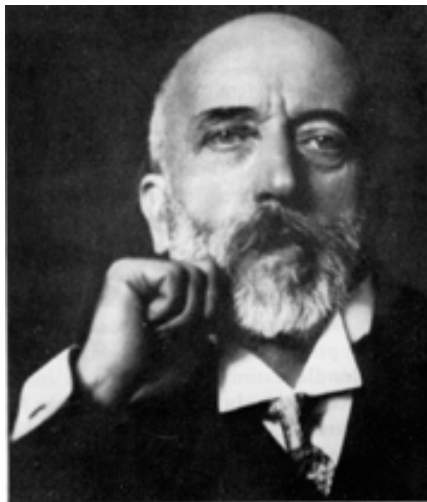


Discovering Major boundaries

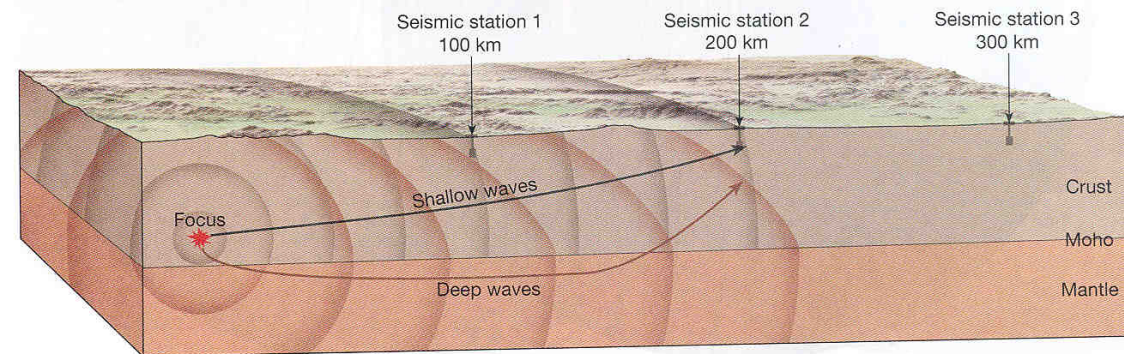
◆ The “Moho”

Boundary
between the
crust and mantle

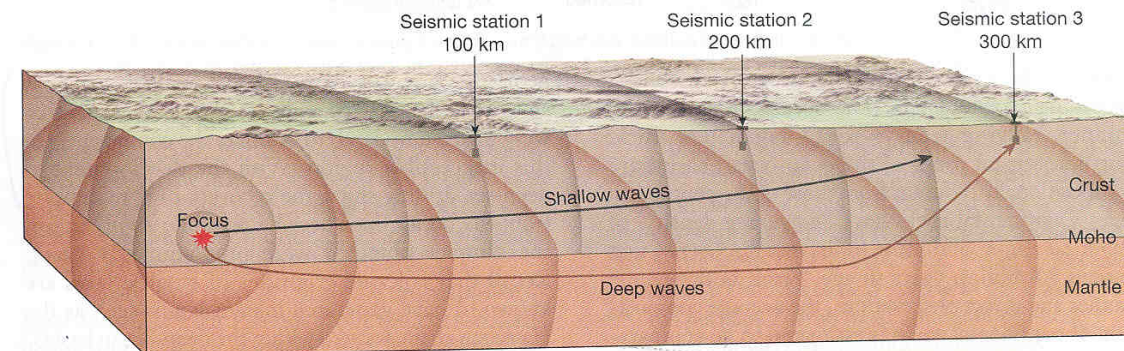
Discovered in 1909
by Andrija
Mohorovicic



A. Time 1 – Slower shallow waves arrive at seismic station 1 first.



B. Time 2 – Slower shallow waves arrive at seismic station 2 first.



C. Time 3 – Faster deeper waves arrive at seismic station 3 first.

Discovering Major boundaries

◆ The Mantle

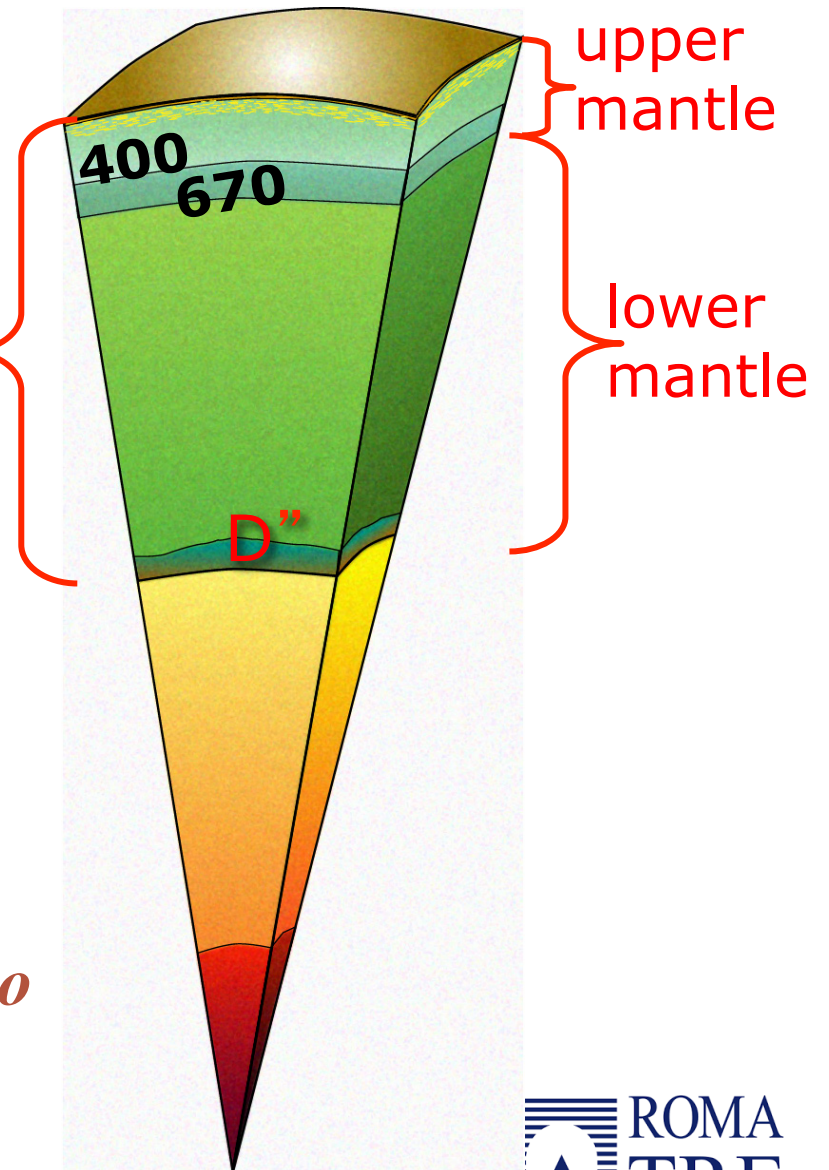
Over 82% of Earth's volume

upper mantle 0 - 670 km
lower mantle 670-2900 km
D" region 2600-2900 km

400 & 670 km depth
“phase transitions”

*Material suddenly compresses to
a more compact form*

mantle



Discovering Major boundaries

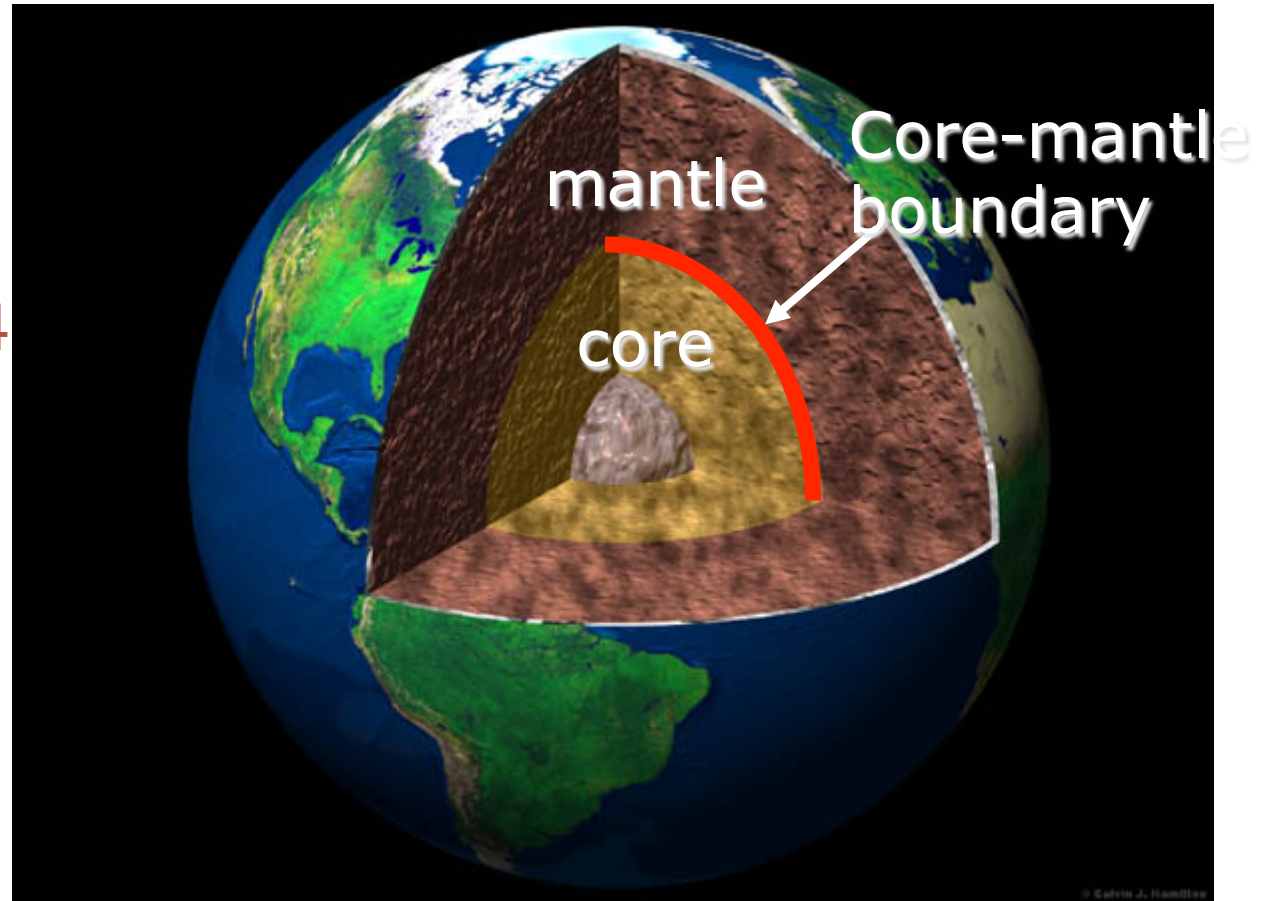
✦ The core-mantle boundary

Boundary
between the
mantle and core

Discovered in 1914
by Beno
Gu

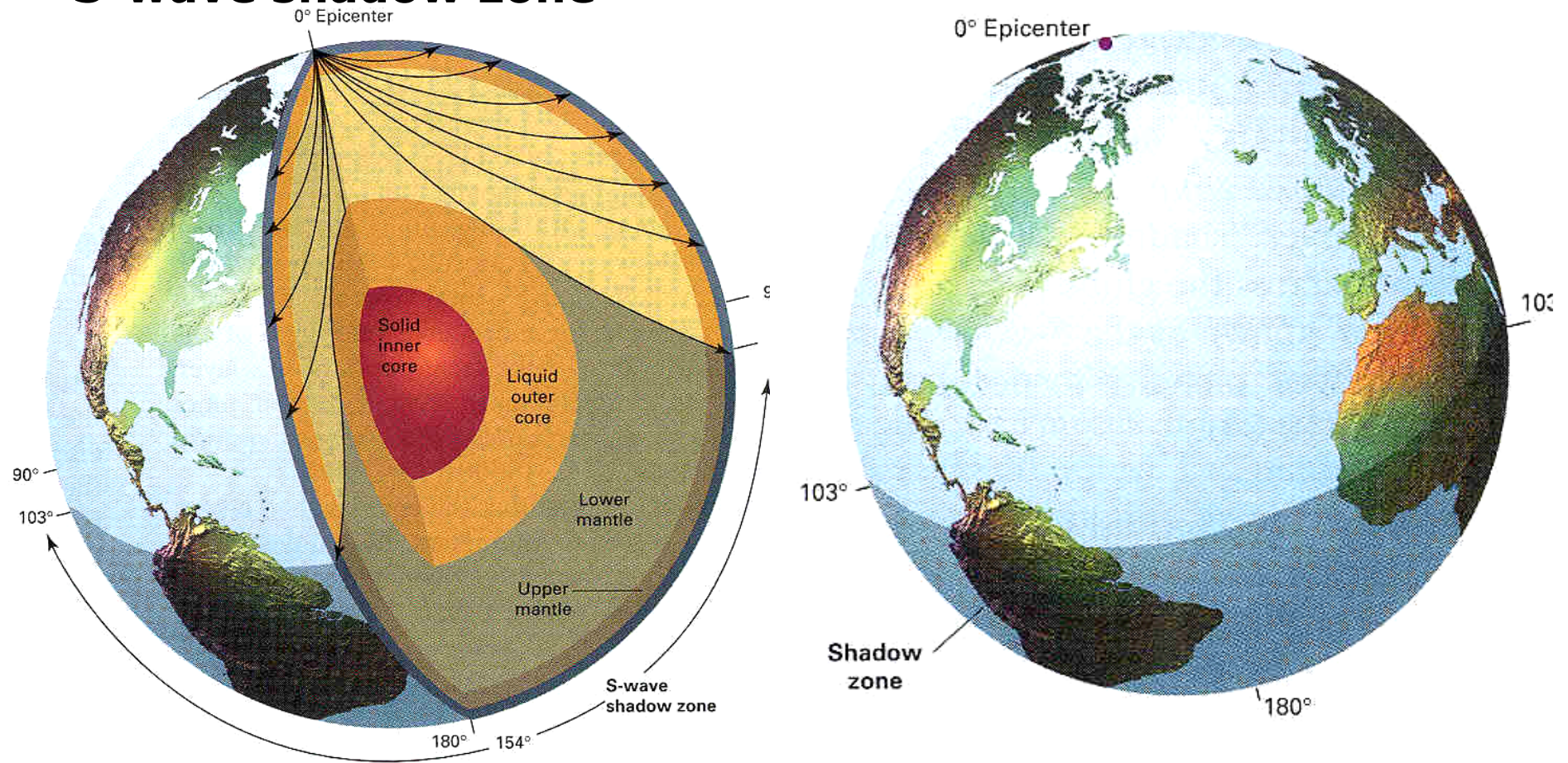


...how?



Discovering Major boundaries

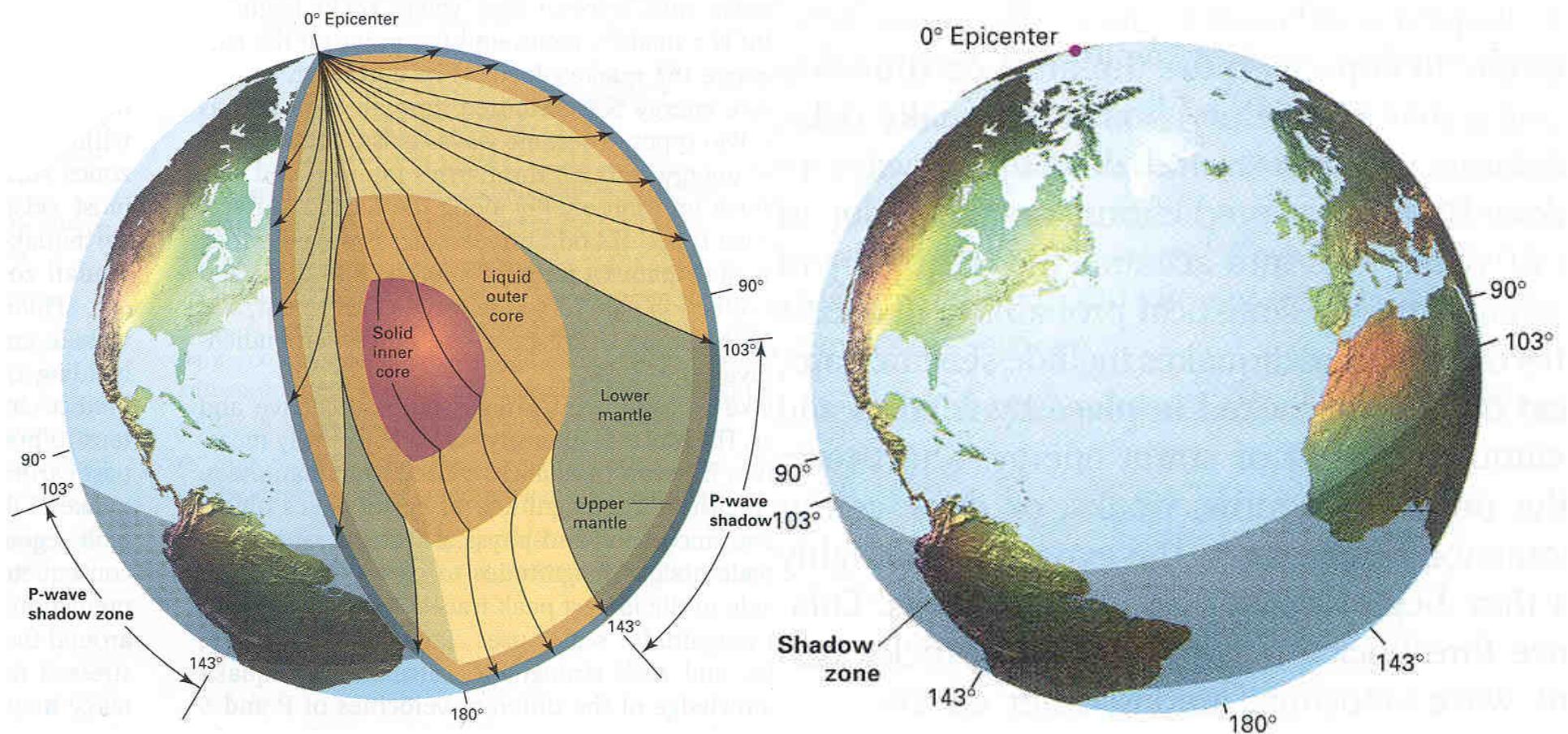
S-wave shadow zone



Core was discovered ...from a “shadow zone”

Discovering Major boundaries

P-wave shadow zone



Discovering Major boundaries

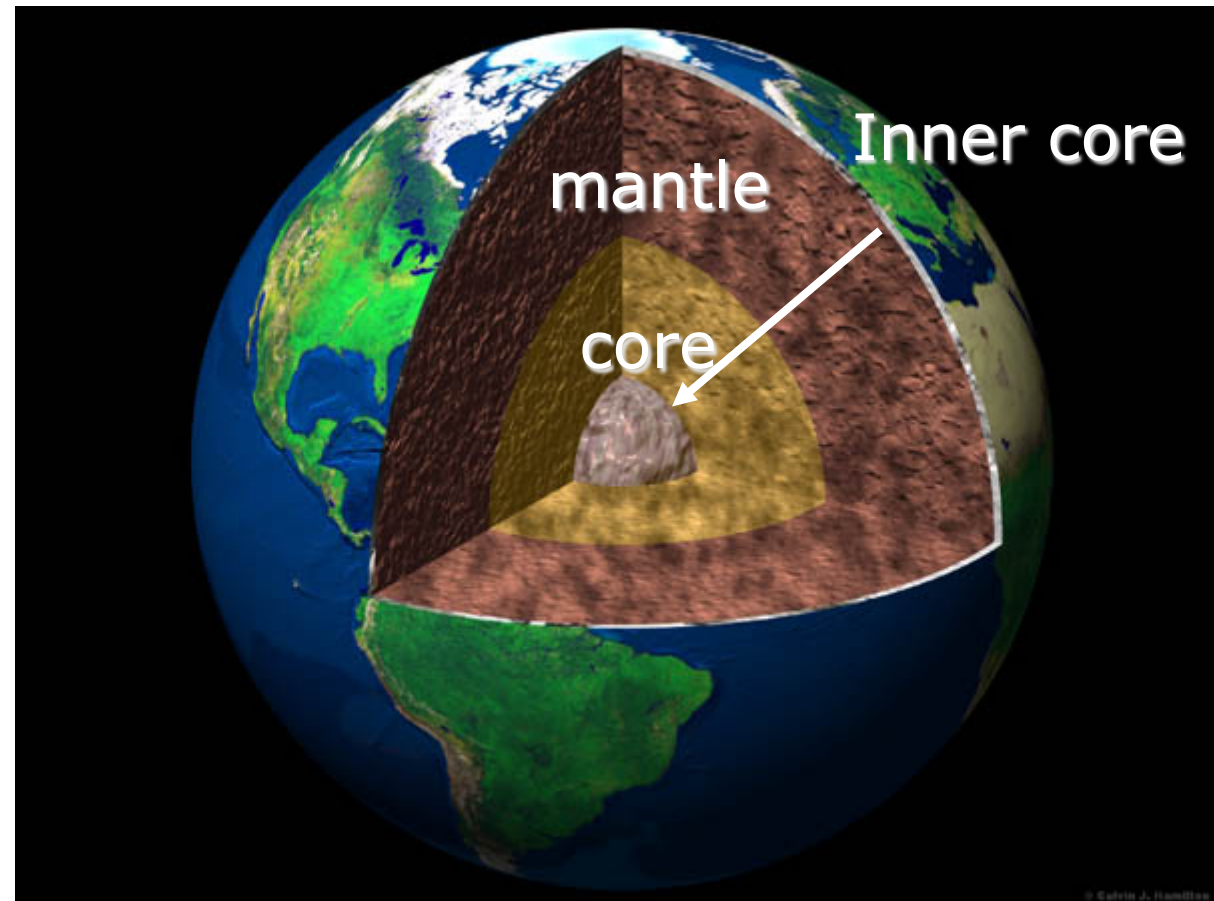
◆ The inner core

Boundary between
the outer liquid and
solid inner core

Discovered in 1936 by
Inge Lehman



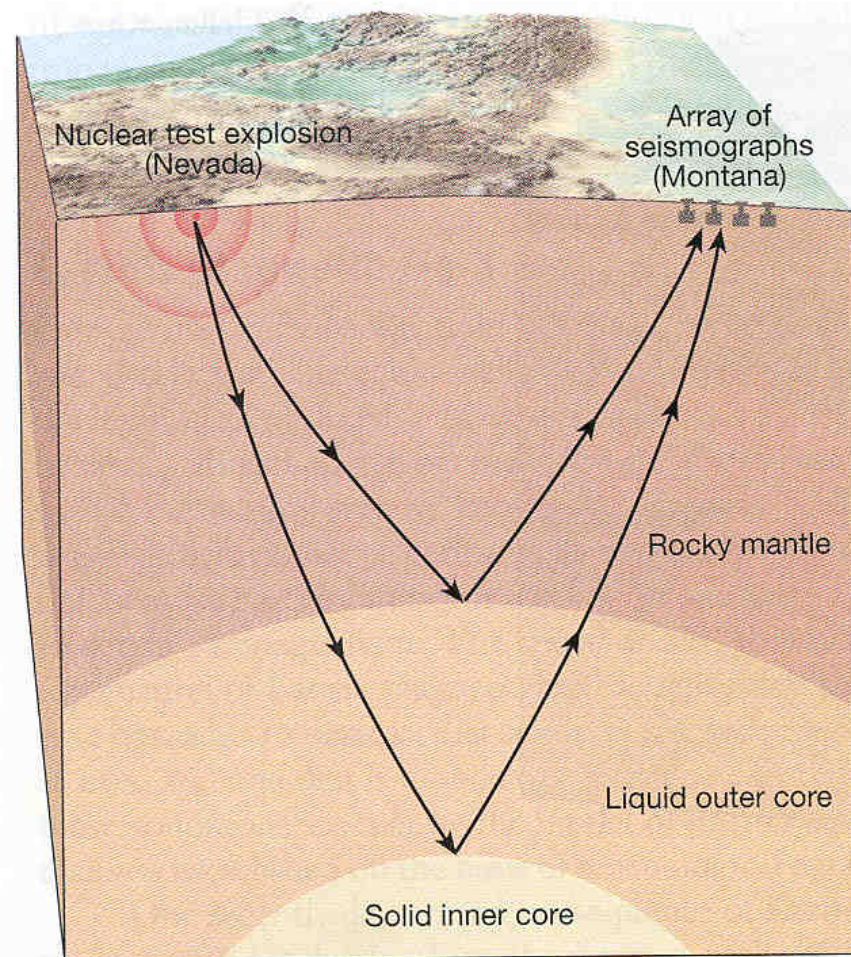
...how?



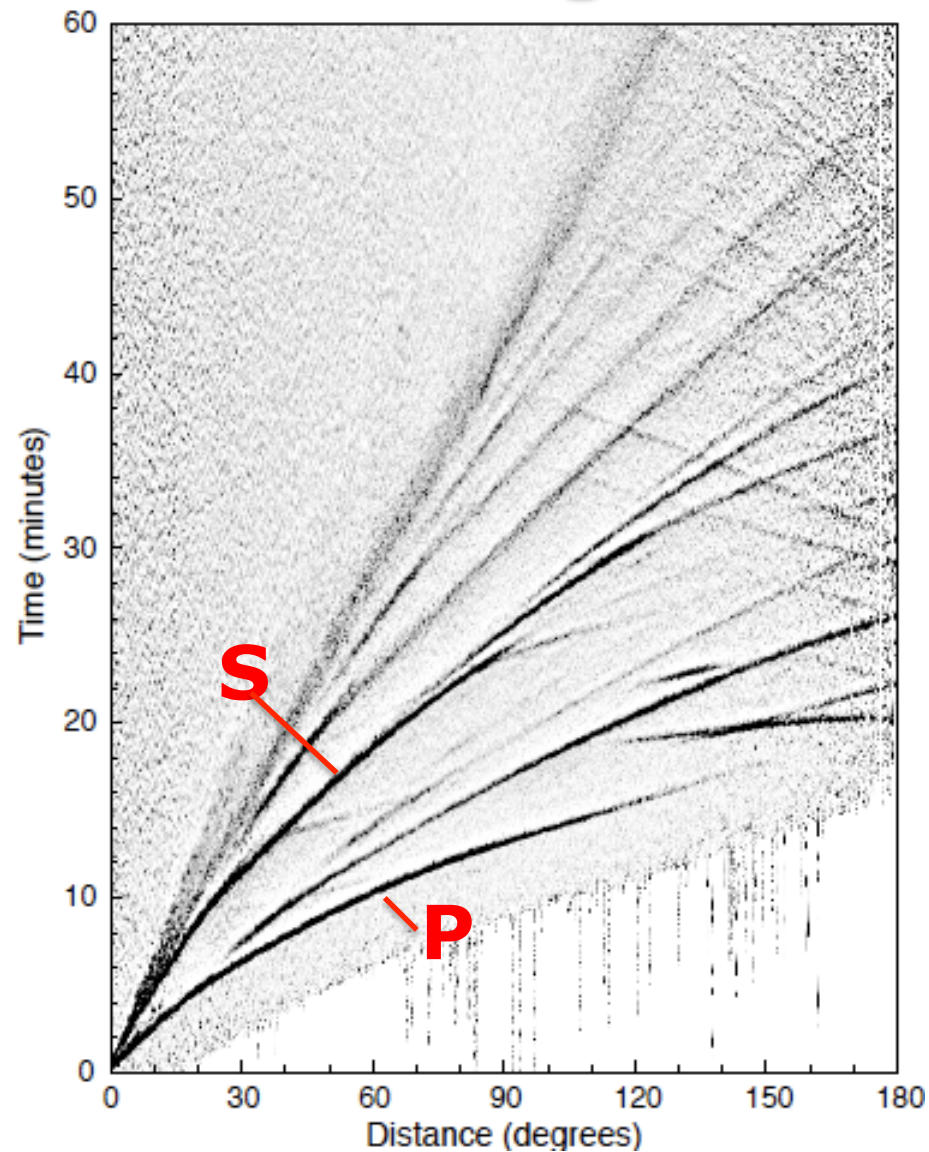
Discovering Major boundaries

◆ The inner core

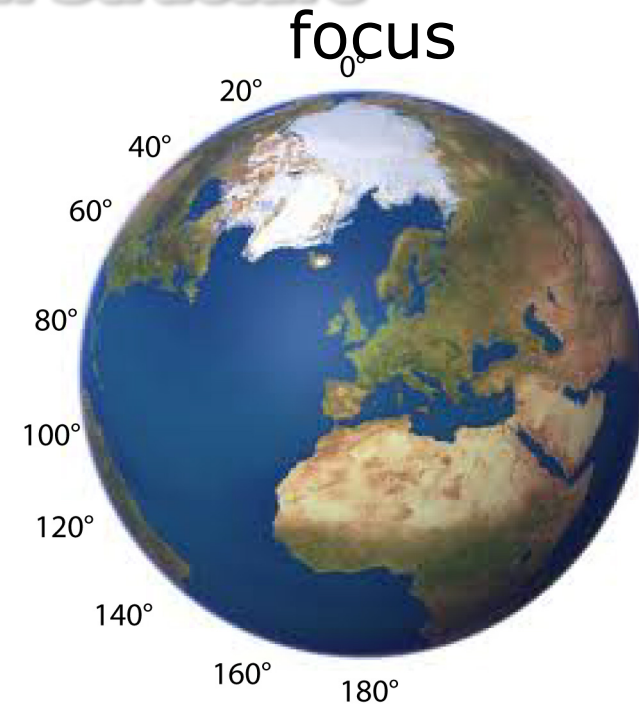
She discovered reflections of seismic waves



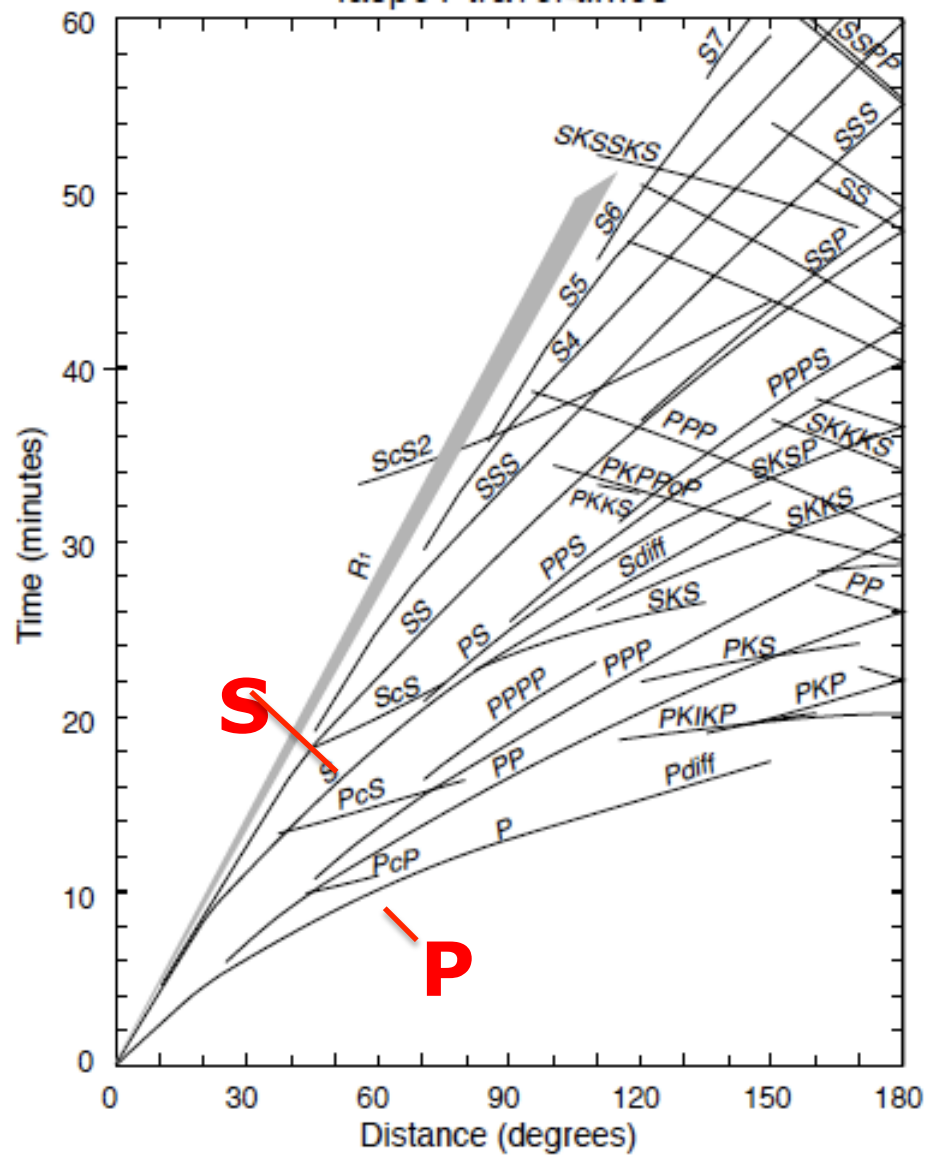
Seismograms and Earth Structure



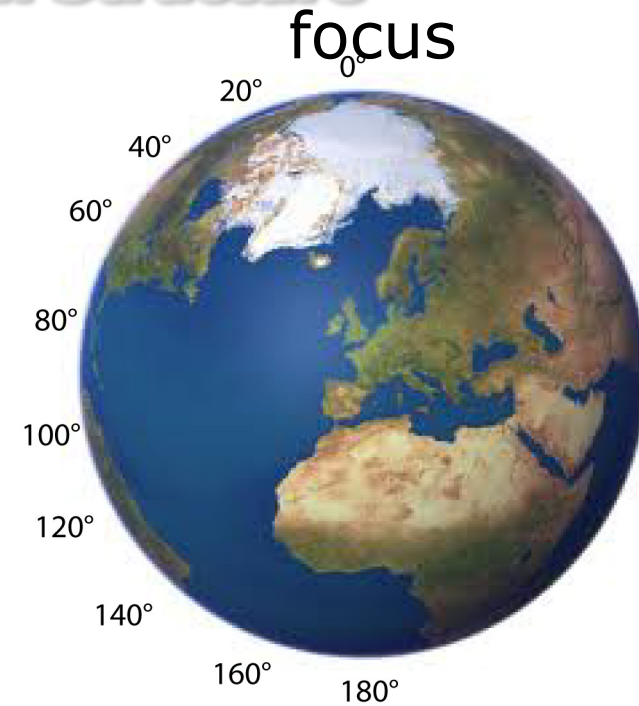
Global stack of broadband seismograms



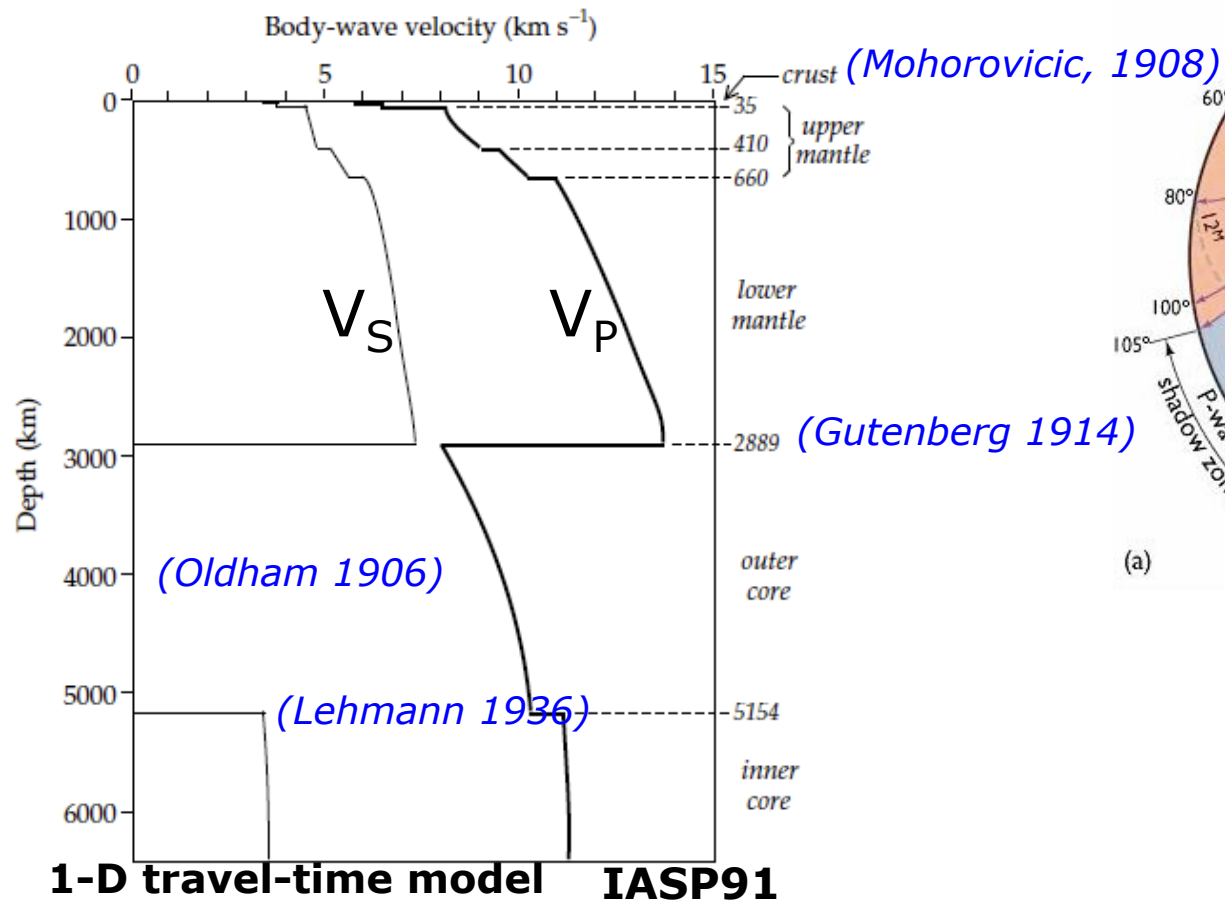
Seismograms and Earth Structure



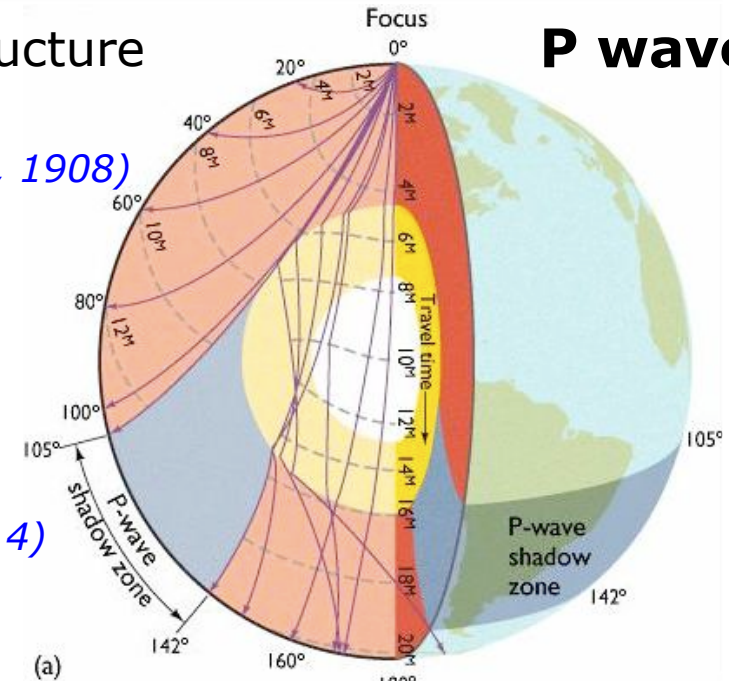
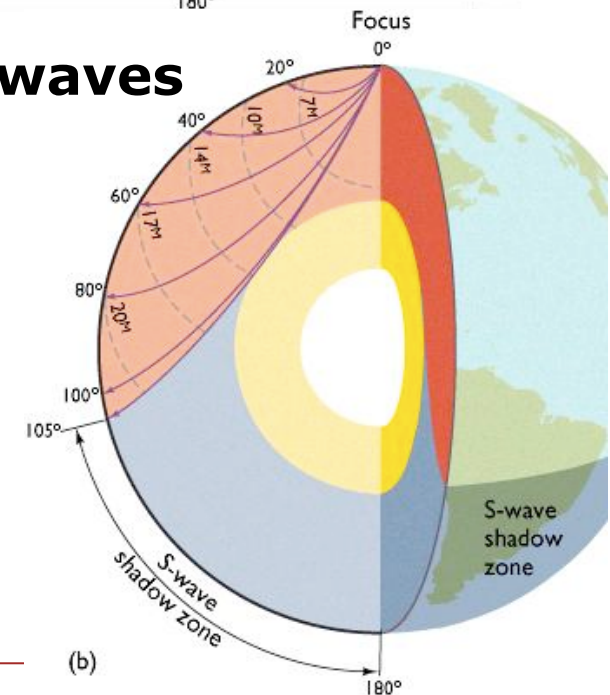
Seismic phases for IASP91 model



First-order Seismic constraints on Earth's structure

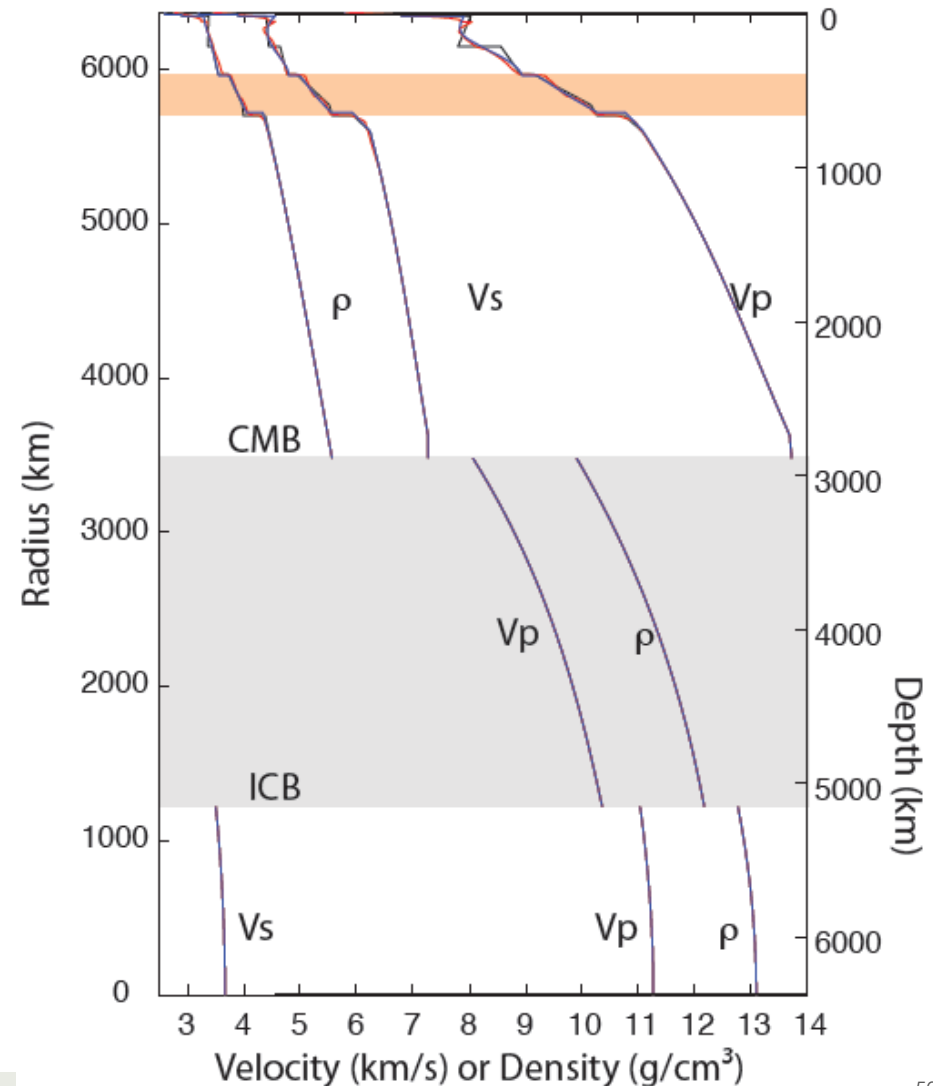
P waves**The Earth's layers**

- **CRUST** - <Oceanic> ~5 km , <Continental> ~33 km
- **MANTLE** - Upper-Lower ~670km
- **CORE** - Outer (liquid) – inner (solid)

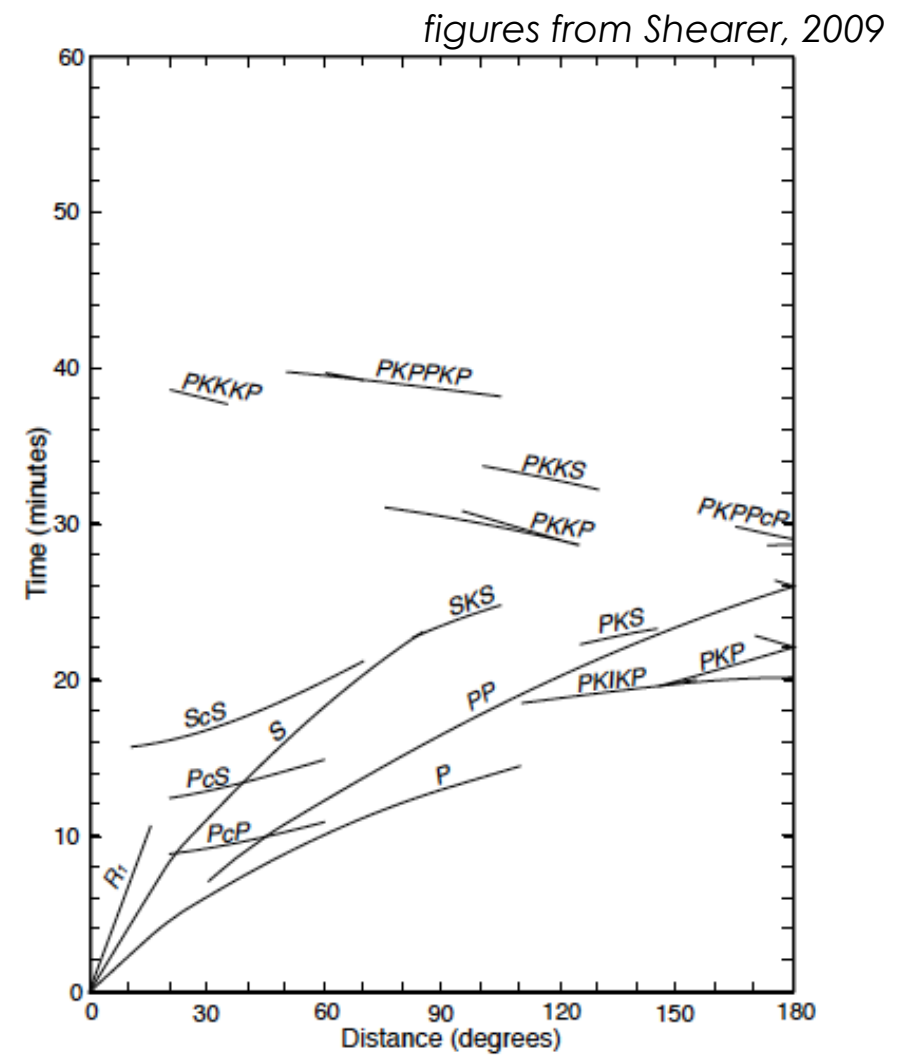
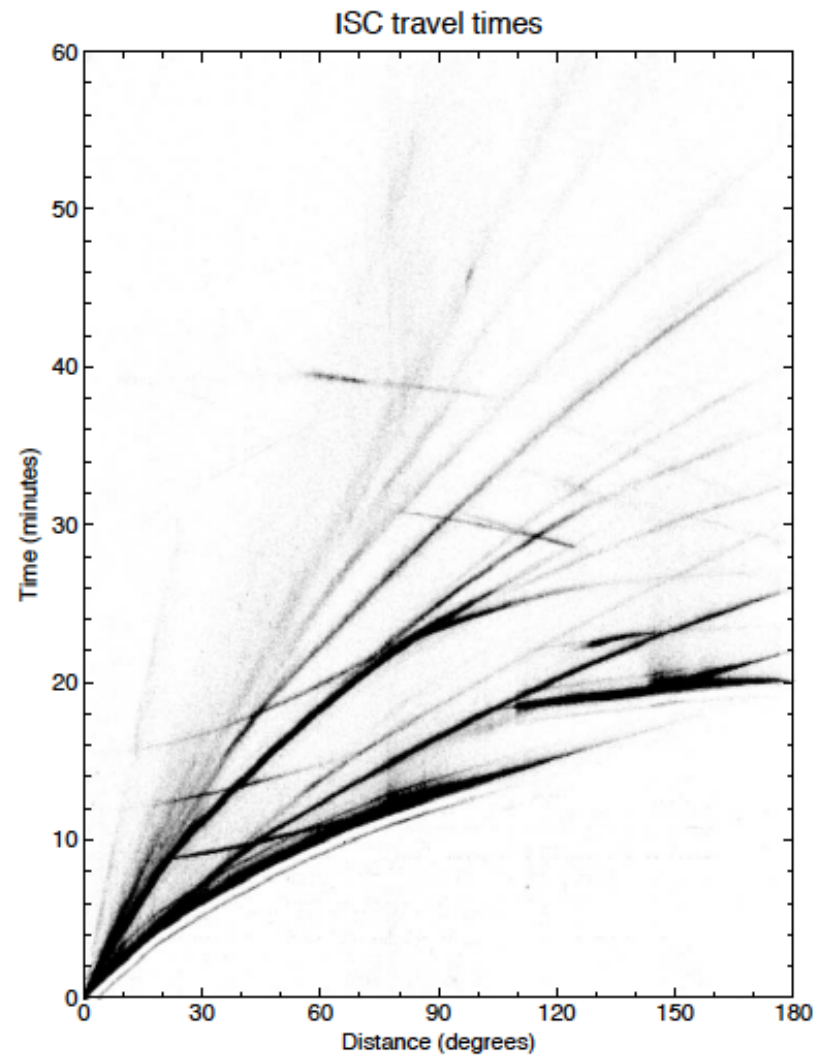
**S waves**

Earth's 1D (radial) structure

- A number of 1D Earth models have been developed: Jeffrey & Bullen (1941), PREM (Dziewonski and Anderson, 1981), ak135 (Kennett et al., 1995), IASP91 (Kennett and Engdahl, 1991).
- Seismically fast lithosphere
- Seismically slow asthenosphere (LVZ)
- Velocity jumps at 410 and 660 km define the transition zone from the upper and lower mantle
- CMB is at ~2891 km depth
- ICB is at ~5150 km depth

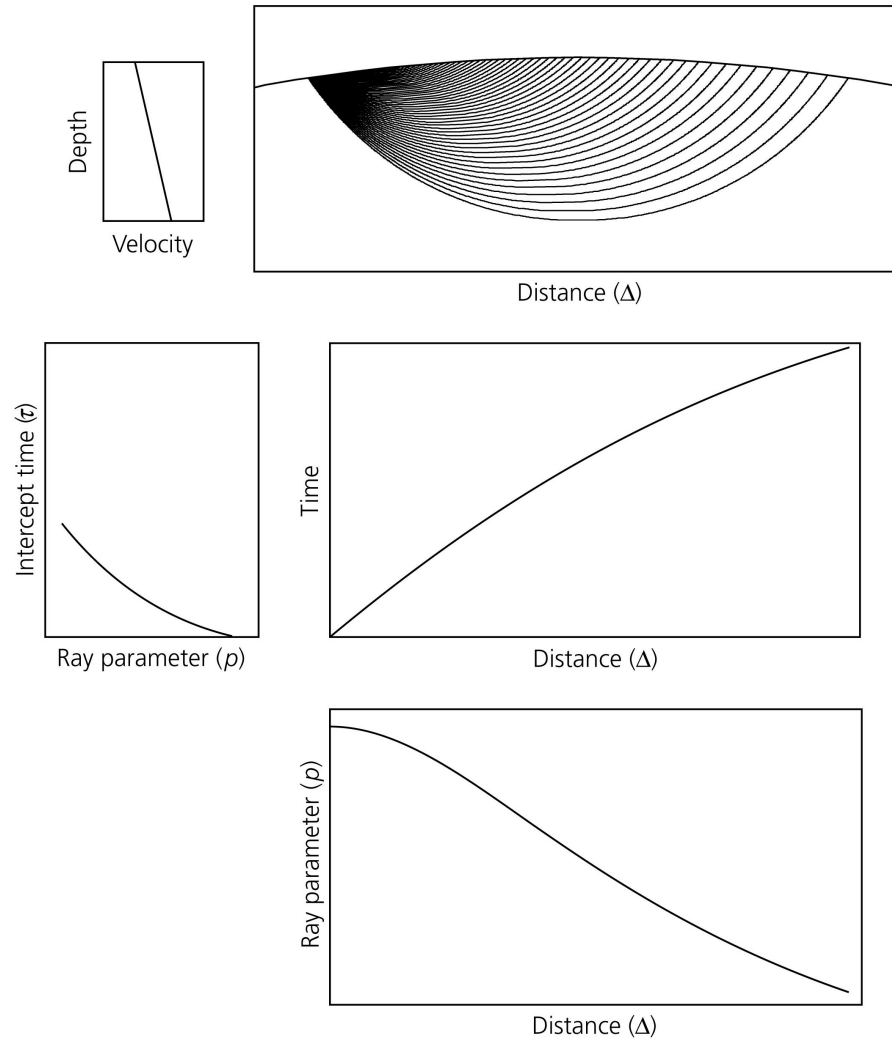


Body wave observations



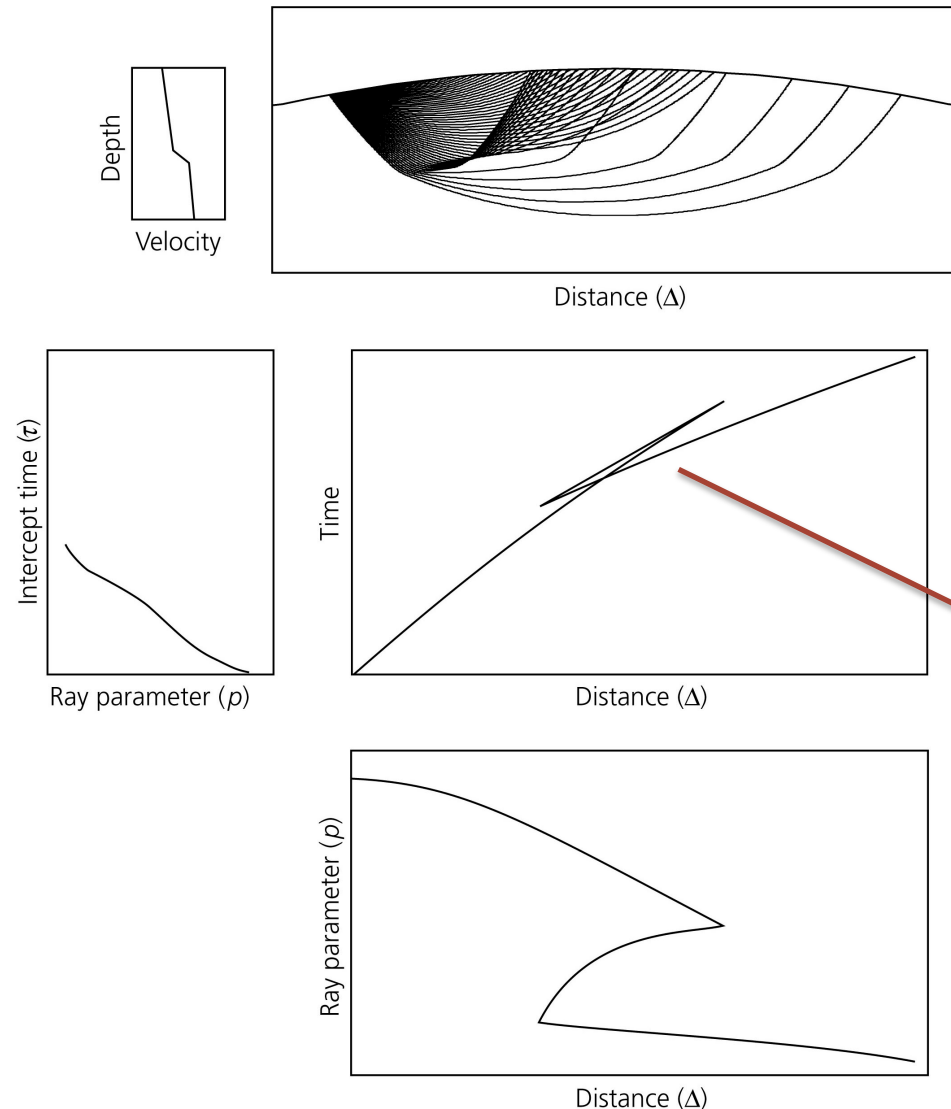
Body wave travel time studies

Figure 3.4-5: Ray path effects for increasing velocity.



Body wave travel time studies

Figure 3.4-6: Ray path triPLICATION effects for a velocity increase.

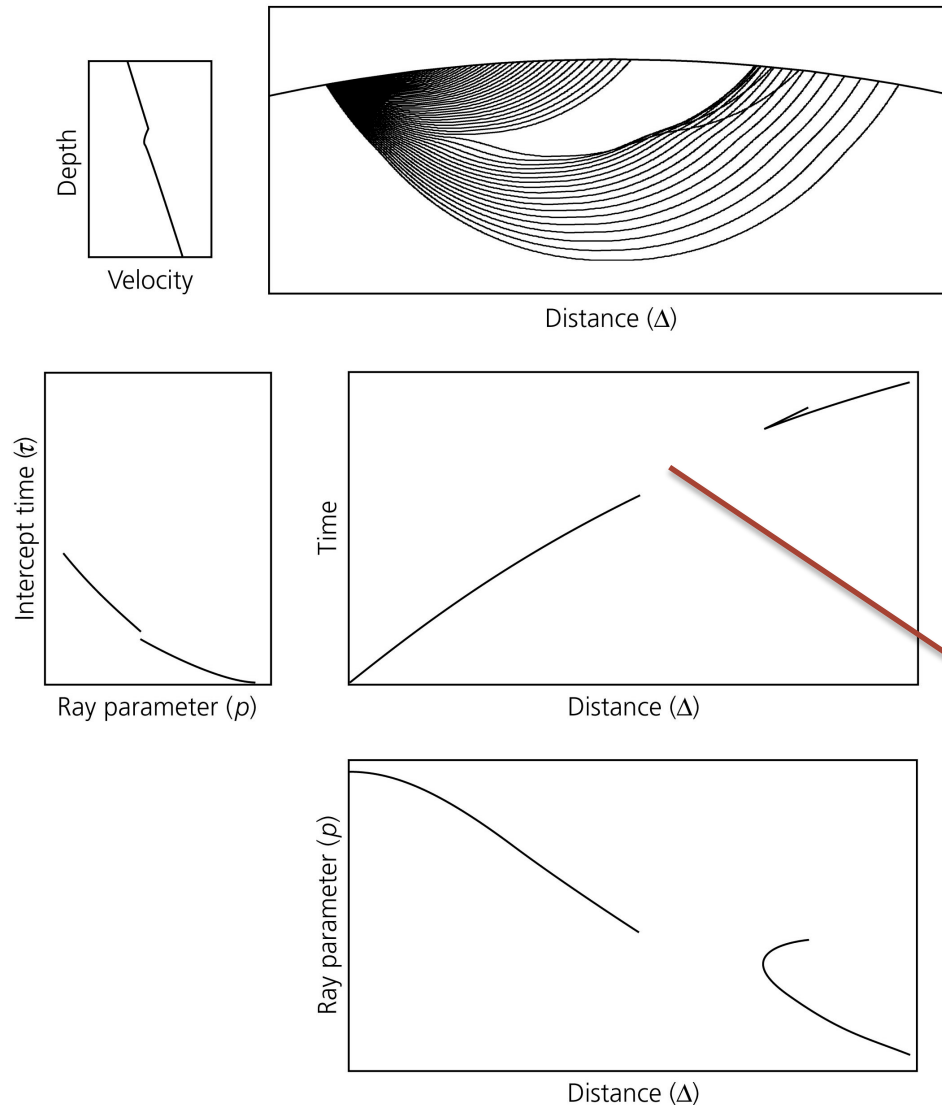


- Depth ranges in which velocity increases rapidly with depth can produce triplications: multiple rays (with different horizontal slownesses) arrive at the same time
- Transition zone (300-800 km depth) discontinuities produce triplications
- At epicentral distances $> 30^\circ$ rays bottom in the lower mantle and no triplications are (typically) observed

triplications

Body wave travel time studies

Figure 3.4-7: Ray path shadow-zone effects for a velocity decrease.



Rays cannot bottom in a depth range where velocity decreases with depth*

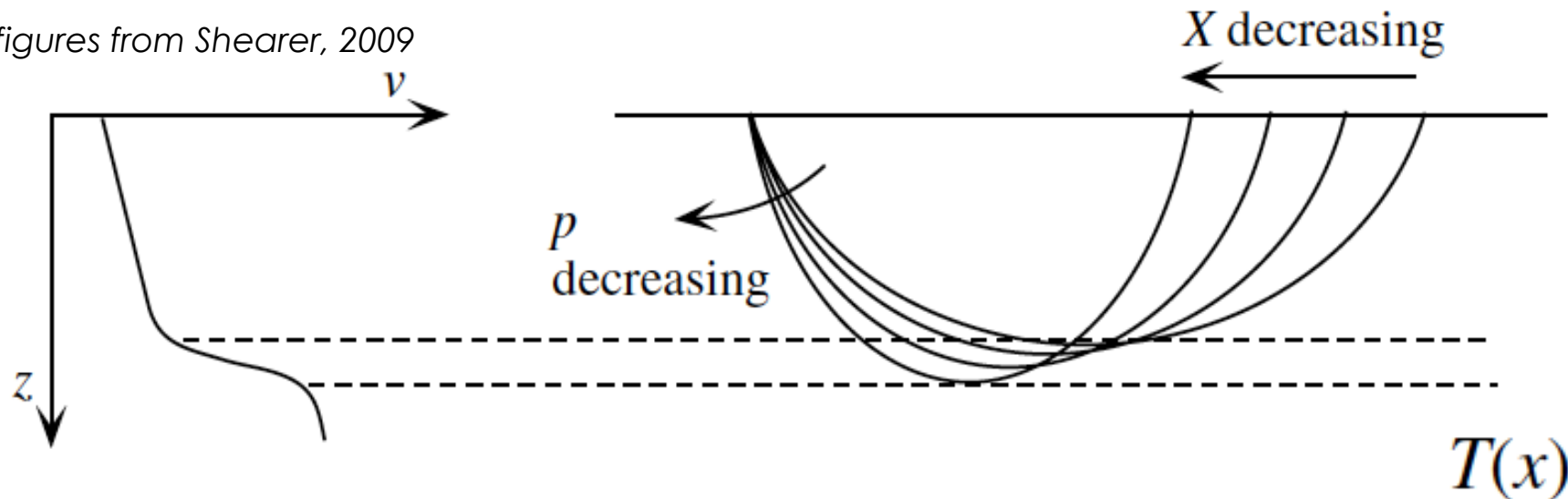
Low-velocity zones produce shadow zones

Prominent shadow zone in PKP waves due to low velocities in the outer core

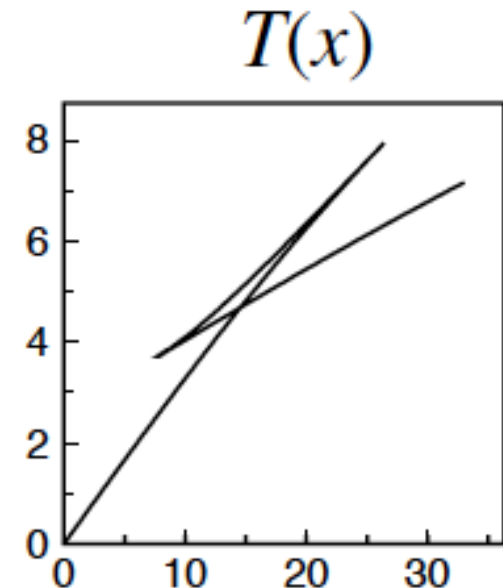
Shadow zone

Tripletations

figures from Shearer, 2009



- Depth ranges in which velocity increases rapidly with depth can produce triplications: multiple rays (with different horizontal slownesses) arrive at the same time
- Transition zone discontinuities produce triplications
- At epicentral distances $> 30^\circ$ rays bottom in the lower mantle and no triplications are (typically) observed

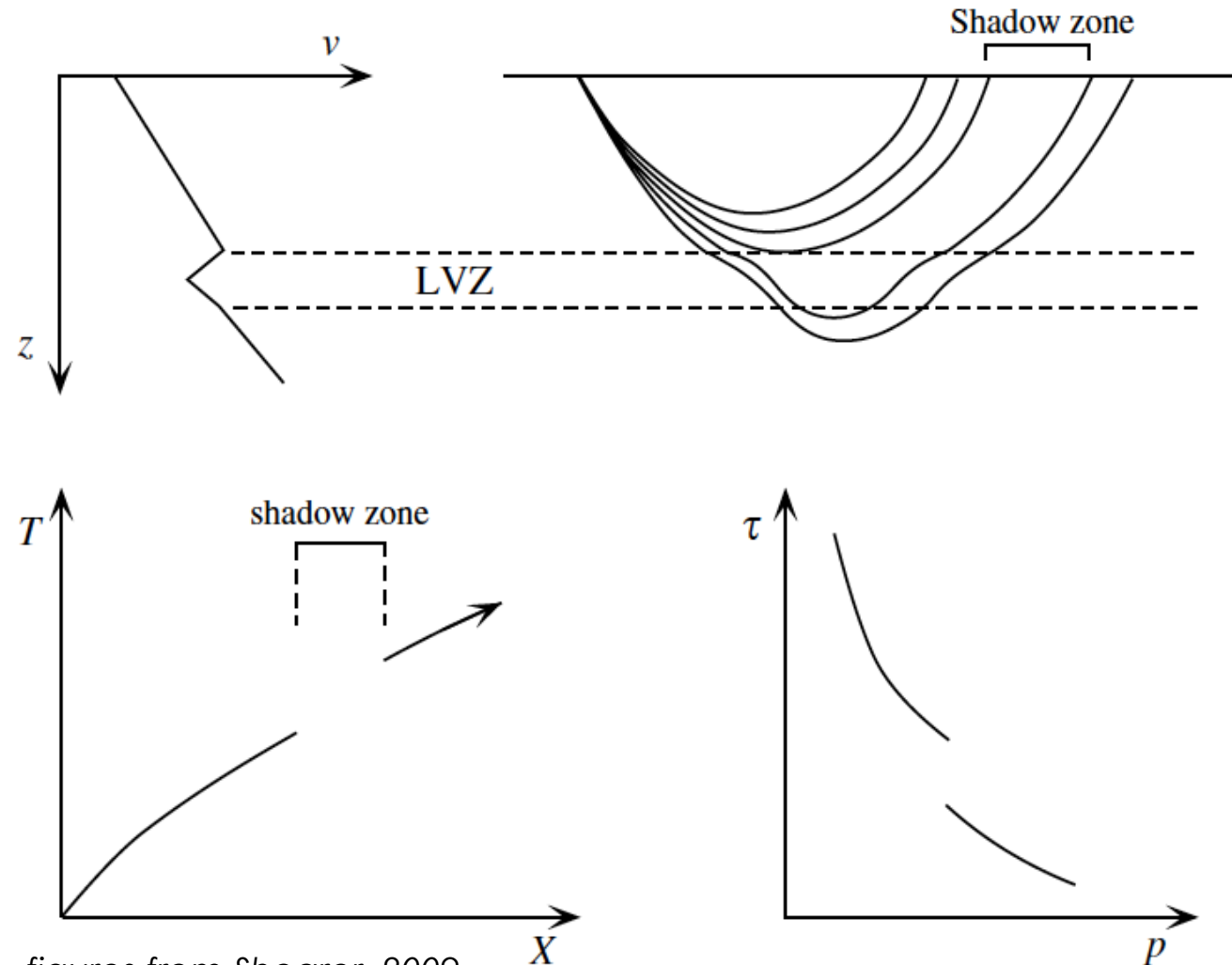


Shadow zones

Rays cannot bottom in a depth range where velocity decreases with depth*

Low-velocity zones produce shadow zones

Prominent shadow zone in PKP waves due to low velocities in the outer core



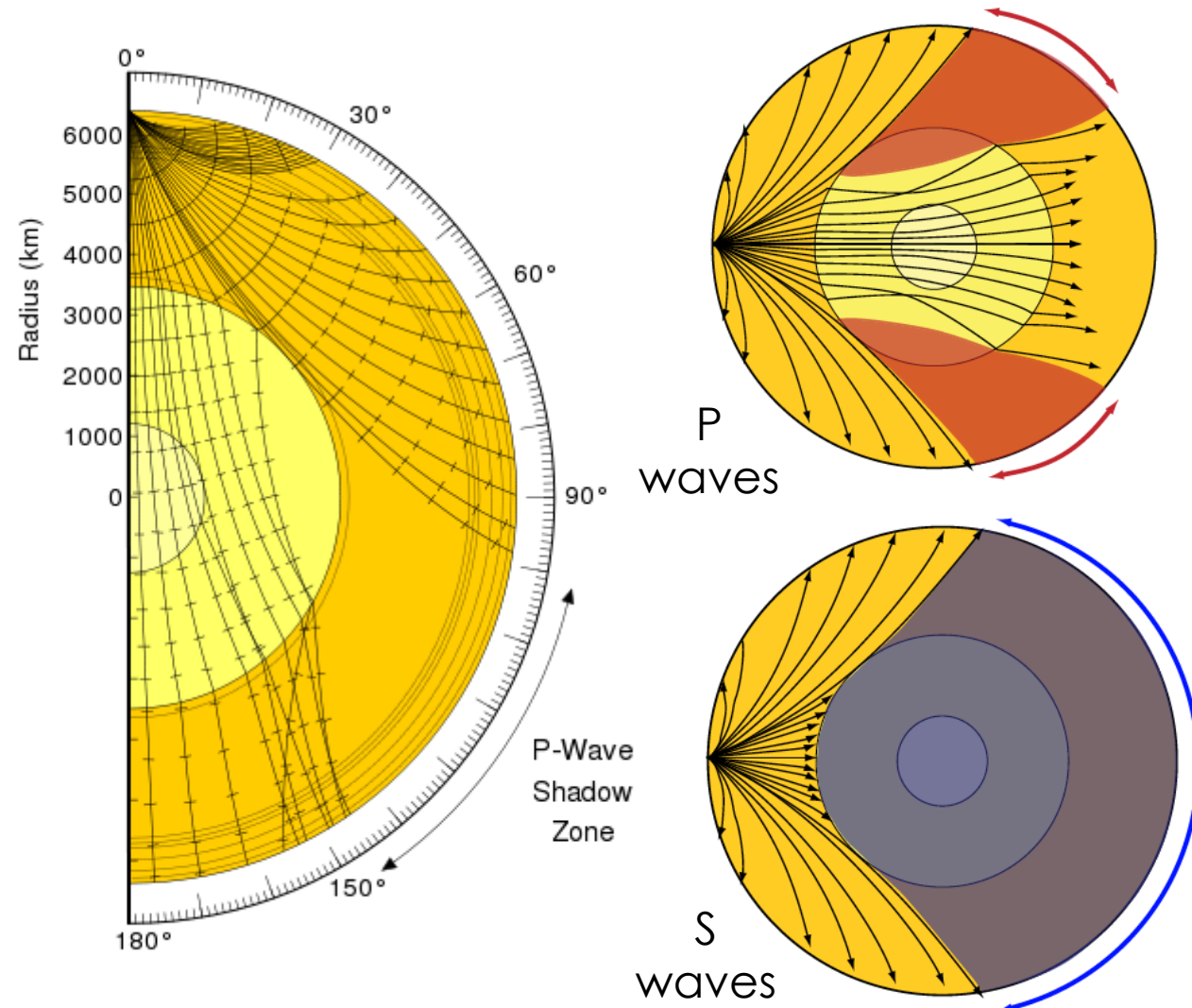
figures from Shearer, 2009

Shadow zones

Rays cannot bottom in a depth range where velocity decreases with depth*

Low-velocity zones produce shadow zones

Prominent shadow zones result from low velocities in the liquid outer core



Body wave travel time studies

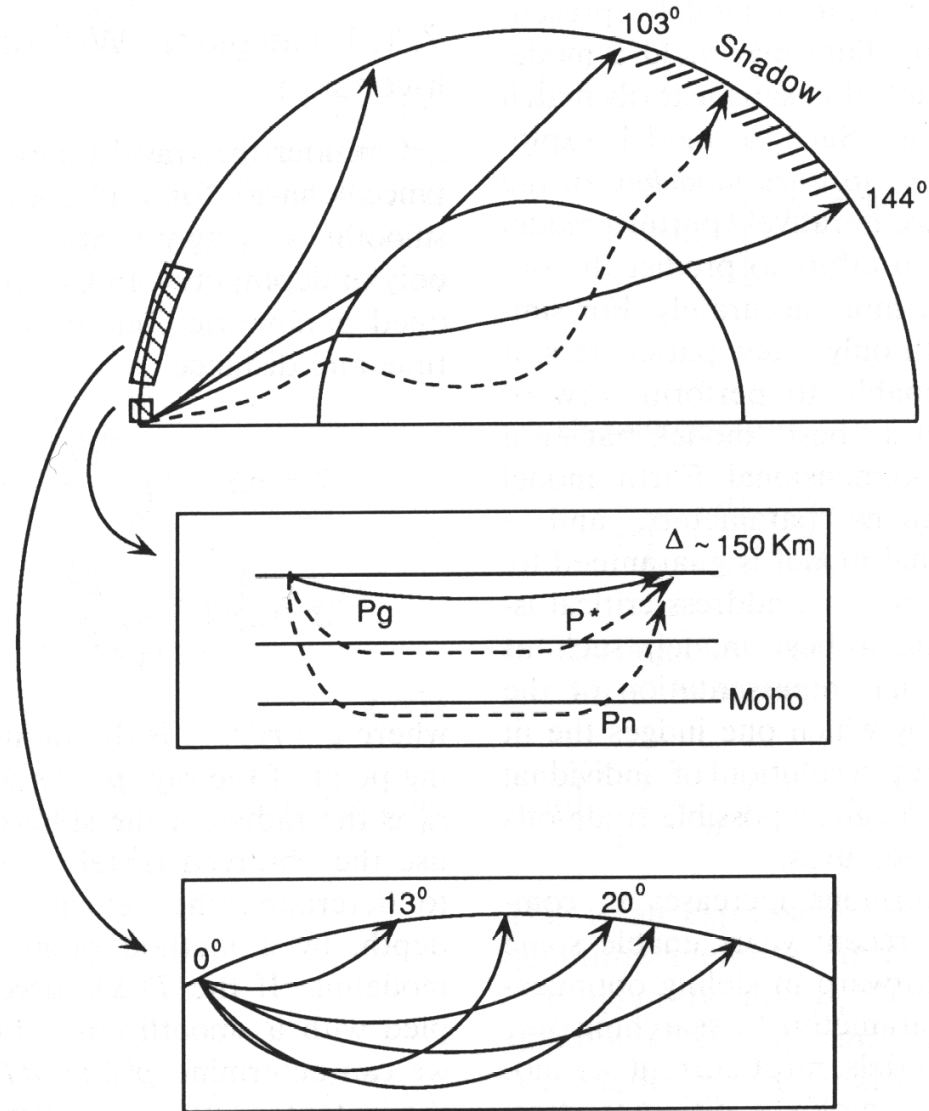
Epicentral Ranges

Three characteristic ranges used in seismic studies:

0°-13° near-field or regional range: crustal phases, spherical geometry can be neglected

13°-30° upper-mantle distance range. Dominated by upper mantle triplications.

30°-180° teleseismic range: waves that sample lower mantle, core, upper mantle reverberations.



Surface wave observations

Figure 2.7-1: Seismograms recorded at a distance of 110°, showing surface waves.

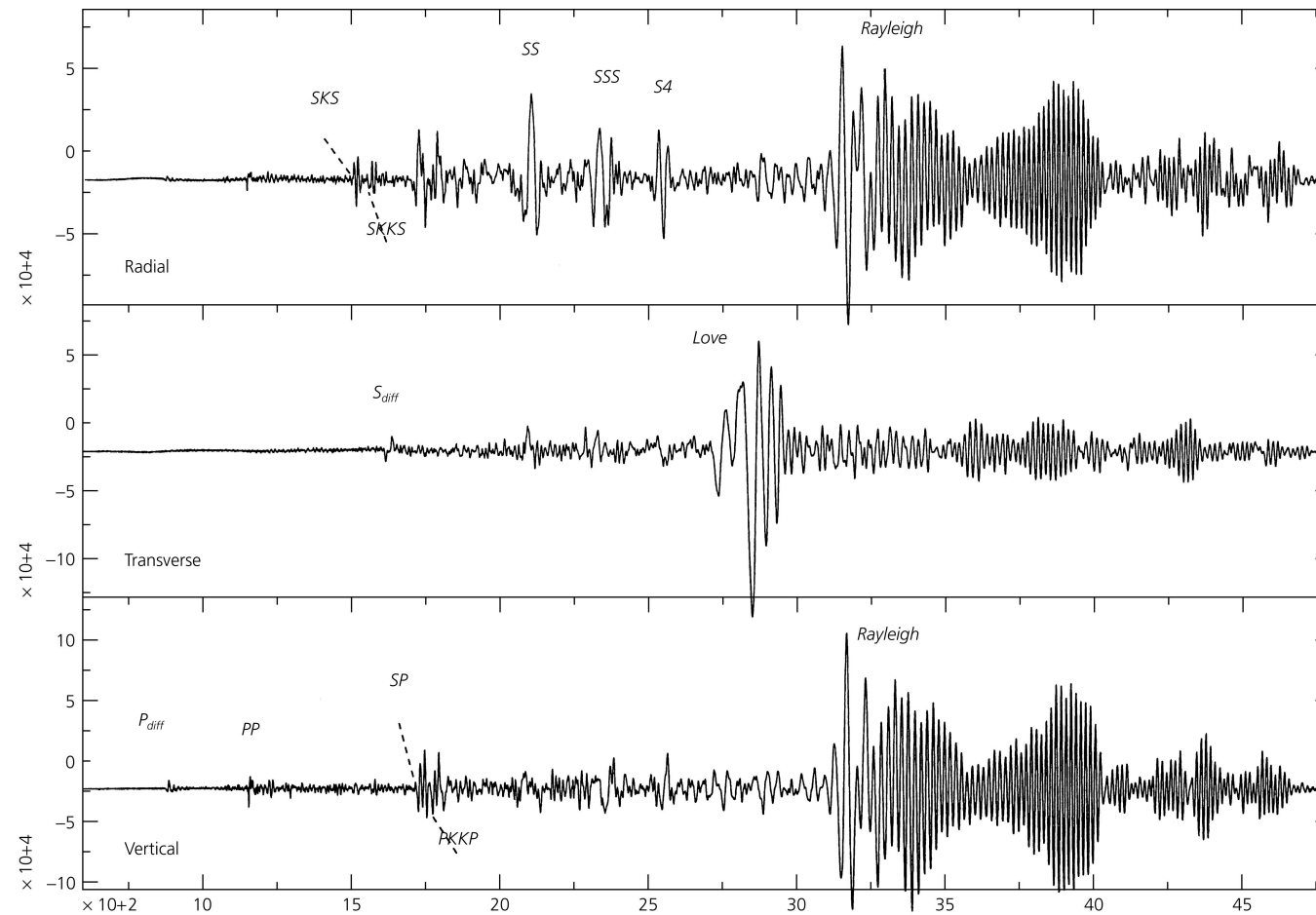


figure from Stein & Wysession, 2003

Relationship to body waves

Love waves

- Constructive interference between surface-bouncing SH waves

Rayleigh waves

- Constructive interference between post-critically reflected P and SV waves



figures from Shearer, 2009

Surface waves

- Surface waves dominate teleseismic records
- Rayleigh (P-SV) and Love (SH) waves

Figure 2.7-1: Seismograms recorded at a distance of 110°, showing surface waves.

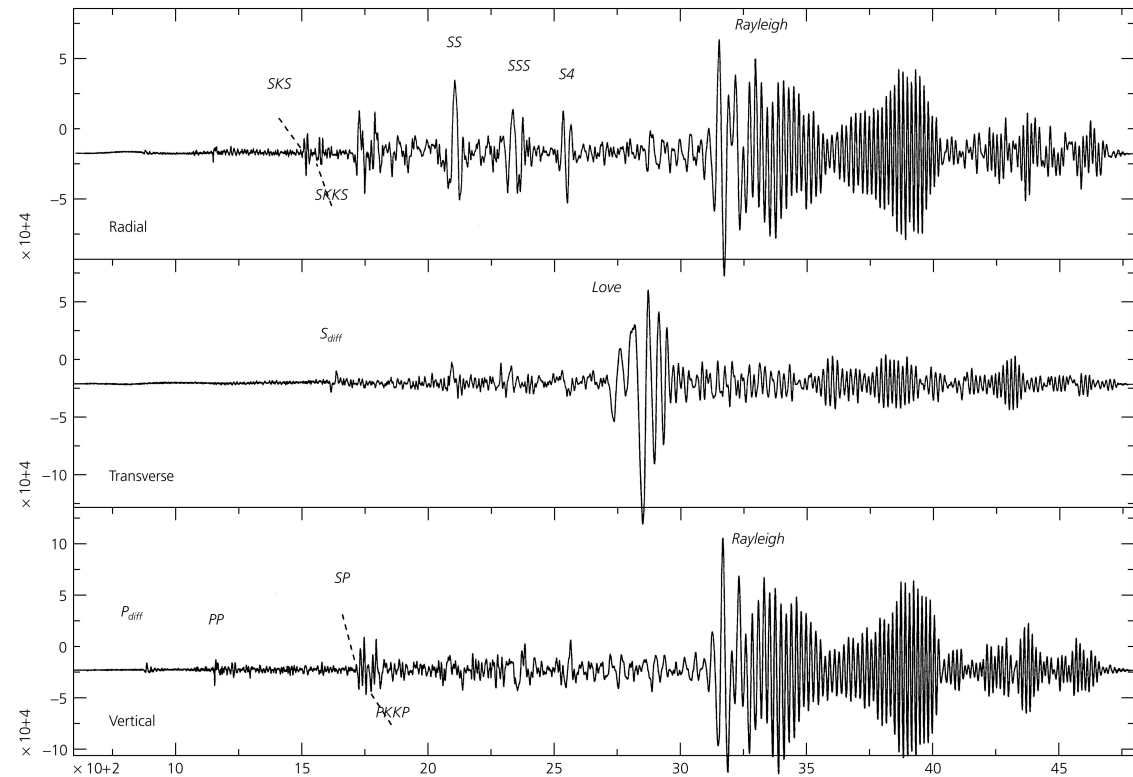
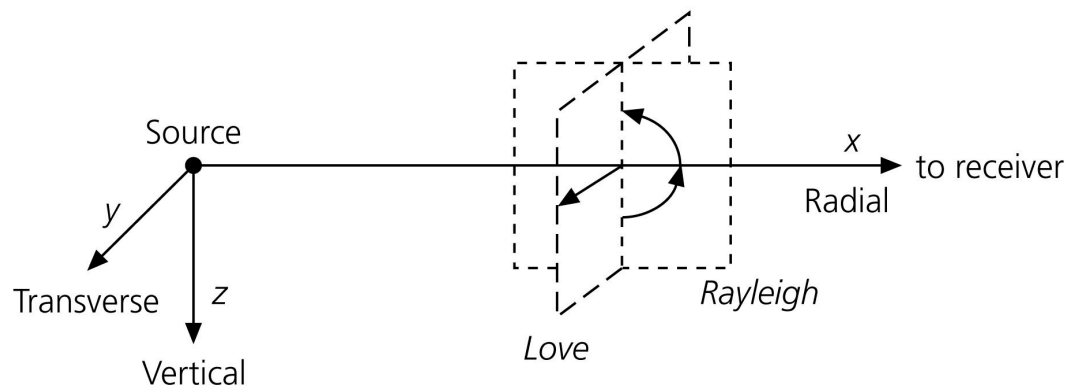


Figure 2.7-2: Geometry for Love and Rayleigh wave motions.



Surface waves

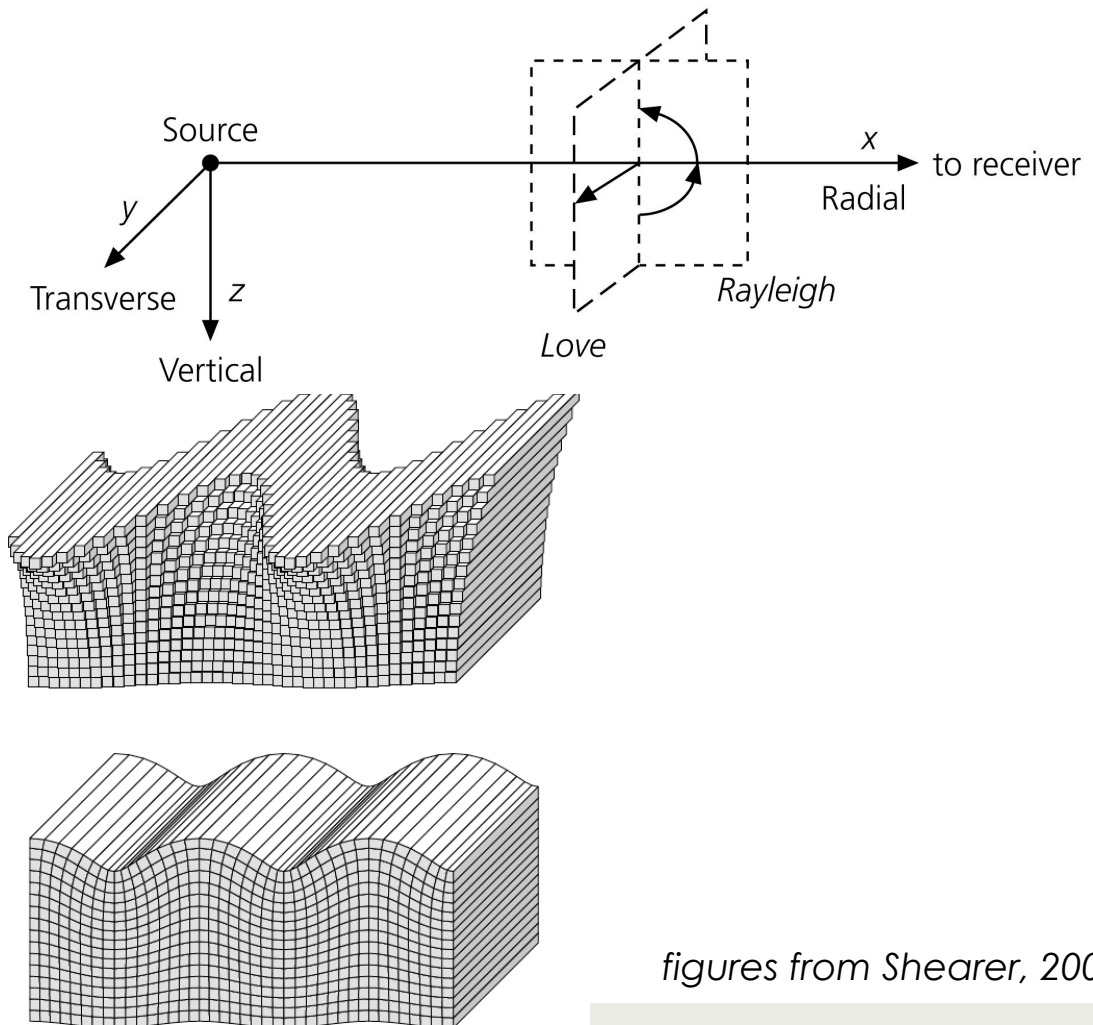
Love Waves

Particle motion is in the horizontal plane perpendicular to direction of propagation

Rayleigh Waves:

Particle motion is confined to the vertical plane joining source-receiver.

Figure 2.7-2: Geometry for Love and Rayleigh wave motions.



figures from Shearer, 2009

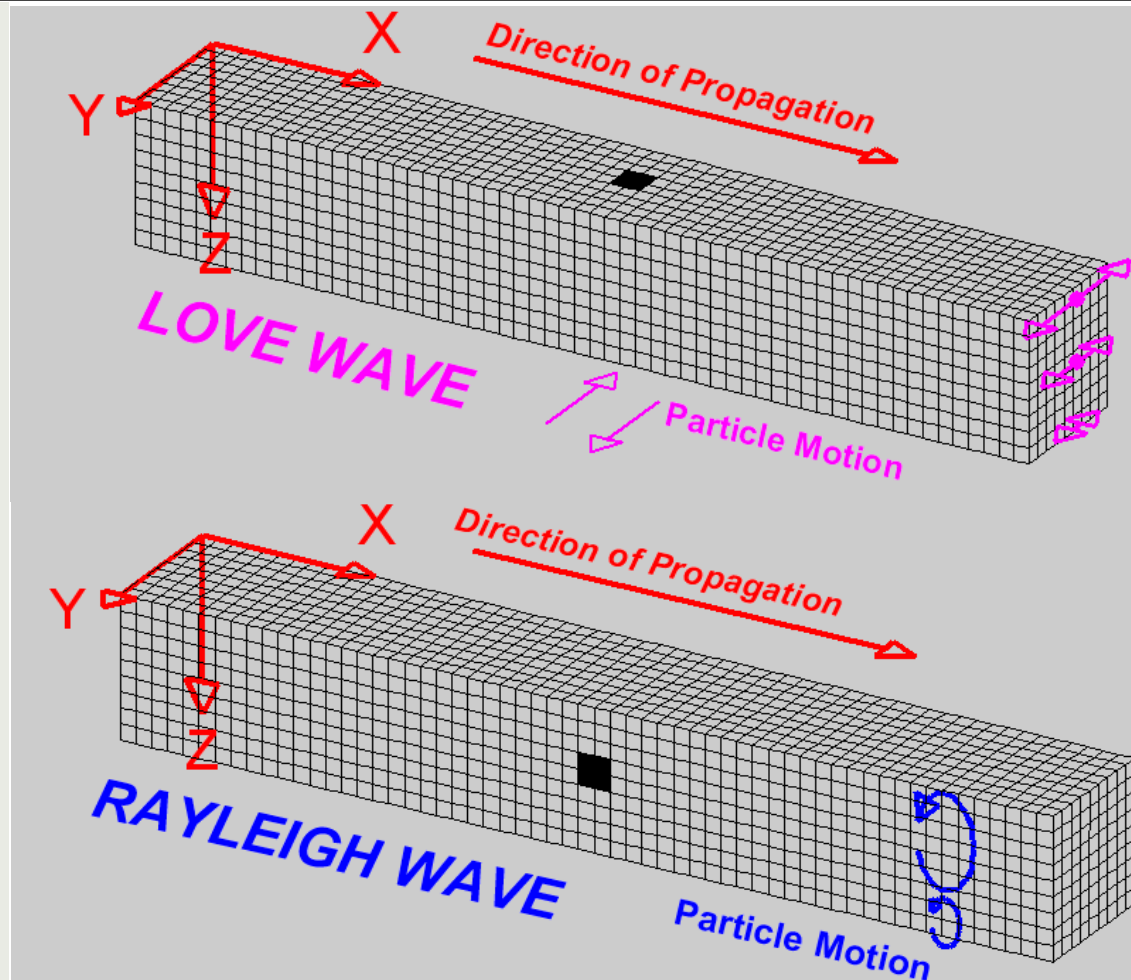
Surface waves

Love Waves

Particle motion is in the horizontal plane perpendicular to direction of propagation

Rayleigh Waves:

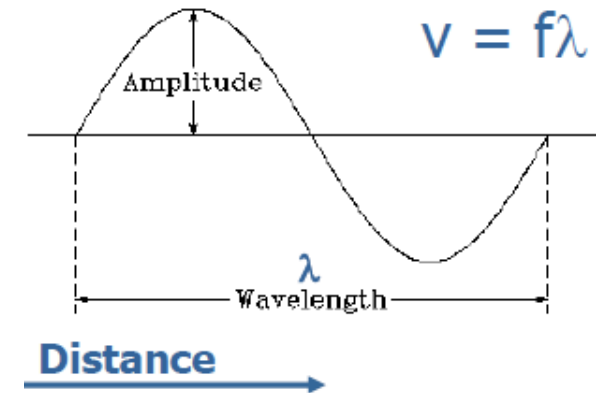
Particle motion is confined to the vertical plane joining source-receiver.



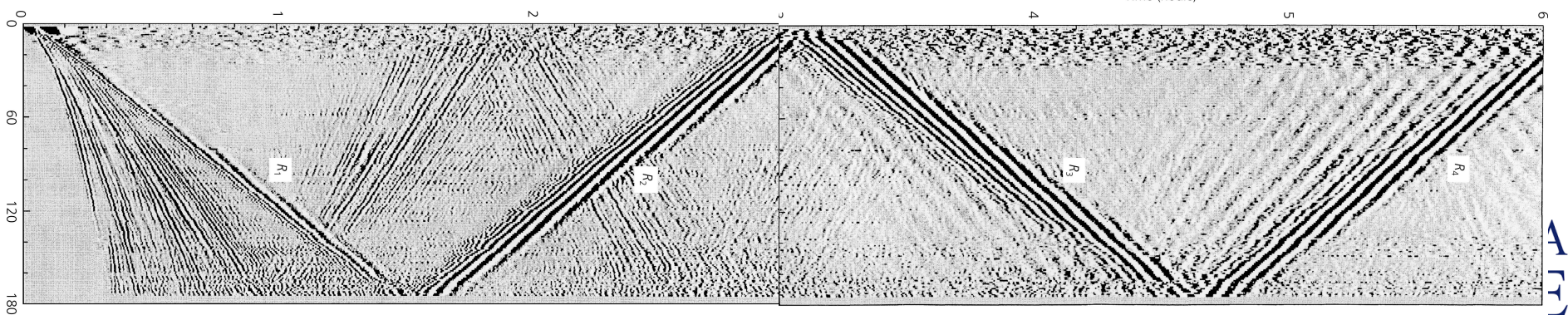
<http://www.geo.mtu.edu/UPSeis/images/>

Surface waves - DISPERSION

- ✓ **Dispersion:** When the velocity of a single-frequency wave, called **phase velocity**, varies with frequency
- ✓ The combination of waves at different frequencies gives the total wave.
- ✓ The result of this interference gives the envelope (or wavecrest) which moves with a different velocity, called **group velocity**



In other words: group velocity is the velocity of the wave-packet.



Surface waves

- Surface waves dominate teleseismic records
- Rayleigh (P-SV) and Love (SH) waves
- Because they are less attenuated than body waves, they can circle the globe few times

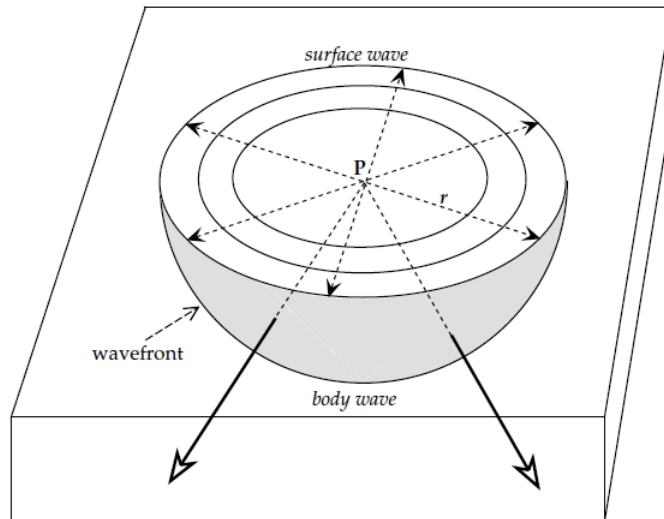
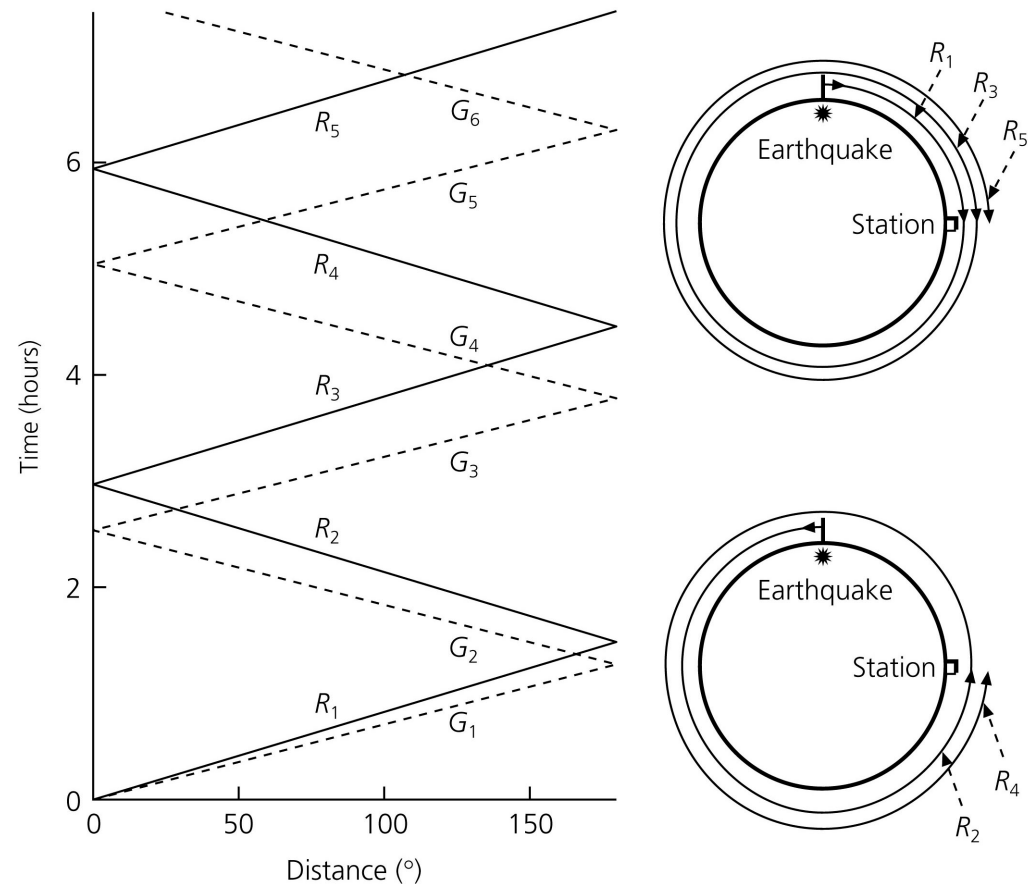
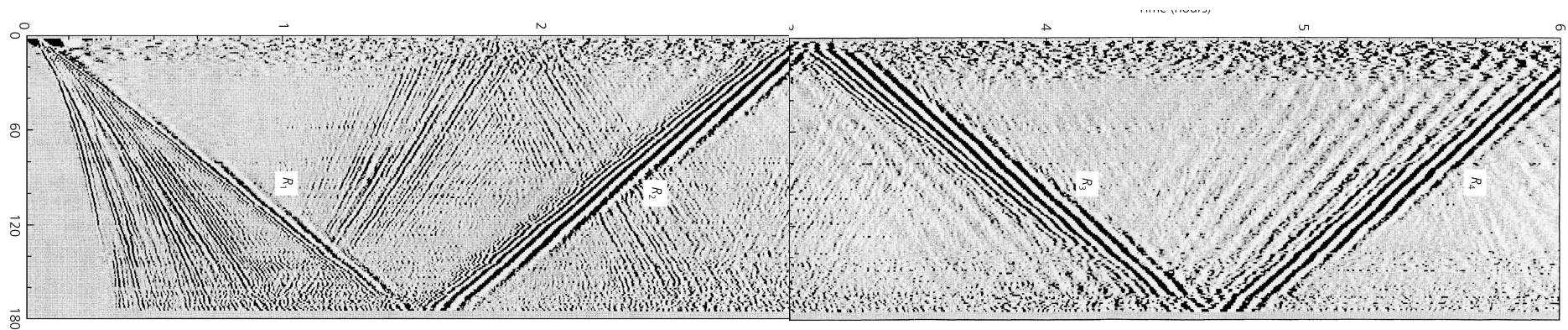


Fig. 3.9 Propagation of a seismic disturbance from a point source P near the surface of a homogeneous medium; the disturbance travels as a body wave through the medium and as a surface wave along the free surface.

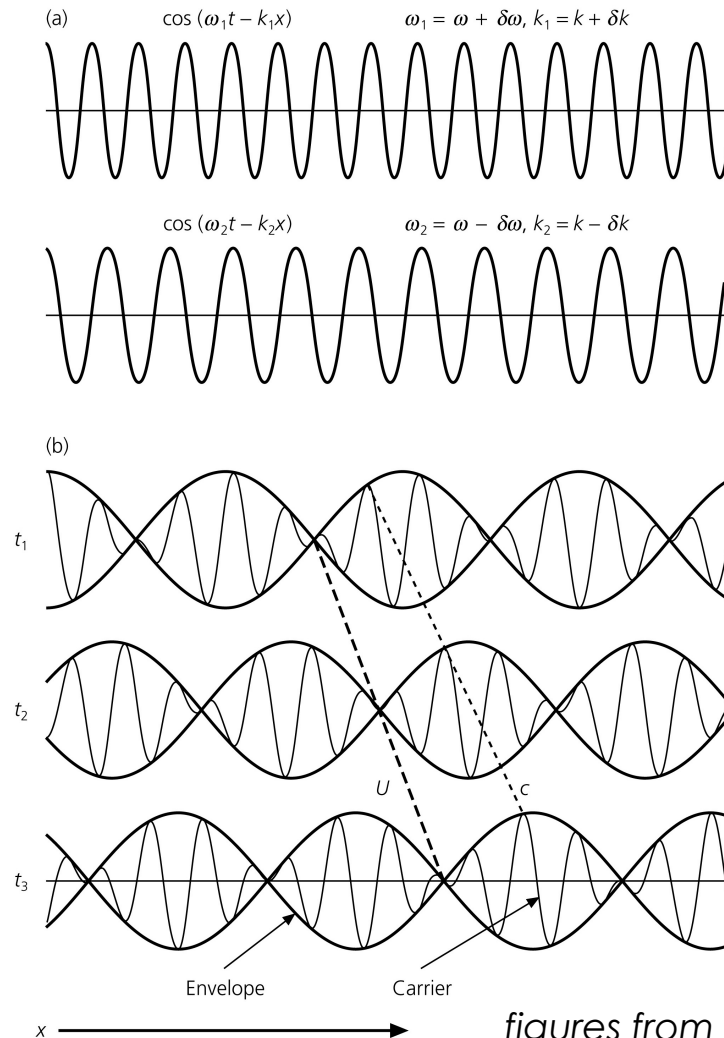
Figure 2.7-4: Six-hour stacked IDA record section.



- Surface waves are **dispersive**: waves at different period travel at different velocity => wave-train becomes broader with time



Phase vs Group velocity

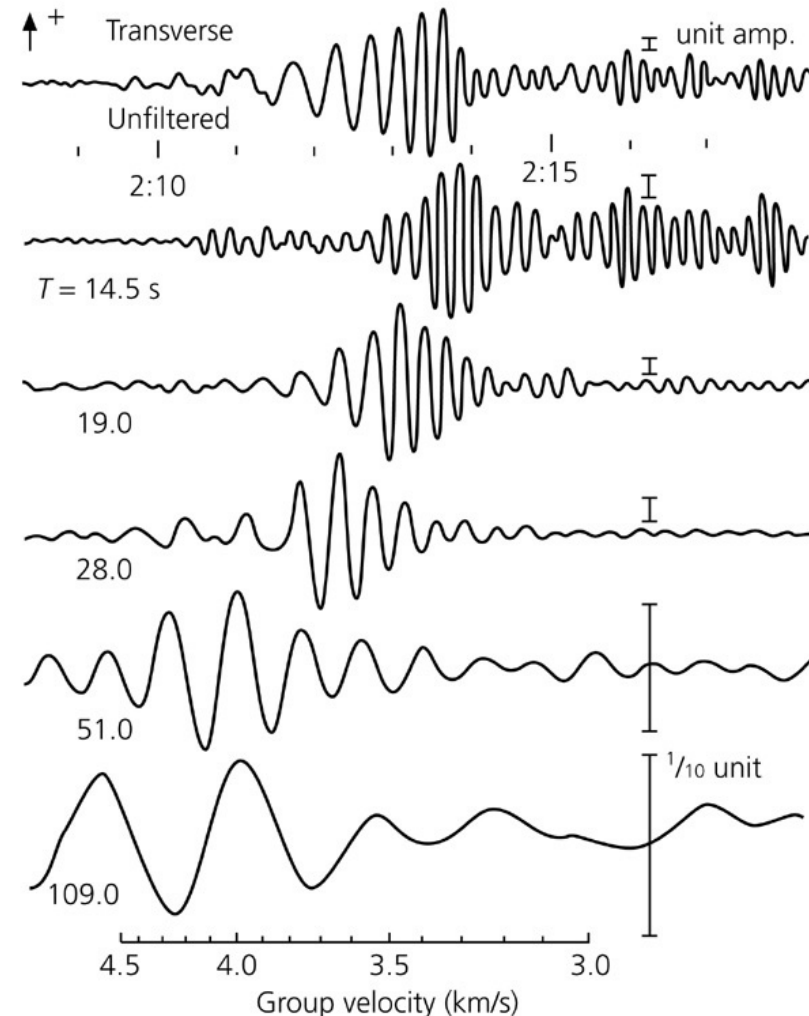


figures from Shearer, 2009

- When different frequencies propagate at different (phase) velocities, packets of seismic energy travel at a different velocity (group)
- Phase velocity: $c = \omega / k$
- Group velocity: $U = d\omega / dk$
- Group velocity is always slower than phase velocity
- At high frequencies, it is easier to measure group velocities since measuring phase velocities has the potential for cycle skipping

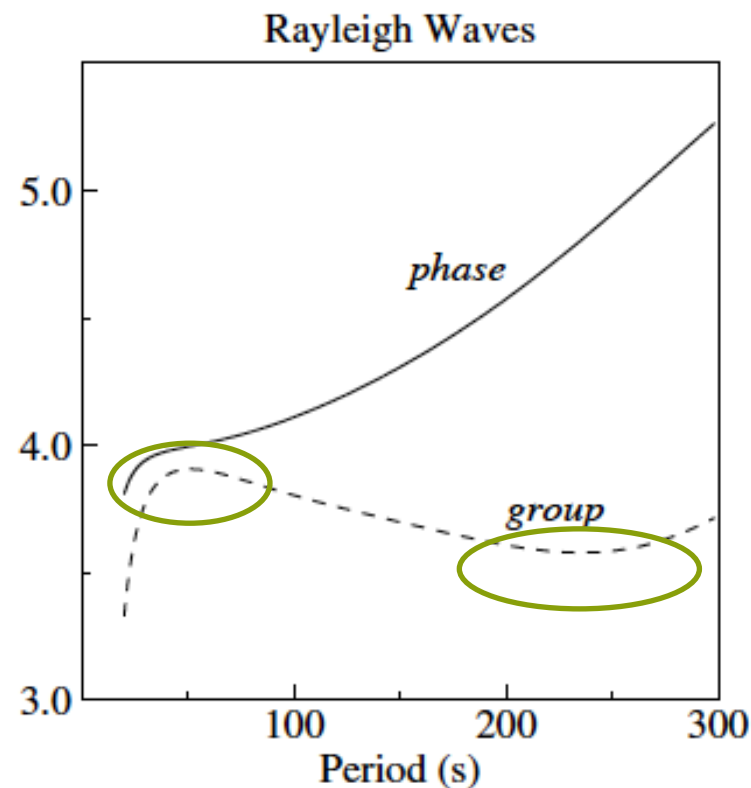
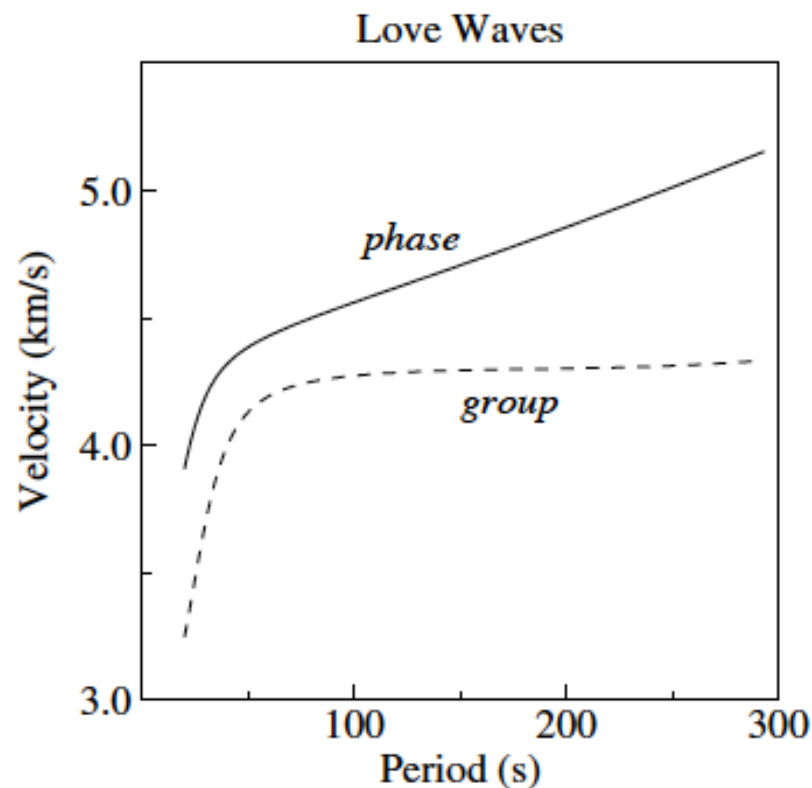
Measuring dispersion

- By filtering a seismogram to include waves of different frequencies, we can measure the phase and group velocities as a function of frequency
- Longer period waves “feel” deeper in the earth than shorter period waves
- Longer period surface waves travel faster → velocity increases with depth



figures from Shearer, 2009

Love & Rayleigh Dispersion



At periods where group velocity attains a maximum or minimum, large amplitude surface waves are seen → “Airy” phases

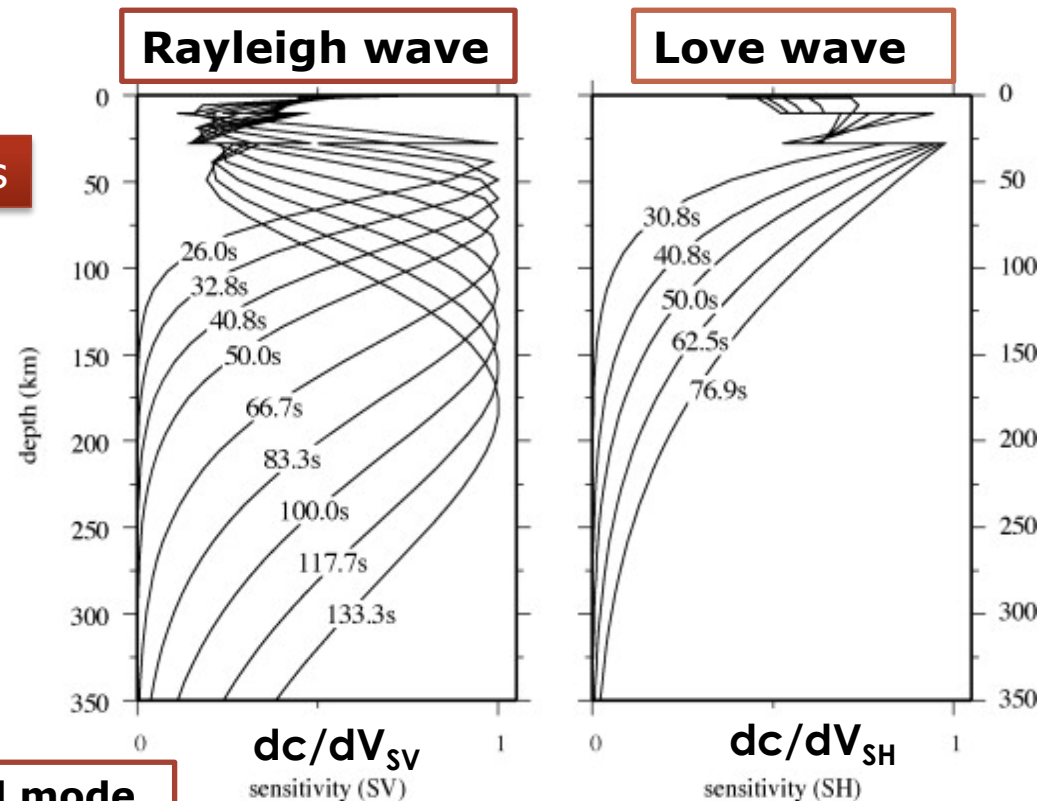
Figure 8.6 Fundamental Love and Rayleigh dispersion curves computed from the isotropic PREM model (courtesy of Gabi Laske).

figures from Shearer, 2009

Surface-wave dispersion studies

- Measuring group and/or phase velocity (how they change with period) gives information about Earth's structure
- The longer the period, the deeper (and broader) is the sensitivity
- Since seismic velocities increase with depth, generally, long period travel faster

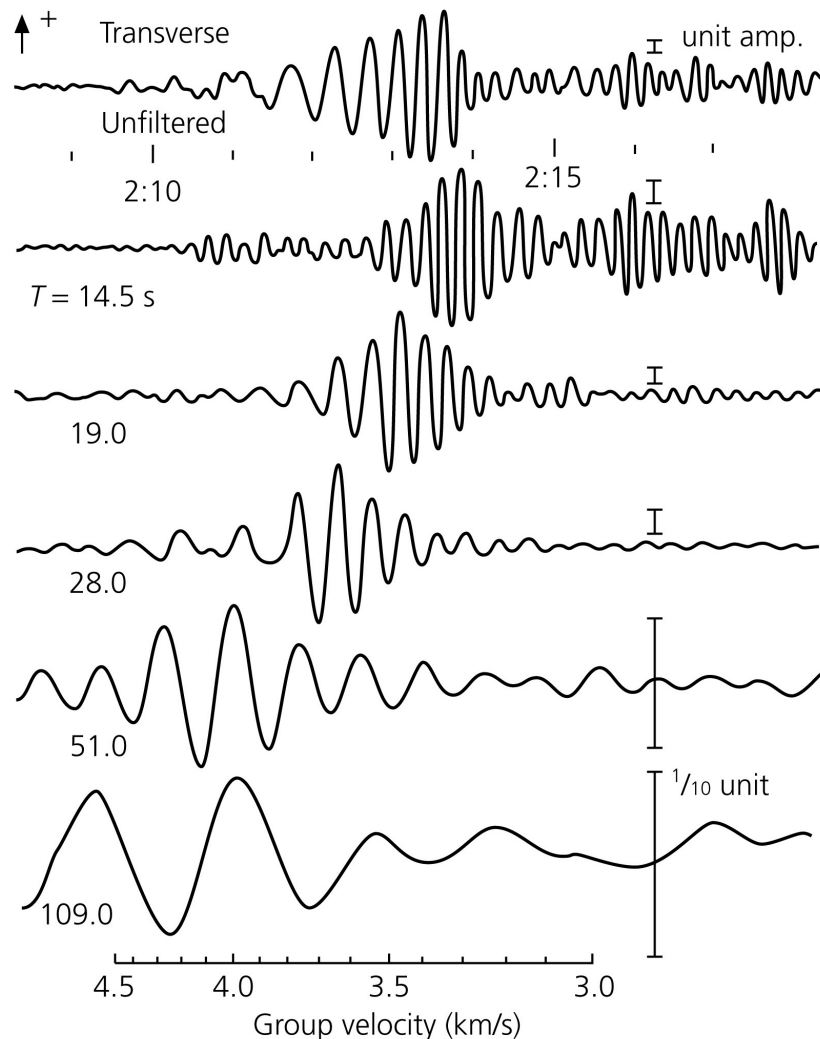
Sensitivity kernels



Fundamental mode

Surface-wave dispersion studies

Figure 2.8-4: Example of Love wave group velocity dispersion through bandpass filtering.



Pick arrival time of group at different periods and compute vel (distance/time)

⇒ build group vel/period plots, compare with a model

⇒ find a model that fit the observations

We use Fourier transform to filter the seismograms at different periods

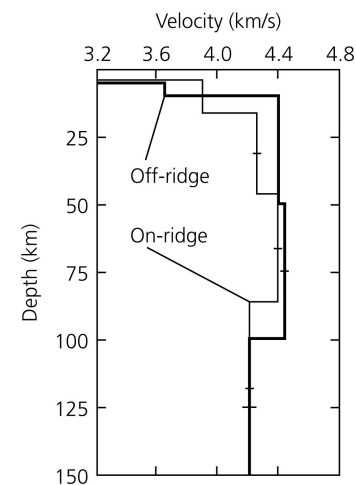
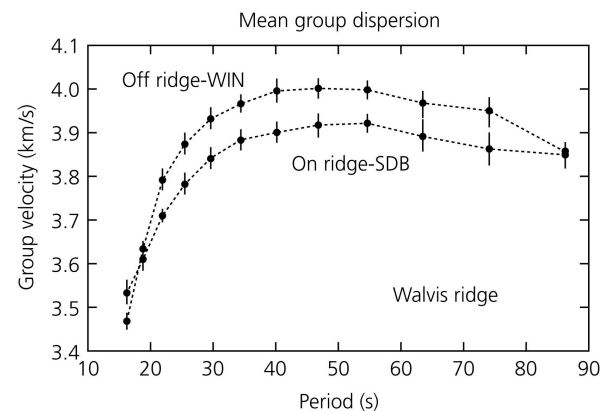
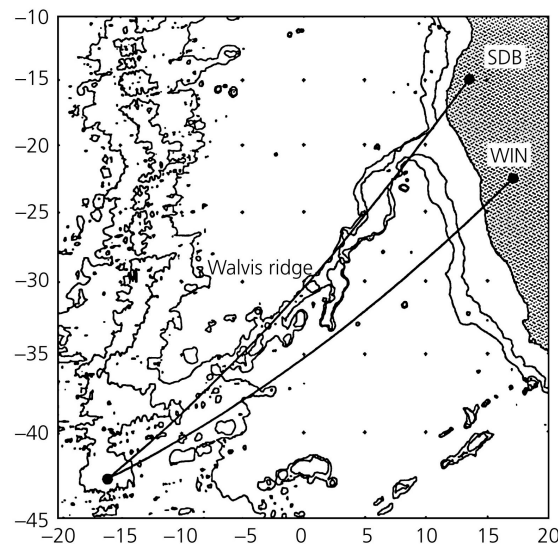
Surface-wave dispersion studies

Comparison of dispersion curves between two corridors indicates the variations in (shallow) structure

Group Velocities

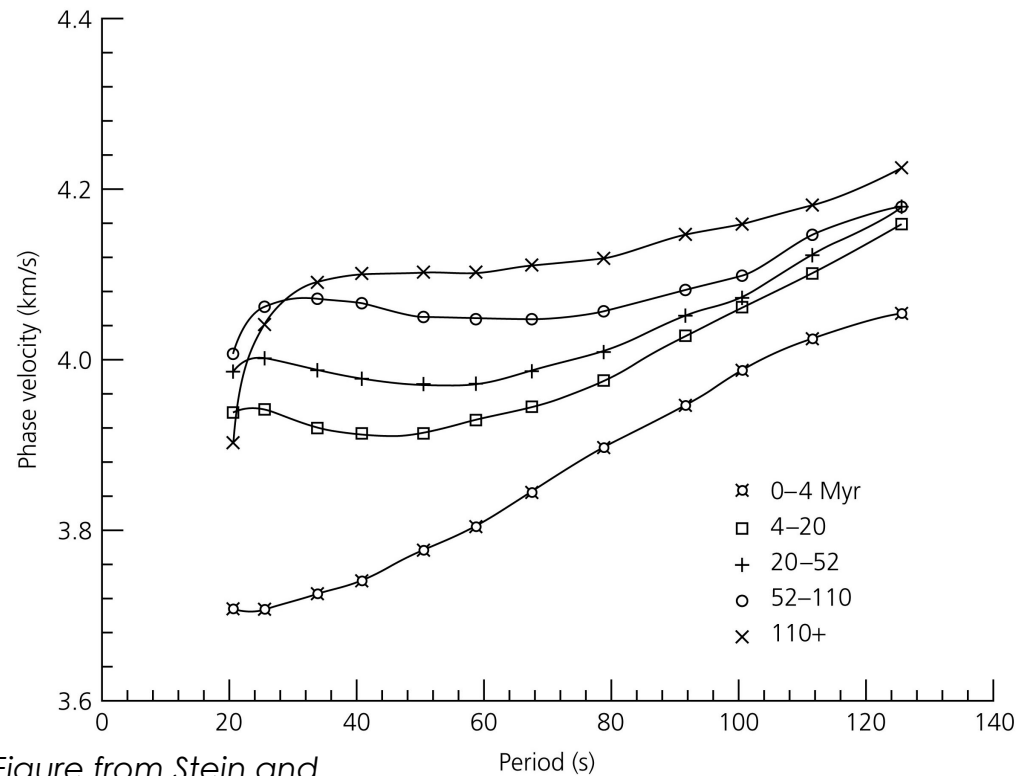
Example: off-ridge path faster for $P > 20$ s \Rightarrow higher velocity upper mantle material to a depth of ~ 45 km

Figure 2.8-5: Rayleigh wave group velocity study of the Walvis ridge.

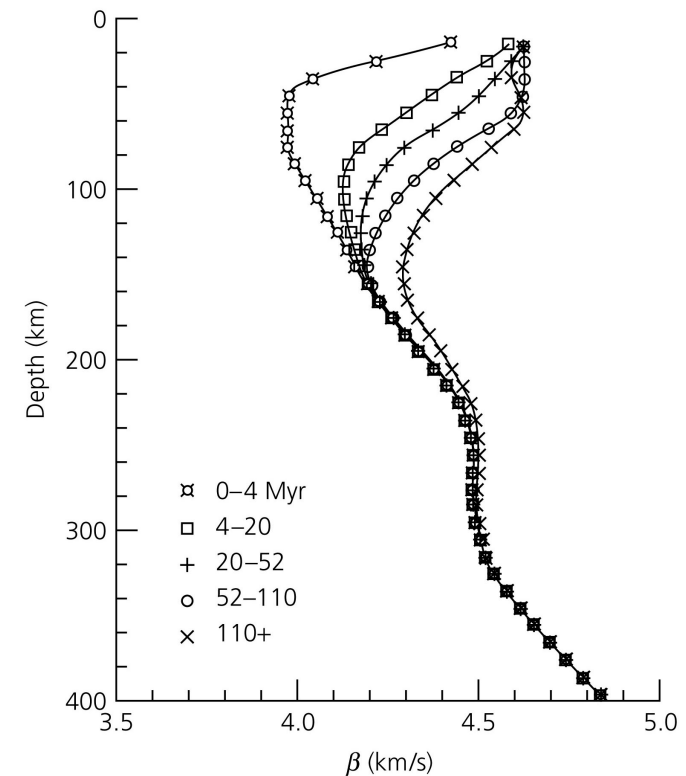


Signature of plate cooling

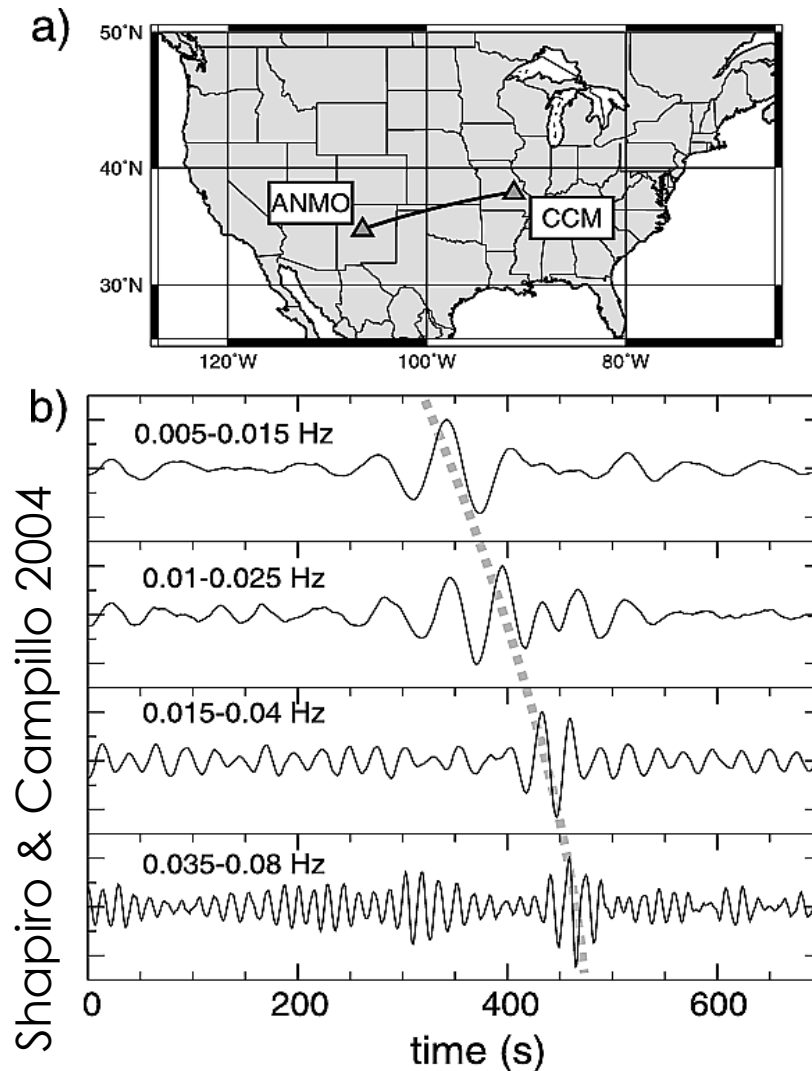
Phase velocity measurements of Rayleigh waves allowed seismologists to infer how velocities increase with plate age (colder temperatures → faster velocities)



(Figure from Stein and Wysession, 2003)



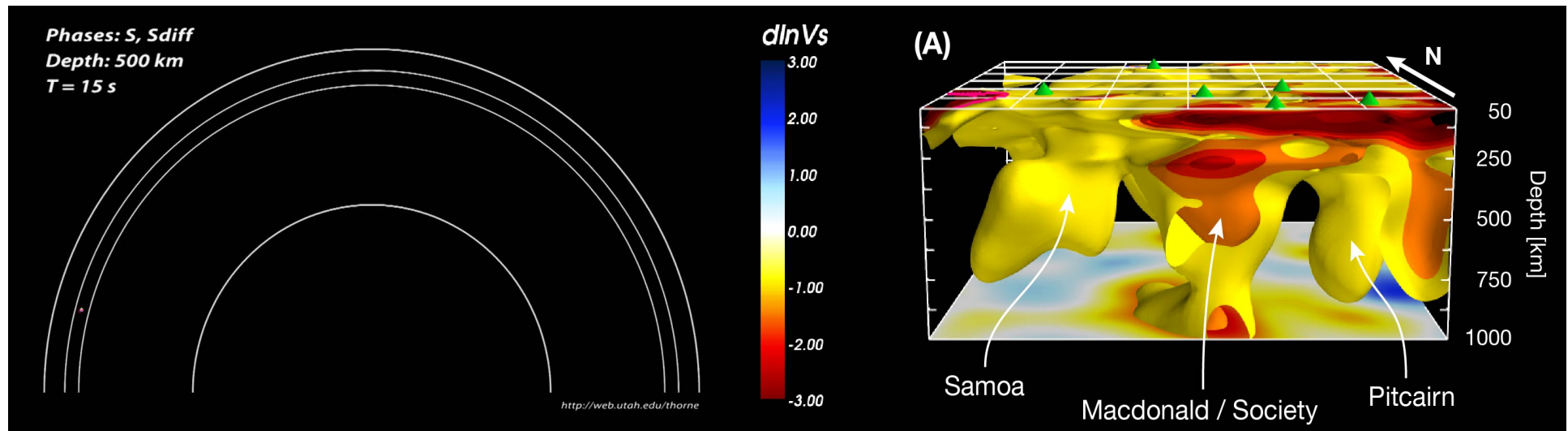
Exploiting ambient noise



- Impact of ocean waves on the shores (primary microseism) and pressure variations on the ocean floor due to ocean waves (secondary microseism) create Rayleigh waves that propagate around the Earth in all directions
- By computing cross-correlations of noise at pairs of seismometers we can extract and measure Rayleigh wave dispersion
- These measurements can be used to image the Earth's interior (ambient noise tomography)

Lateral variations in structure

- We can infer 3D velocity distribution using:
 - Absolute and differential travel-times measured across many different paths
 - Similarly, phase / group velocity measurements at different frequencies and on different paths
 - Directly analyzing full waveforms recorded on different paths



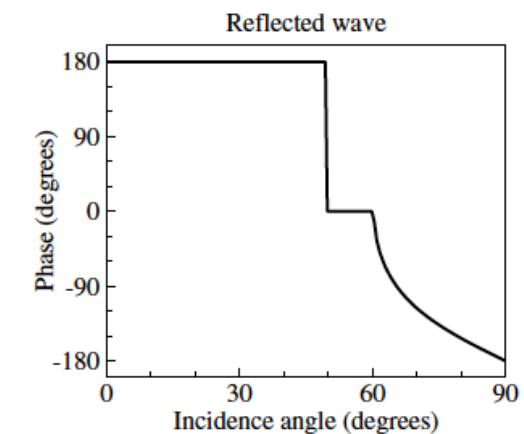
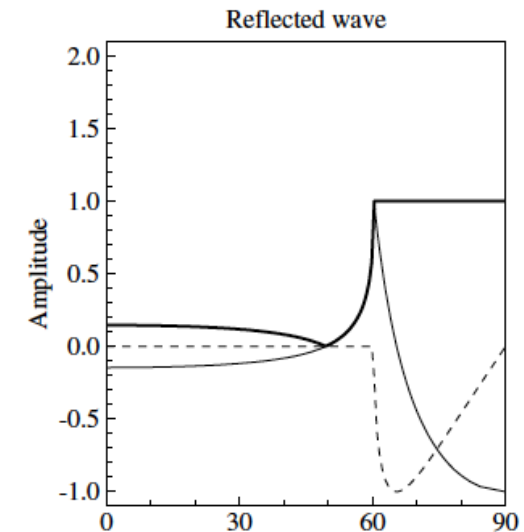
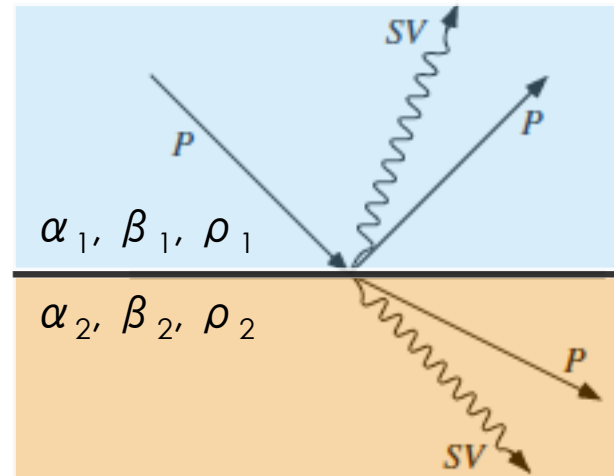
French et al. 2013

Amplitudes - Relative

- So far, we have just discussed travel times of waves through the Earth (only depend on velocity)
- What factors cause amplitudes to change as waves propagate?
 - Reflection / transmission coefficients
 - Geometric spreading
 - Scattering / redistribution of seismic energy
 - Focusing / defocusing by structure
 - Intrinsic attenuation

Reflection/transmission coefficients

- Impose continuity of displacements and tractions across solid-solid interface
- R/T coefficients depend on **impedance**: the product of velocity with density



figures from Shearer, 2009

$$\frac{\dot{S}}{S} \equiv \frac{\dot{A}_1}{A_1} = \frac{\rho_1 \beta_1 \cos \theta_1 - \rho_2 \beta_2 \cos \theta_2}{\rho_1 \beta_1 \cos \theta_1 + \rho_2 \beta_2 \cos \theta_2}$$

$$\frac{\dot{S}}{S} \equiv \frac{\dot{A}_2}{A_2} = \frac{2 \rho_1 \beta_1 \cos \theta_1}{\rho_1 \beta_1 \cos \theta_1 + \rho_2 \beta_2 \cos \theta_2}$$

SS and PP precursors (reflection)

- SS (or PP) precursors are waves reflected from a discontinuity in the subsurface and observed before the arrival of the surface-reflected wave
- Their amplitude (as a function of epicentral distance) can constrain both V_p , V_s and density jumps across mantle discontinuities!

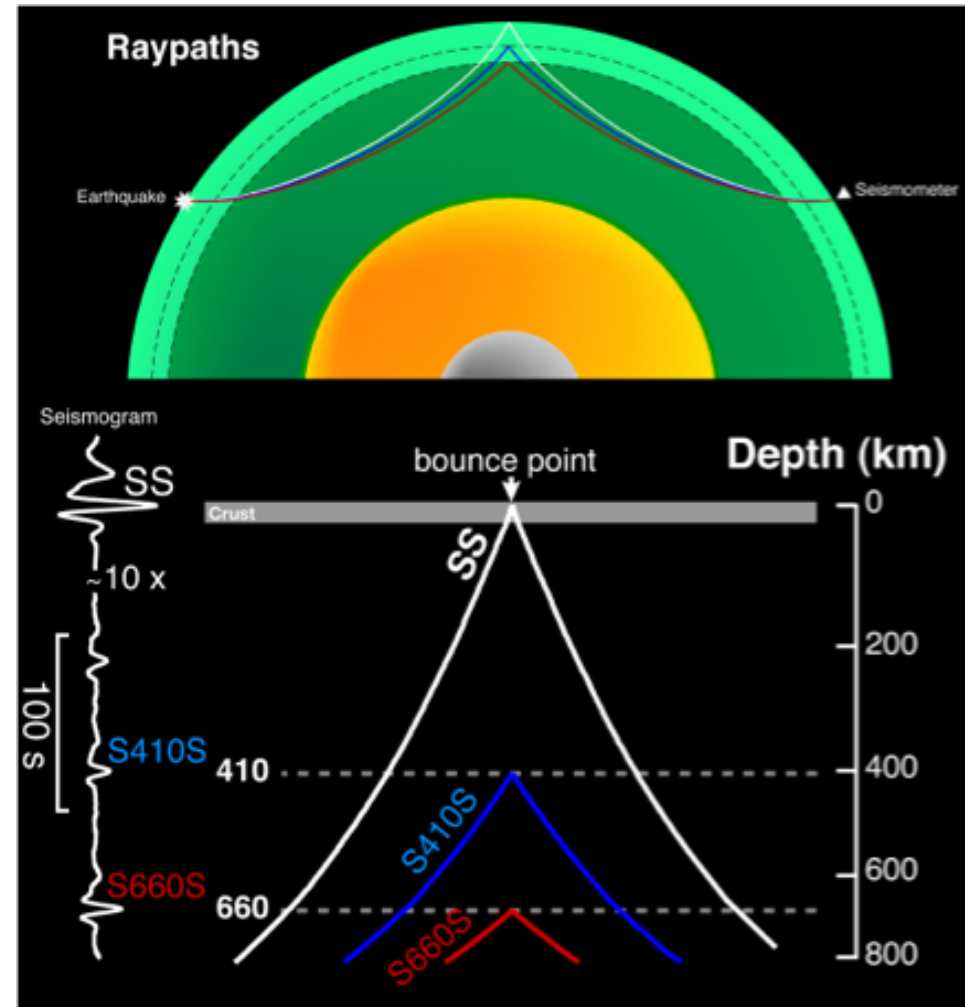
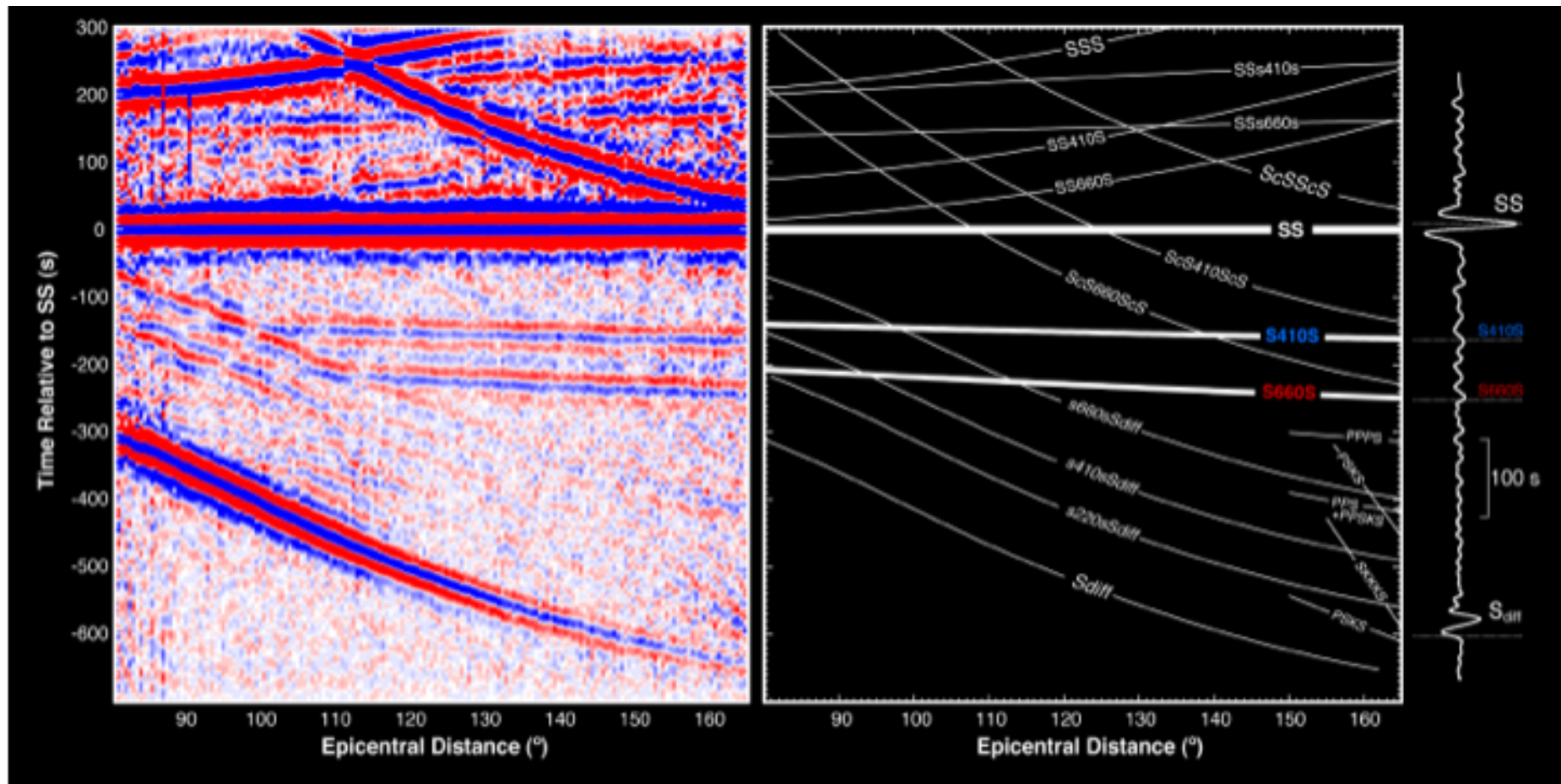


Figure by Schmerr

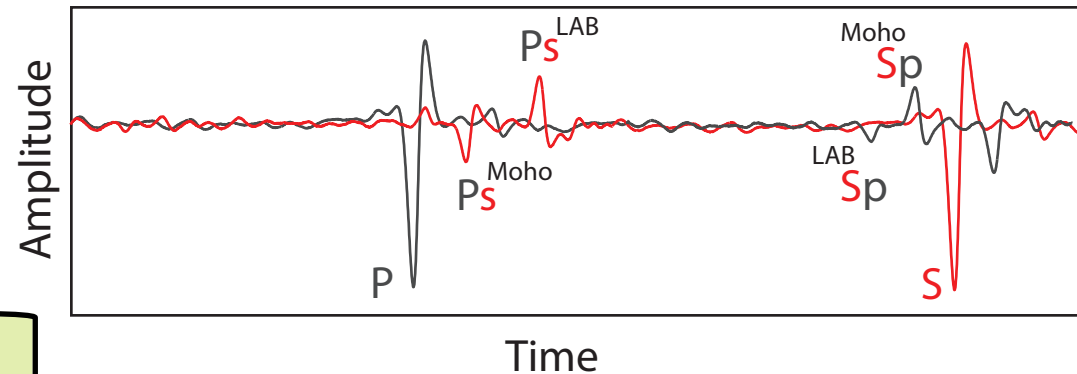
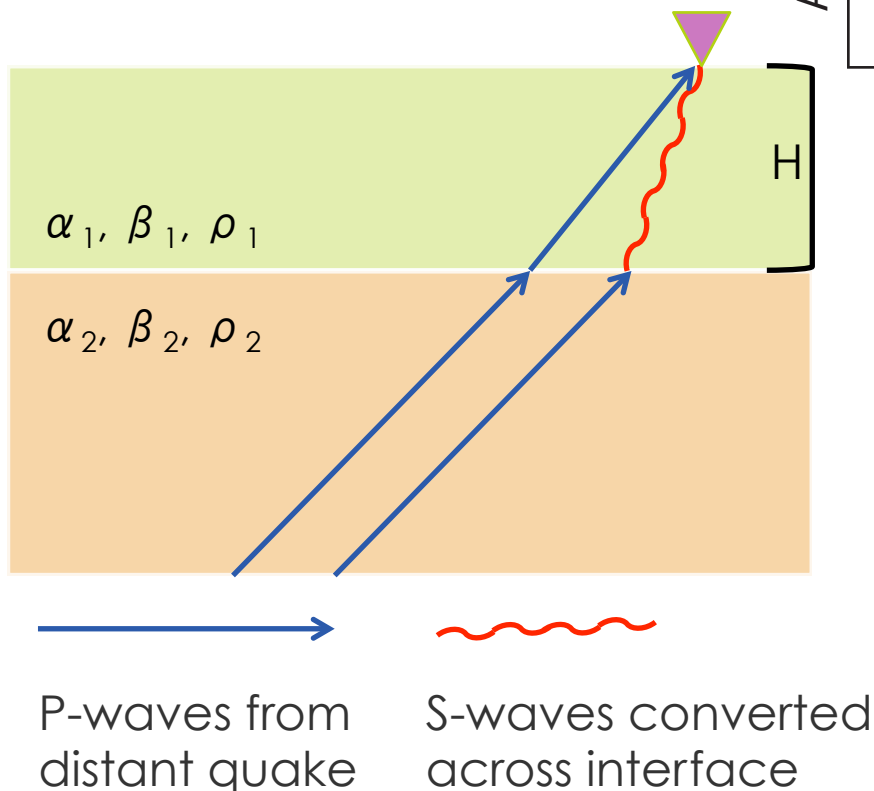
SS precursors (reflection)



<http://terpconnect.umd.edu/~nschmerr/Research.html>

Receiver Functions (transmission)

$$T_P - T_{Ps} = H (\eta_S - \eta_P)$$

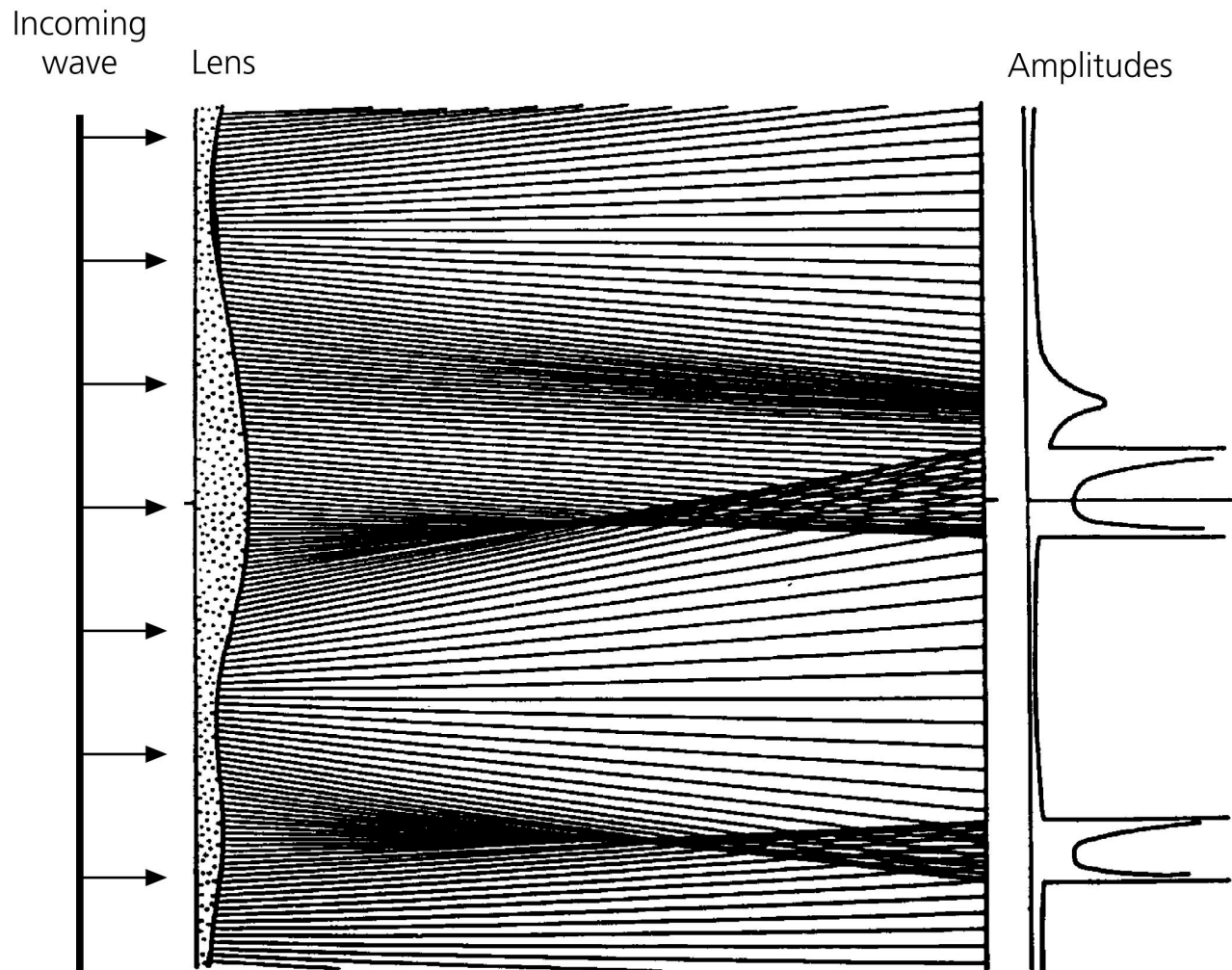


- Teleseismic waves can convert from P-to-S or S-to-P beneath a seismometer
- Relative timing between P(S) and Ps(Sp) arrivals constrains the depth of the interface
- Relative amplitude of P/Ps and S/Sp constrains impedance contrast across interface

Focusing-Defocusing

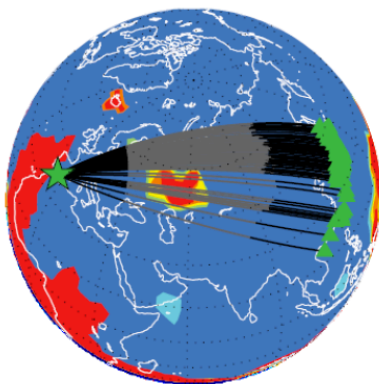
Velocity heterogeneity can focus (like a lens) or defocus the energy
=> note amplitude of waves recorded far away can still be affected

Figure 3.7-5: Example of velocity heterogeneities affecting wave amplitudes.

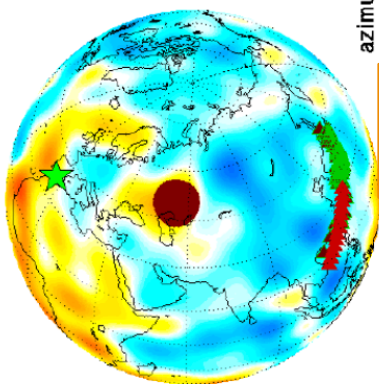


Focusing by slow anomalies

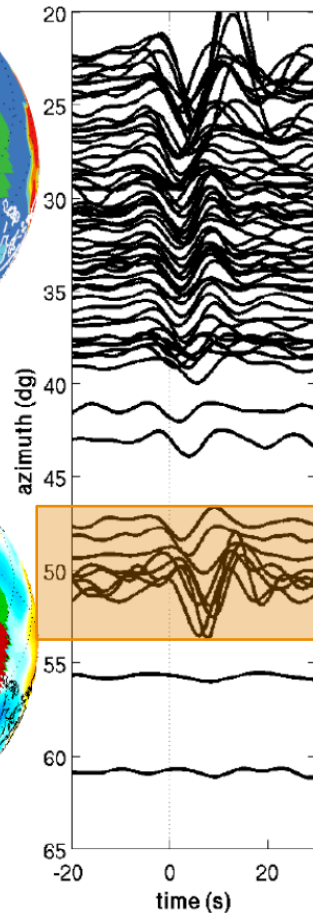
a. Station Coverage



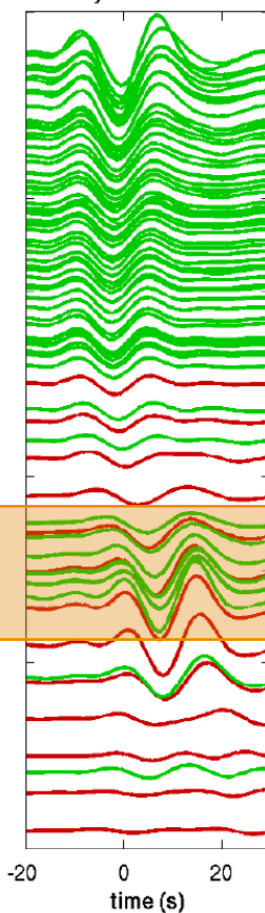
b. 3D model



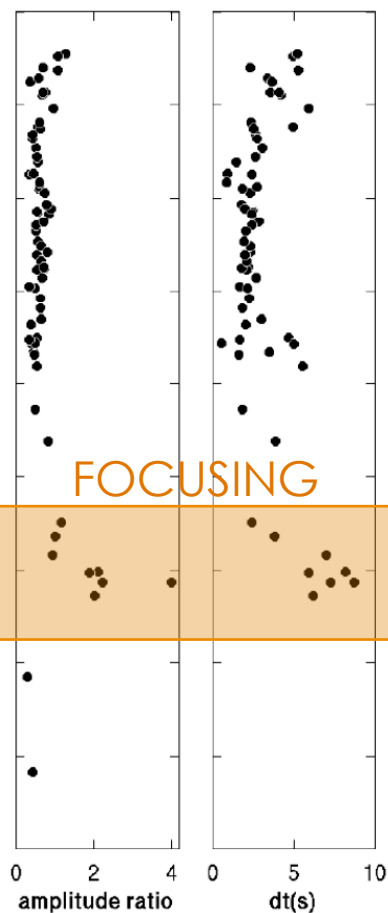
c. Sdiff waveforms



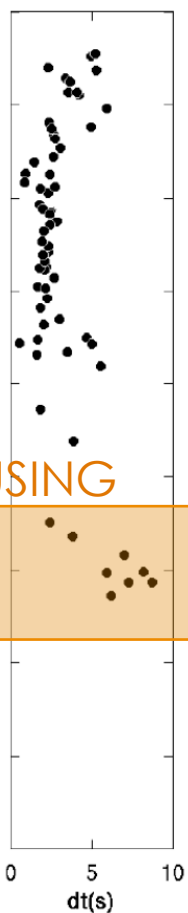
d. 3D synthetics



e. Amplitude ratios



f. Differential travel times



- Transverse-component velocity waveforms from the 4/11/2010 Spain event
- Stations in 91° -102° epicentral distance range → S waves grazing the core-mantle boundary
- S/Sdiff waveforms show amplitude focusing and travel-time delays

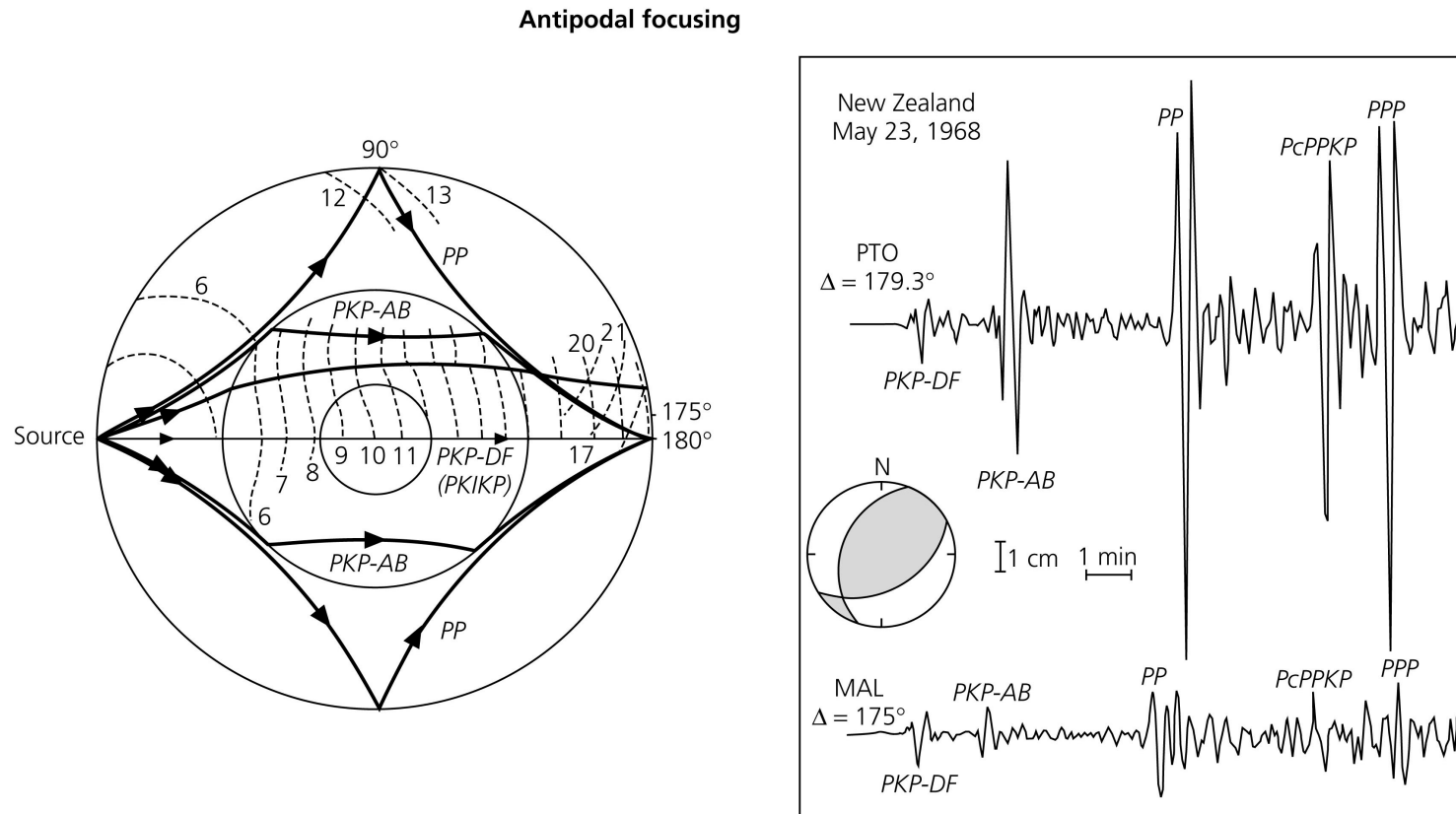
Focusing

At antipodes, energy can focus (can be seen as ray from different directions arriving at the same time) => Amplitude increase

Core phases can be amplified at the antipodes

Core phases

Figure 3.5-11: Focusing of *P* waves at the antipode.

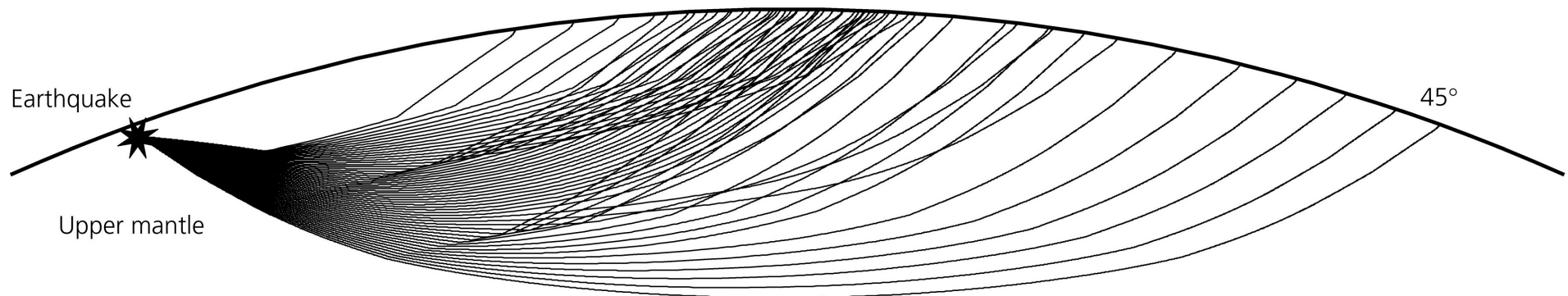


Triplications in the upper mantle

Around 15 and 22 degrees of epicentral distance, triplications due to two mantle discontinuities, ~ 410 and 660 km depth, are observed

Triplications, i.e. arrival of energy from different depth at the same time, are difficult to study

Figure 3.5-12: Ray paths for *P* waves through the upper mantle.

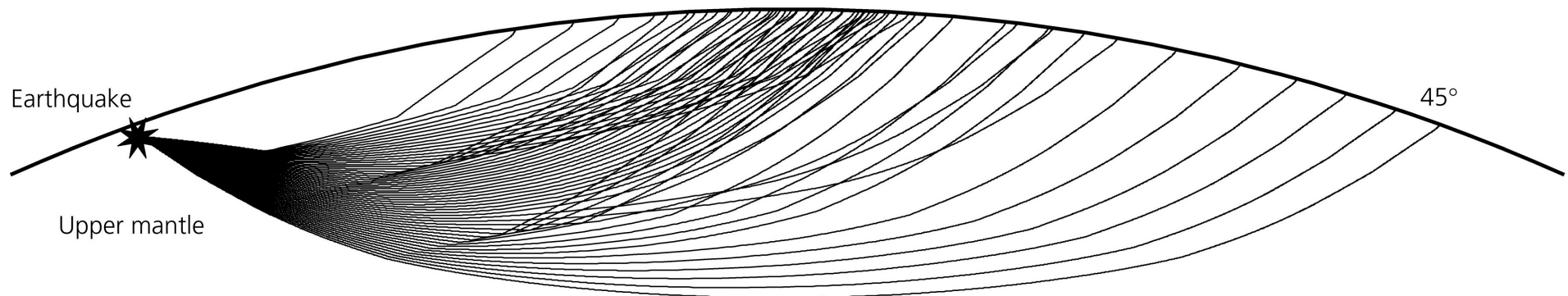


Triplications in the upper mantle

Around 15 and 22 degrees of epicentral distance, triplications due to two mantle discontinuities, ~ 410 and 660 km depth, are observed

Triplications, i.e. arrival of energy from different depth at the same time, are difficult to study \Rightarrow dense arrays of stations, enhance signal-to-noise ratio, waveform modeling and non-linear inversion techniques.

Figure 3.5-12: Ray paths for *P* waves through the upper mantle.

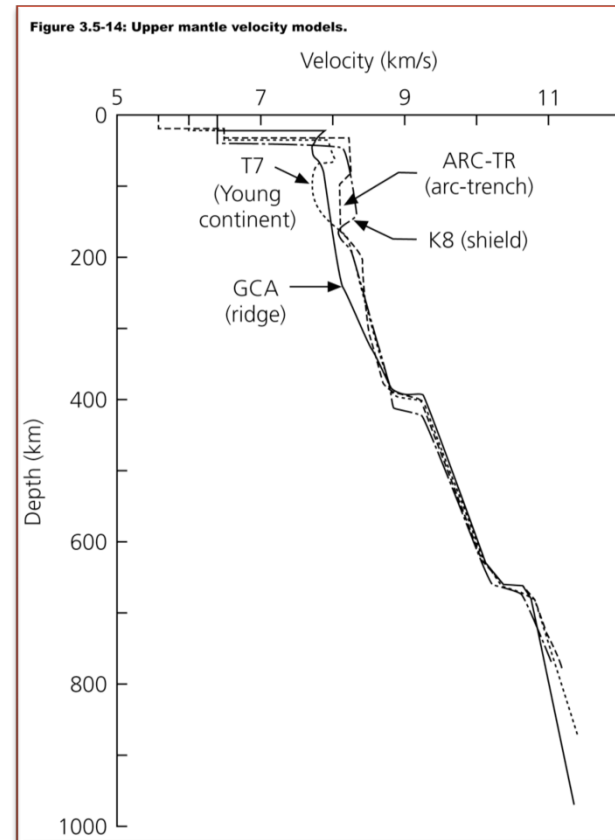
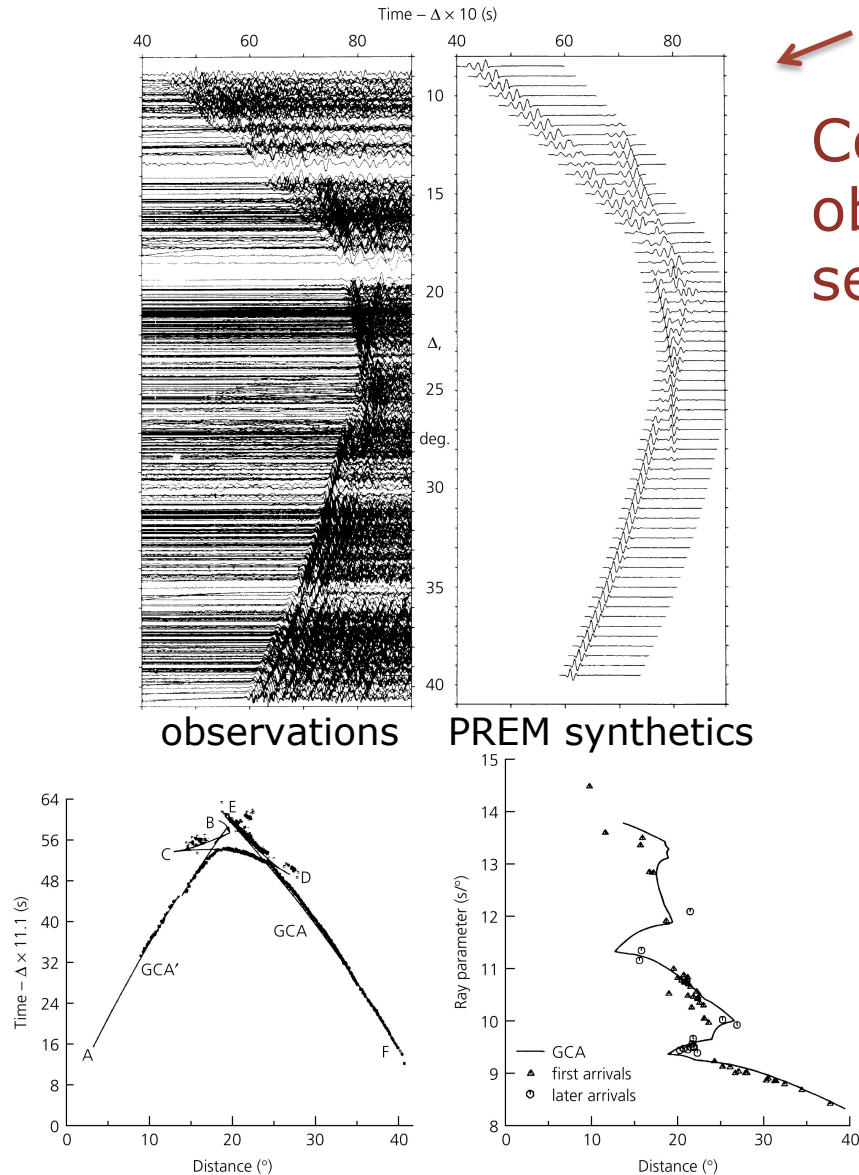


Tripletations in the upper mantle

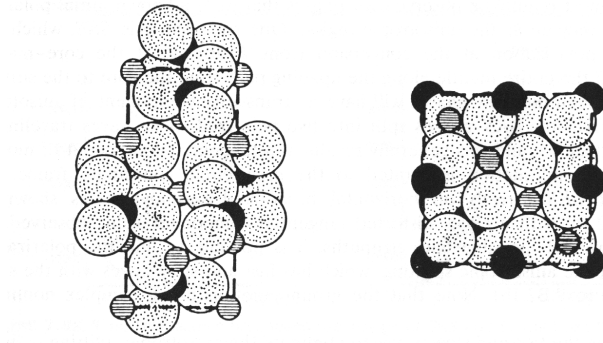
Figure 3.5-13: Seismic array study of upper mantle structure.

Record section in reduced velocities

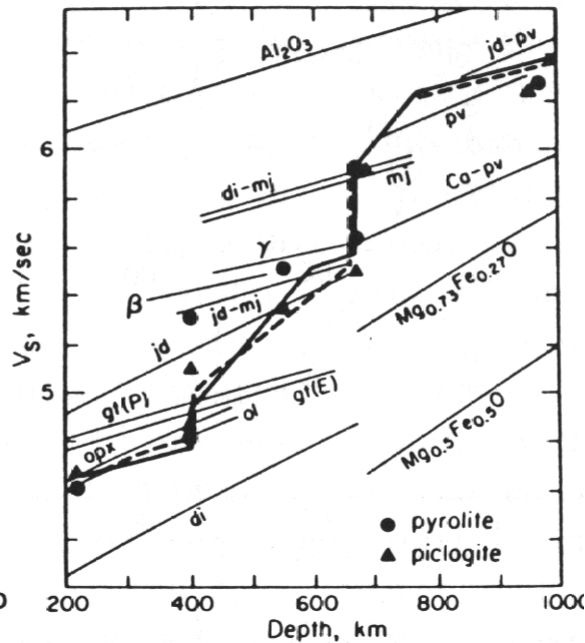
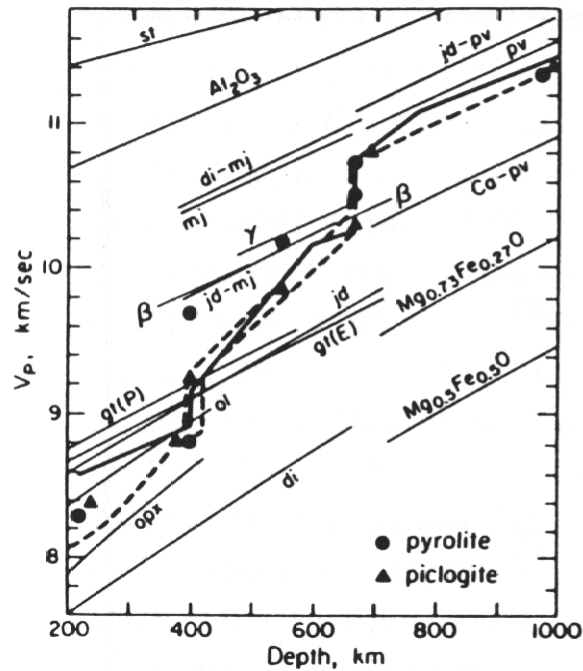
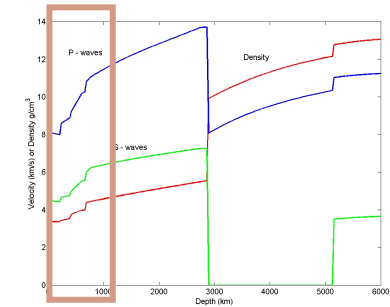
Combined analysis of several observations and prediction of seismograms (GCA model is best fit)



Upper Mantle: Phase transitions



Upper mantle discontinuities (e.g. 410km) are caused by phase transitions (left: low pressure olivine, right: high pressure b-spinel)



Various upper mantle seismic models and experimental results for minerals and mineral assemblages.

Seismic attenuation

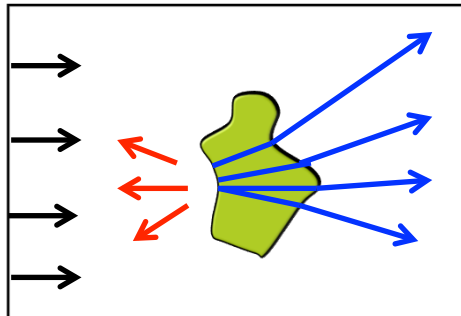
Extrinsic attenuation

incoming elastic energy
is conserved

Geometrical
spreading



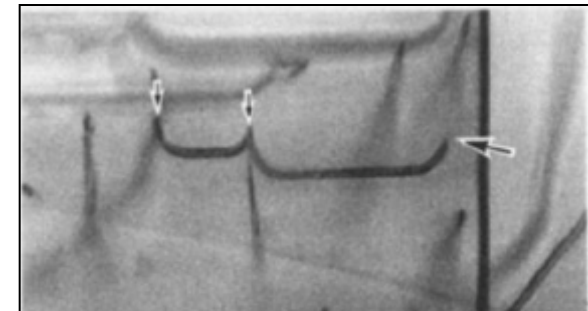
Focusing/Defocusing
Scattering



Intrinsic attenuation

incoming elastic energy
is transformed

Anelasticity
(dislocations, diffusion, ...)



Karato & Spetzler [1990]

Q (*quality factor*) or **q** (*absorption*)

$$q = 1/Q = - \Delta E / 2\pi E = - \Delta A / \pi A$$

no scattering

scattering

Scattering

Seismic waves can scatter from heterogeneities within the elastic medium

Scattering is efficient if the size of the scatterer is similar to the wavelength

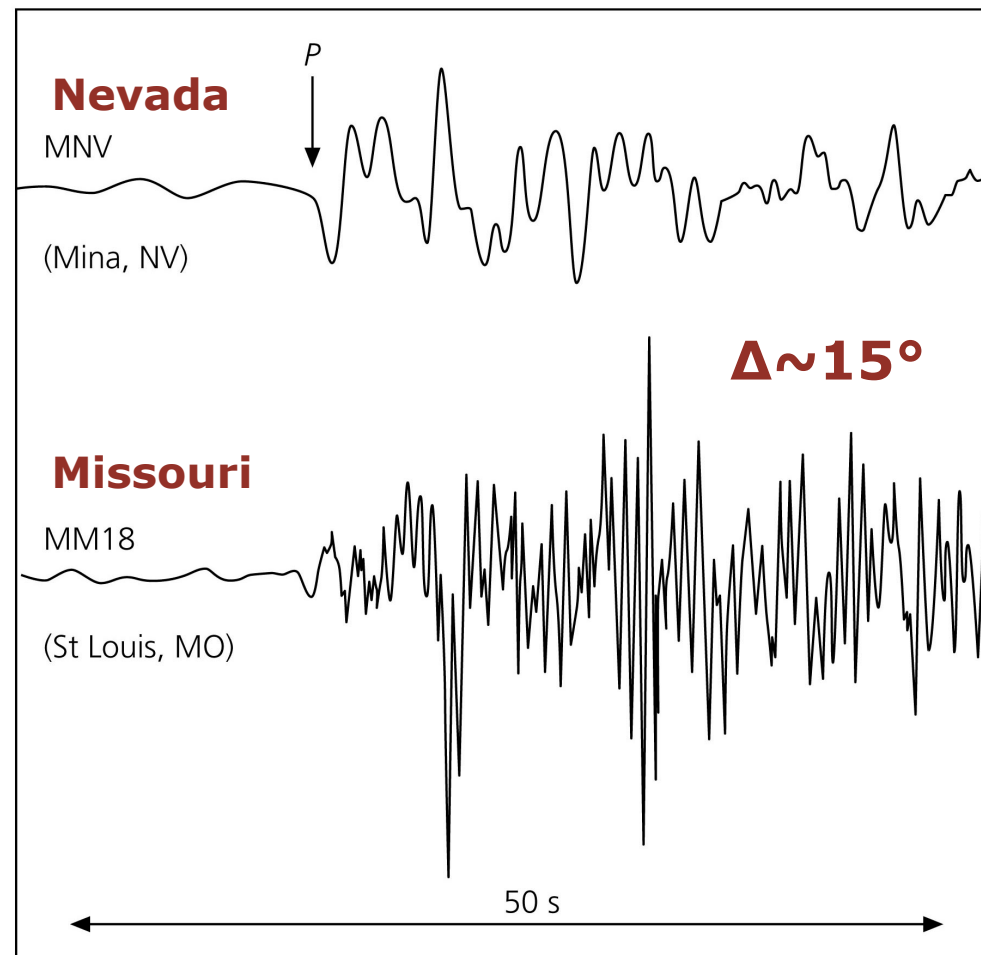
Scattering re-distributes energy, decreasing amplitudes at the beginning of a seismogram, and increasing them in the back (the “coda”)

Attenuation

Seismic attenuation can vary considerably: for example, tectonically active western USA is more attenuating than stable mid-continent.

Note also the major content of high frequency in the less attenuated signal

Figure 3.7-1: Regional effects of attenuation.



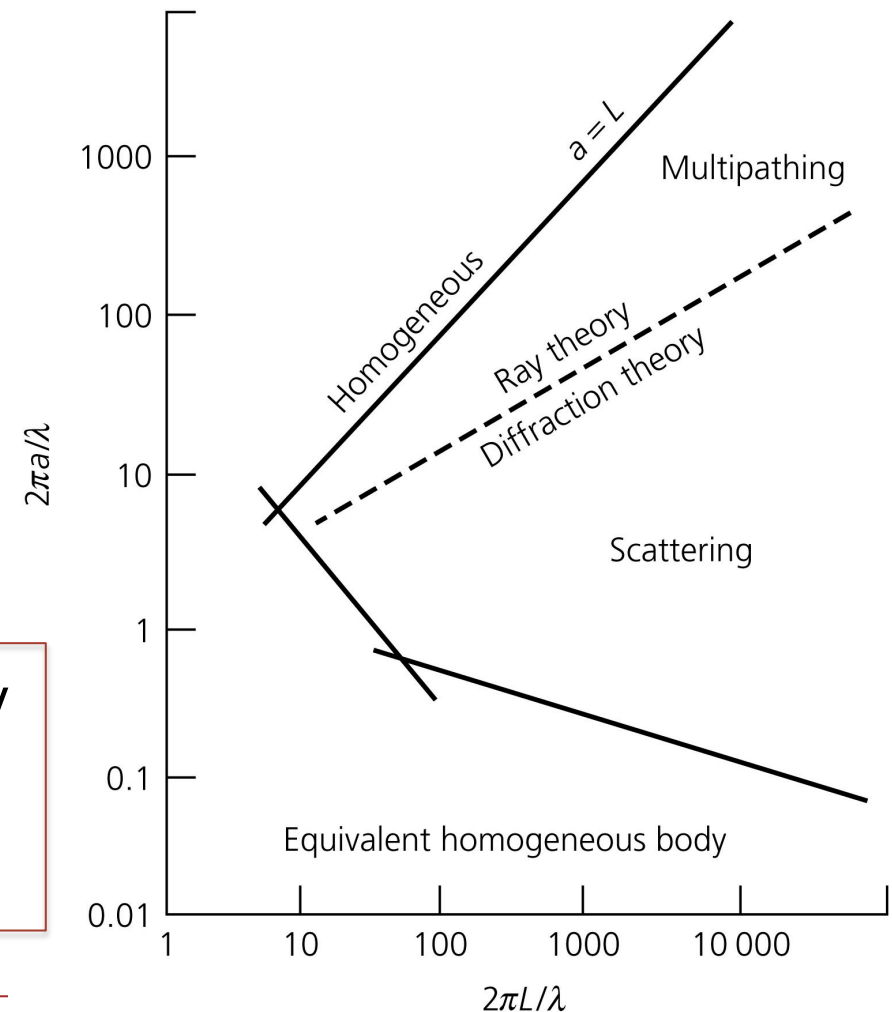
Scattering

Multipathing (consider several rays) can be useful to visualize focusing-defocusing effects. Ray theory, or perturbation to it can be still used.

The phenomena can be pushed further to have scattering => diffusive equation (no ray theory)

a = size of heterogeneity
 L = distance wave travels
 λ = wavelength

Figure 3.7-8: Different approaches to wave propagation in a heterogeneous medium.



Scattering

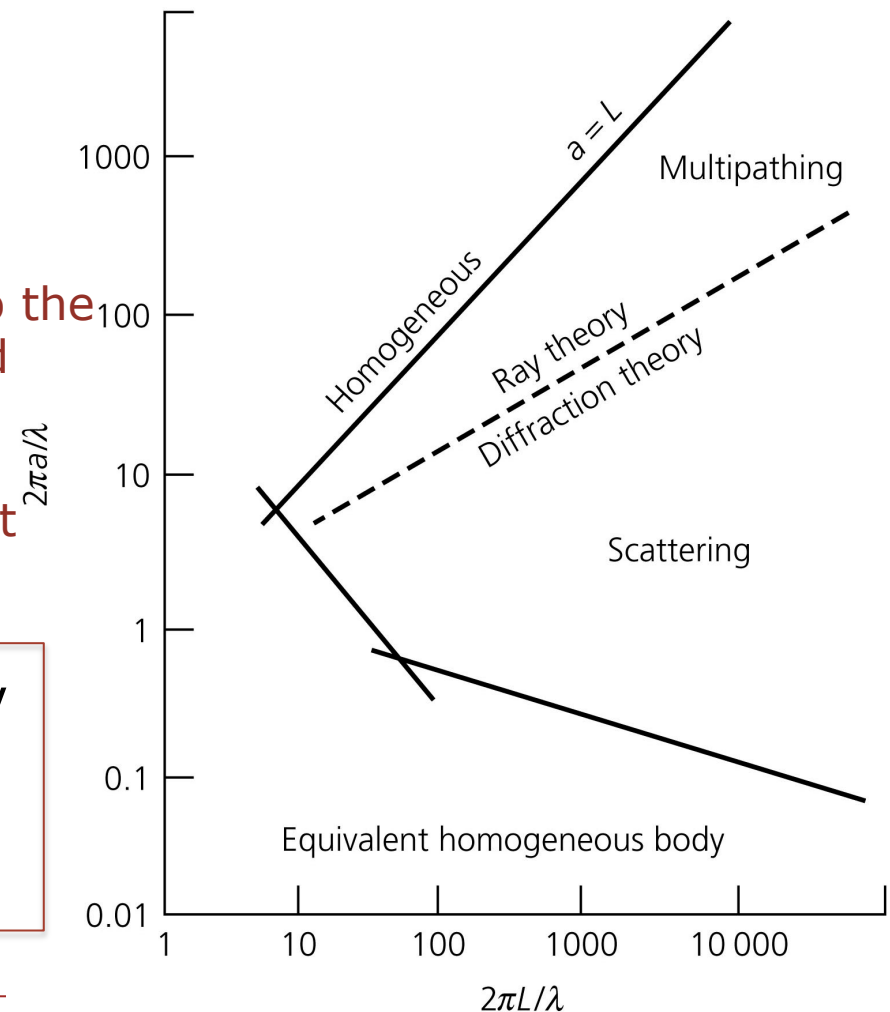
Multipathing (consider several rays) can be useful to visualize focusing-defocusing effects. Ray theory, or perturbation to it can be still used.

The phenomena can be pushed further to have scattering => diffusive equation (no ray theory)

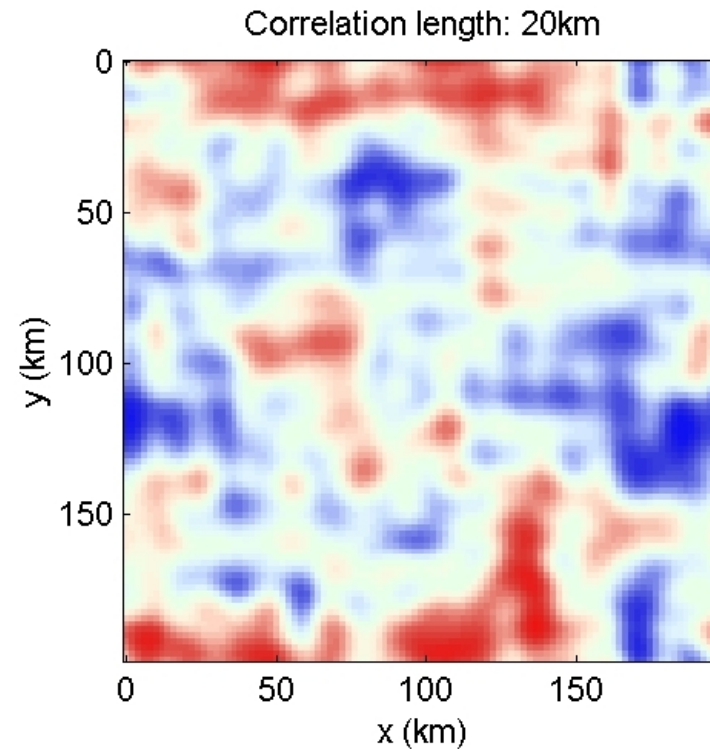
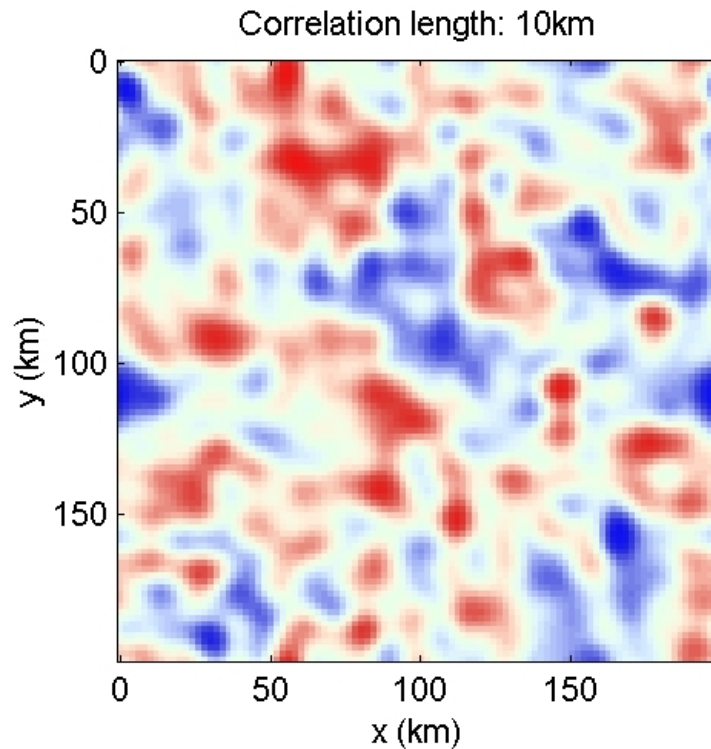
- If heterogeneity becomes comparable to the wavelength, energy is strongly scattered
- If heterogeneity is much larger, ray theory + multipathing, if heterogeneity is smaller, lambda sees an average effect

a = size of heterogeneity
 L = distance wave travels
 λ = wavelength

Figure 3.7-8: Different approaches to wave propagation in a heterogeneous medium.



Scattering

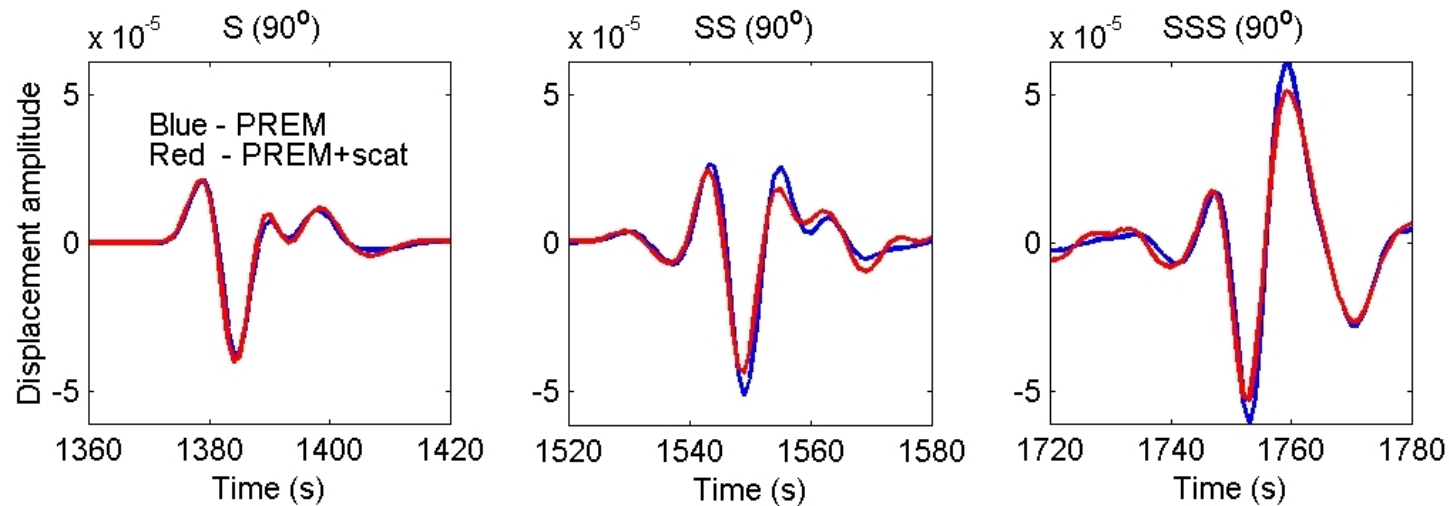
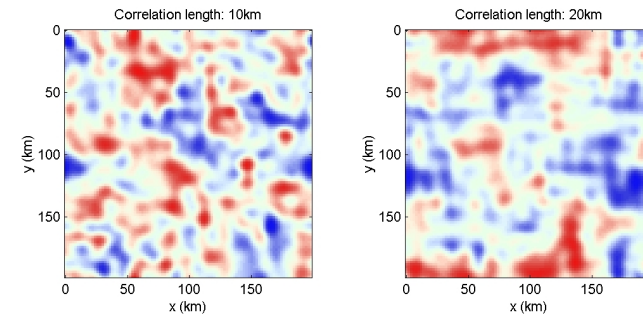


How is a propagating wavefield affected by random heterogeneities?

- $a = L$ homogeneous region
- $a \gg \lambda$ ray theory is valid
- $a \approx \lambda$ strong scattering effects

Scattering

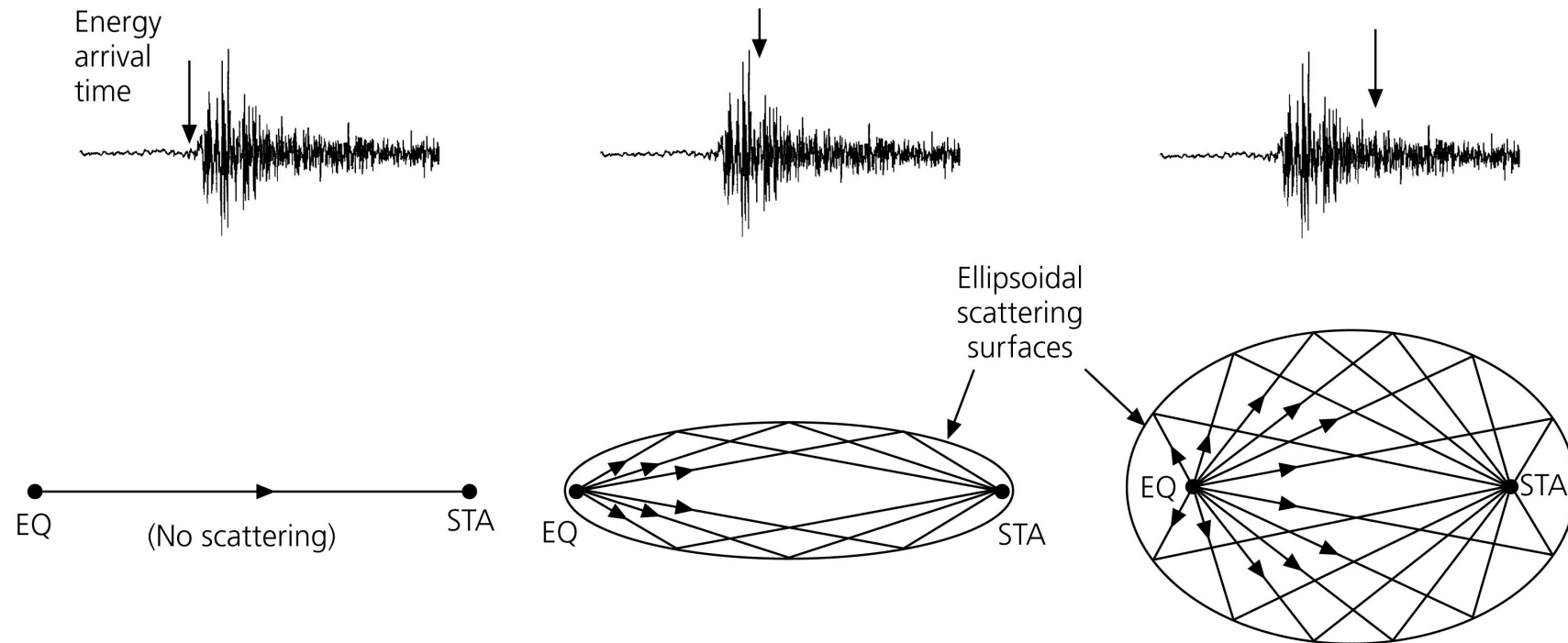
Synthetic seismograms for a global model with random velocity perturbations.



When the wavelength is long compared to the correlation length, scattering effects are difficult to distinguish from intrinsic attenuation.

Scattering

Figure 3.7-9: Development of a *P*-wave coda.

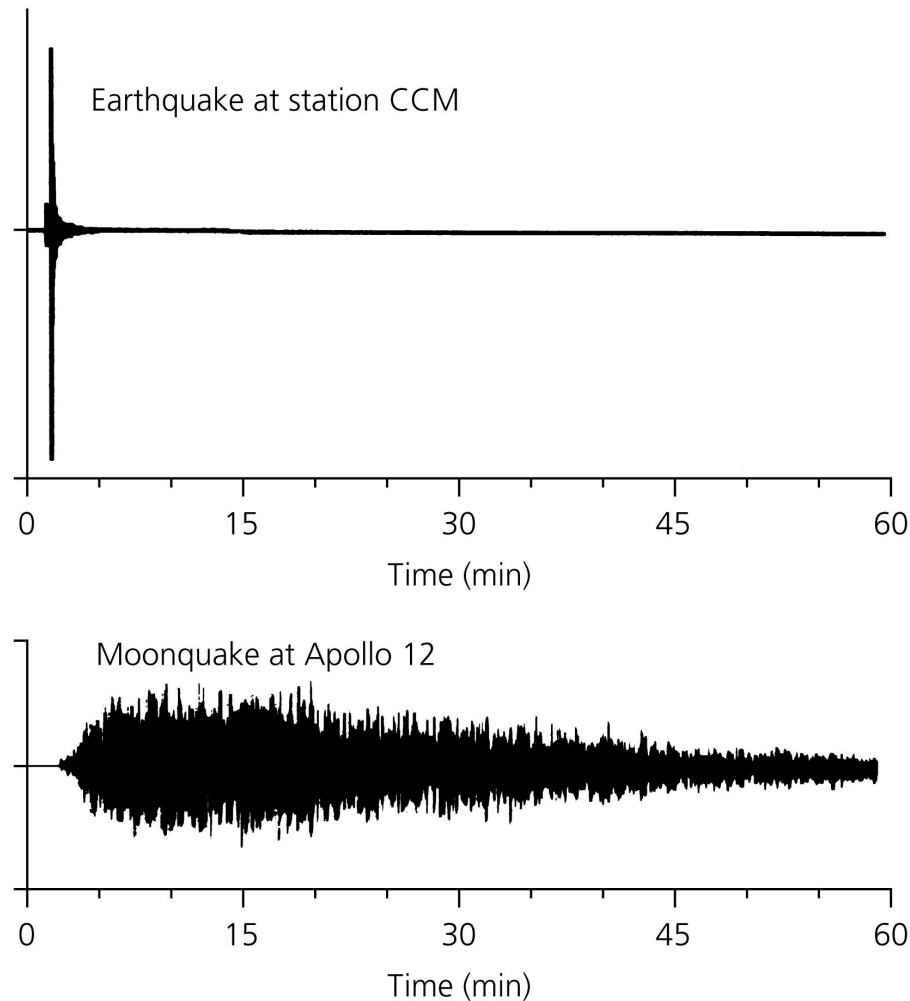


- First-order scattering (Born approximation) (generally, coda at high frequency are due to multiple scattering).

Scattering

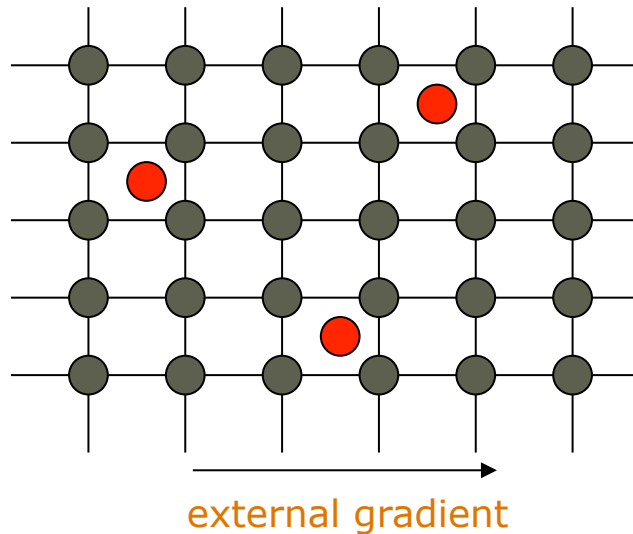
Very strong scattering for the Moon=> shallow regolith layer
(fractured layer due to intense crater impacts and low gravity)

Figure 3.7-10: Comparison of seismograms on the earth and moon.



Characterization of intrinsic attenuation

97



Elastic energy of waves is consumed in dissipative processes (*Knopoff, 1964*)

Many different dissipation mechanisms exist in the mantle (*e.g. Jackson and Anderson 1970*)

Characterization of intrinsic attenuation

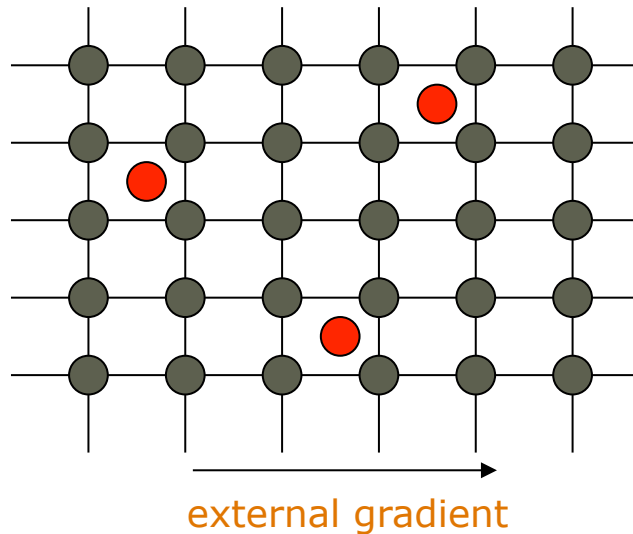
98

Incident seismic wave



Elastic energy of waves
is consumed in
dissipative processes
(*Knopoff, 1964*)

Many different
dissipation mechanisms
exist in the mantle
(*e.g. Jackson and
Anderson 1970*)



Characterization of intrinsic attenuation

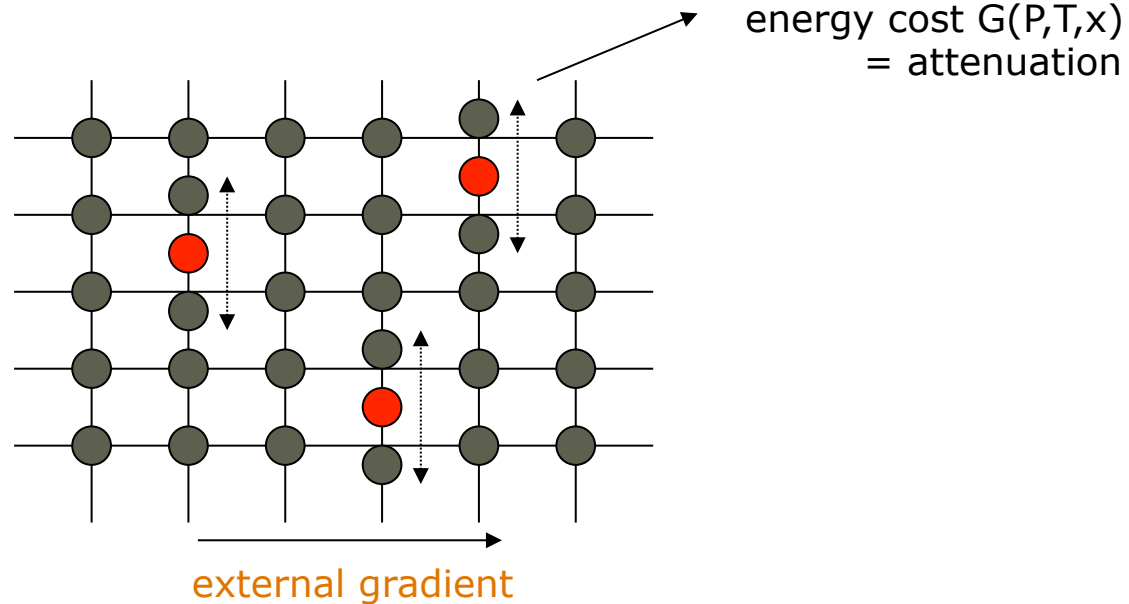
99

Incident seismic wave



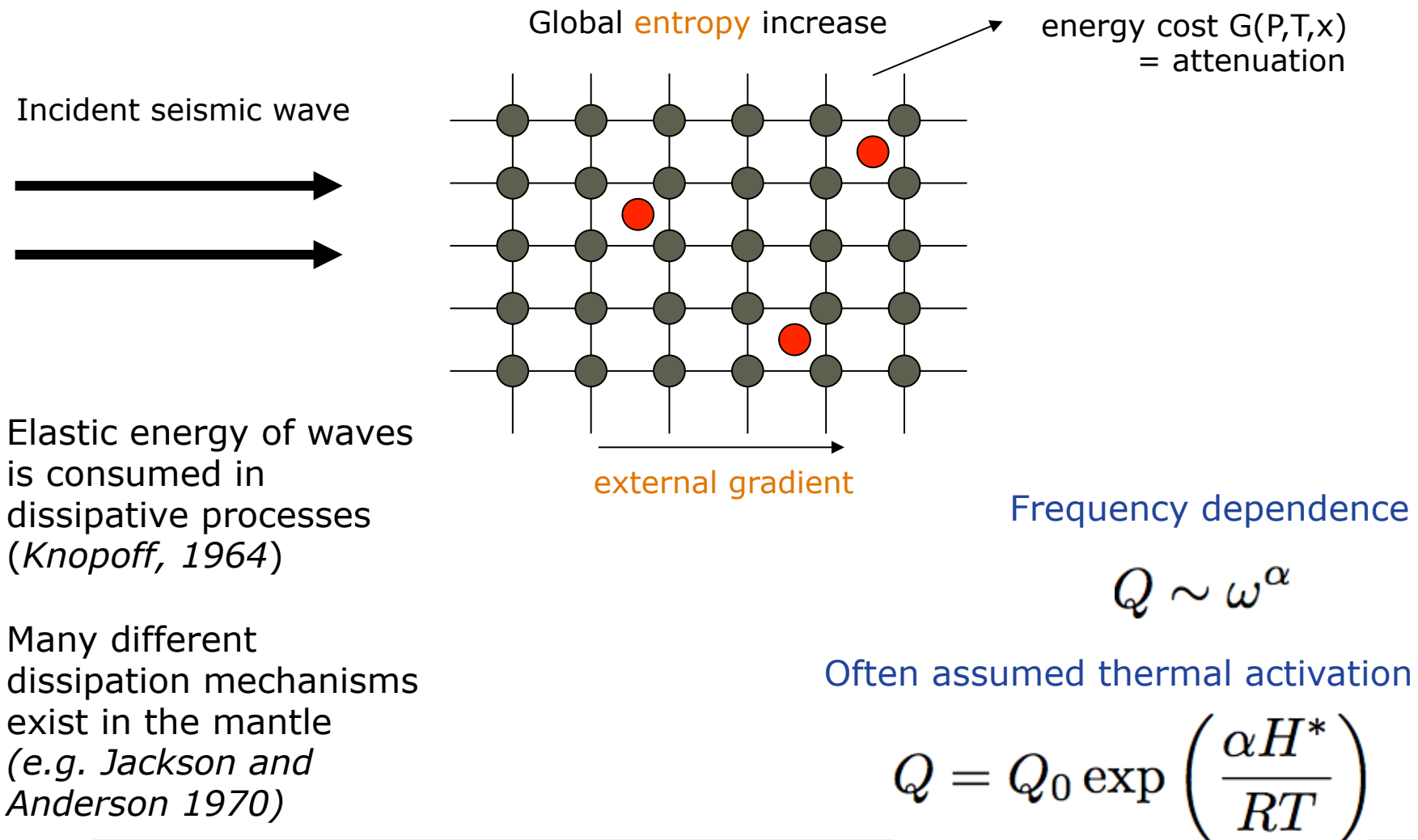
Elastic energy of waves
is consumed in
dissipative processes
(*Knopoff, 1964*)

Many different
dissipation mechanisms
exist in the mantle
(*e.g. Jackson and
Anderson 1970*)



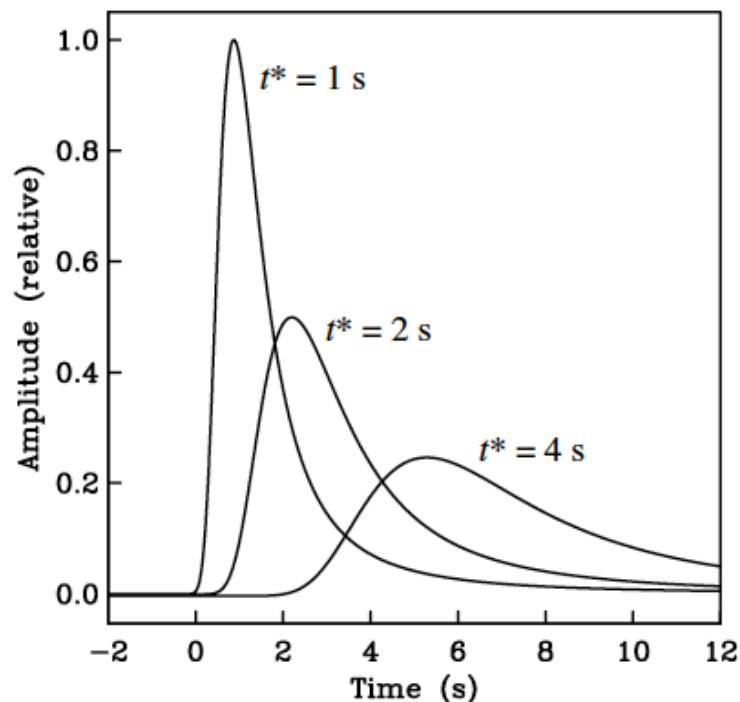
Characterization of intrinsic attenuation

100



Dispersion due to attenuation

$$A(x) = A_0 e^{-\omega x / 2cQ}$$



- Because they have more oscillations per unit distance, higher frequencies are more attenuated
- If all frequencies travelled at the same speed, then causality would be violated
- Low frequency waves are slowed down more than high frequency waves

figures from Shearer, 2009

Earth attenuation structure

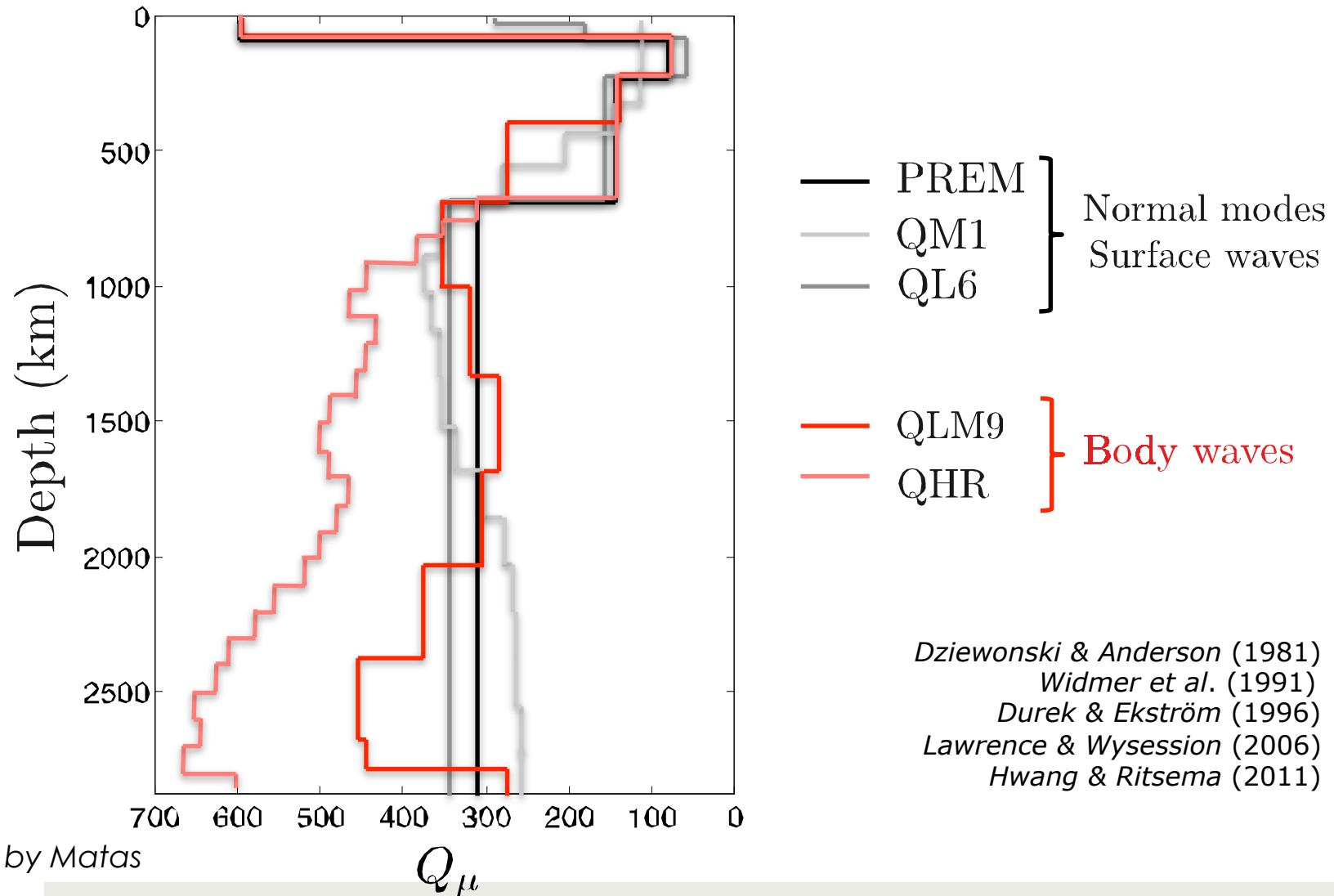
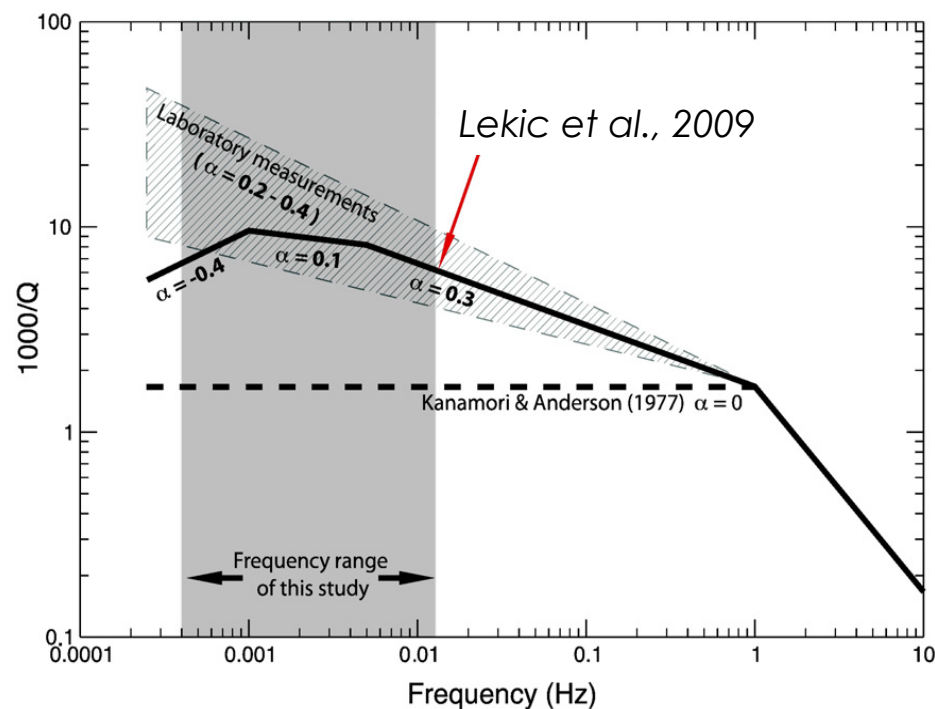


figure by Matas

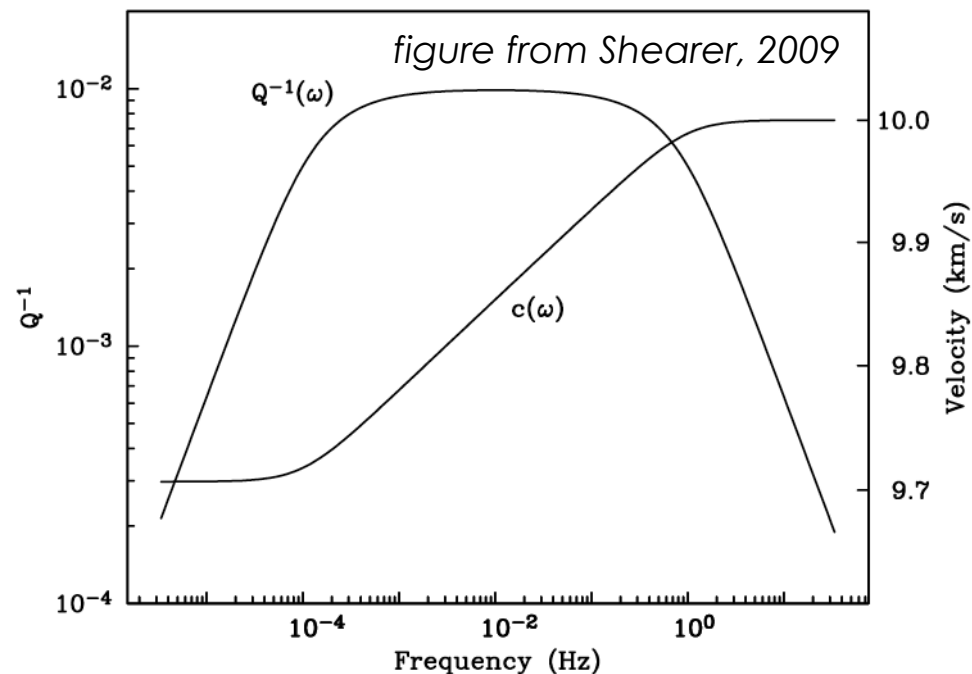
Frequency dependence

Q depends on frequency



$$\frac{V(\omega_2)}{V(\omega_1)} = 1 + \frac{q(\omega_1)}{2} \cot\left(\frac{\alpha\pi}{2}\right) \left[1 - \left(\frac{\omega_1}{\omega_2}\right)^\alpha\right]$$

Q is frequency independent



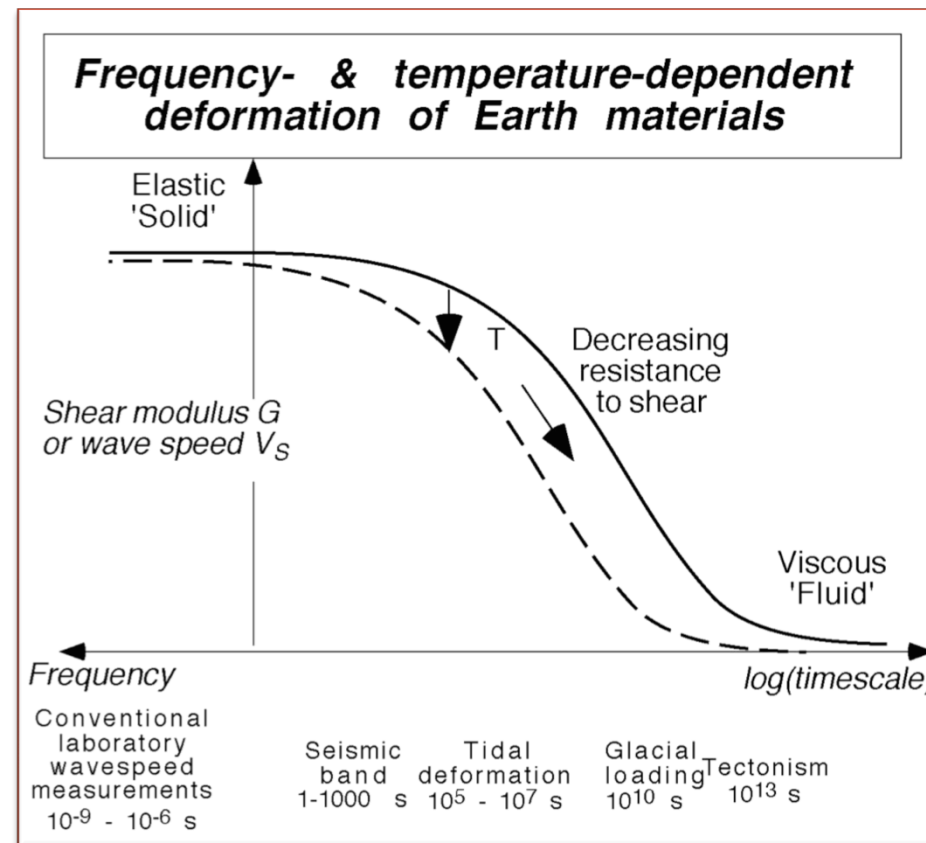
$$\frac{V(\omega_2)}{V(\omega_1)} = 1 + \frac{q}{\pi} \ln\left(\frac{\omega_2}{\omega_1}\right)$$

Intrinsic attenuation - Anelasticity

Rocks are not perfectly elastic → some energy is lost as heat due to (internal) frictional dissipation

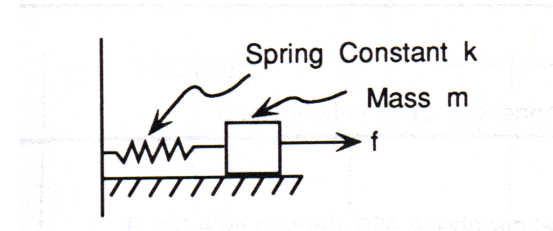
The causes are due to presence of defects within the crystalline structure that introduce a time-dependent response to stress (a sort of delay, called relaxation time), already at seismic frequencies.

The visco-elastic relaxation is thermally activated => inferring from seismic attenuation gives constraints on temperature



Intrinsic attenuation - Anelasticity

To understand the macroscopic effect of seismic attenuation, consider a simple damped harmonic oscillator:



Model of intrinsic attenuation:

damped harmonic oscillator composed of a spring and dashpot

Newton's Law: $\mathbf{F} = m\mathbf{a}$

Case for no damping:

$$m \frac{d^2 u(t)}{dt^2} + k u(t) = 0 \quad \text{where } k \text{ is the spring constant.}$$

Solution is perpetual harmonic oscillation:

$$u(t) = Ae^{i\omega_0 t} + Be^{-i\omega_0 t} \quad \text{or} \quad u(t) = A_0 \cos(\omega_0 t)$$

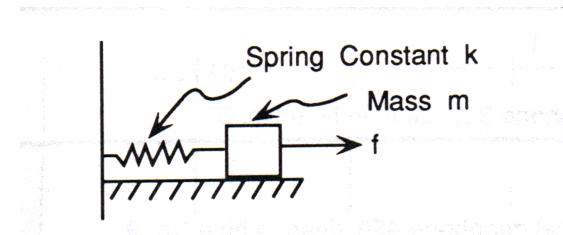
(A and B are constants)

Intrinsic attenuation - Anelasticity

The mass moves back and forth with a natural frequency $\omega_0 = (k/m)^{1/2}$

Once the motion is started, the oscillation continues forever.

Case of damping:



The damping force is proportional to the velocity of the mass and opposes its motion.

$$m \frac{d^2 u(t)}{dt^2} + \gamma m \frac{du(t)}{dt} + k u(t) = 0 \quad (\gamma \text{ is the damping factor.})$$

To simplify, define the *quality factor* $Q = \omega_0/\gamma$ to get:

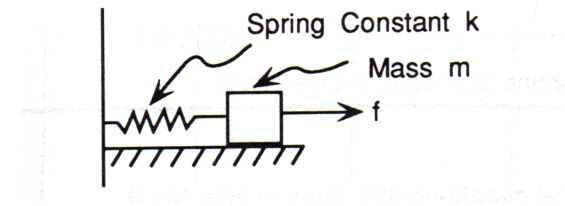
$$\frac{d^2 u(t)}{dt^2} + \frac{\omega_0}{Q} \frac{du(t)}{dt} + \omega_0^2 u(t) = 0$$

Eq. for damped harmonic oscillator

Intrinsic attenuation - Anelasticity

$$u(t) = A_0 e^{-\omega_0 t/2Q} \cos(\omega t)$$

solution for damped harmonic oscillator

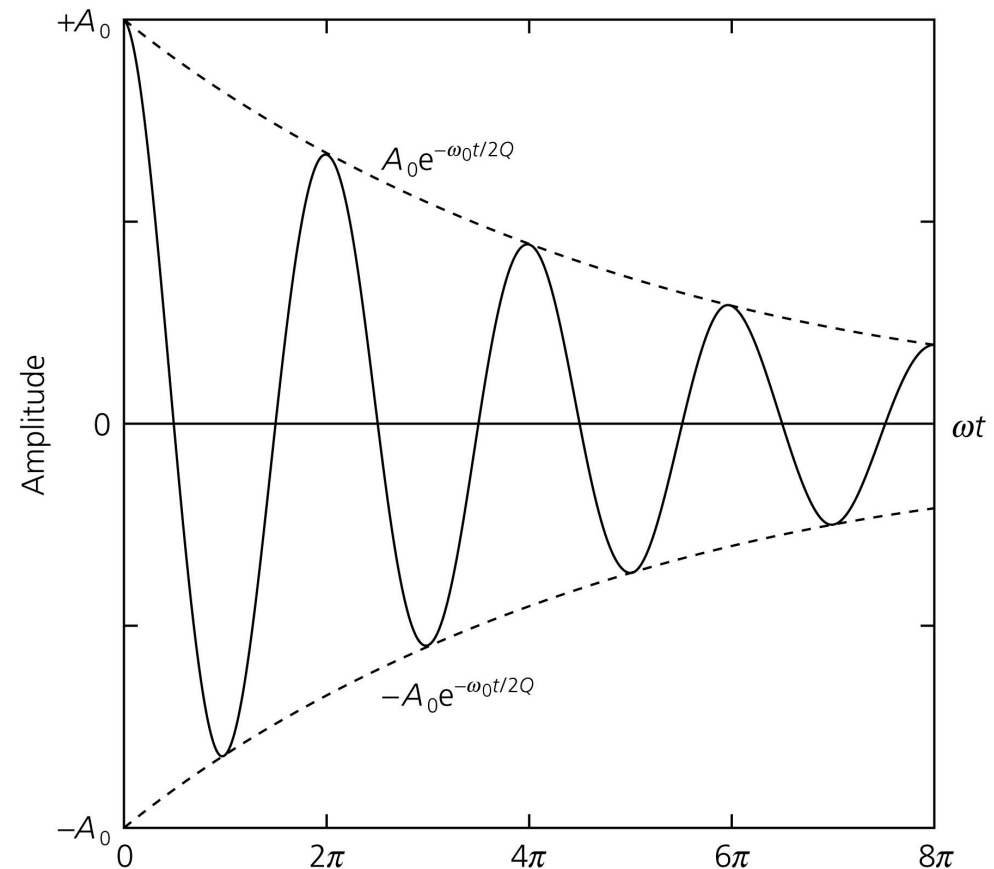


The real exponential term gives the decay of the signal's envelope or overall amplitude:

$$A(t) = A_0 e^{-\omega_0 t/2Q}$$

In addition, the frequency is changed from the natural frequency of the undamped system, ω_0 , by an amount depending on the quality factor.

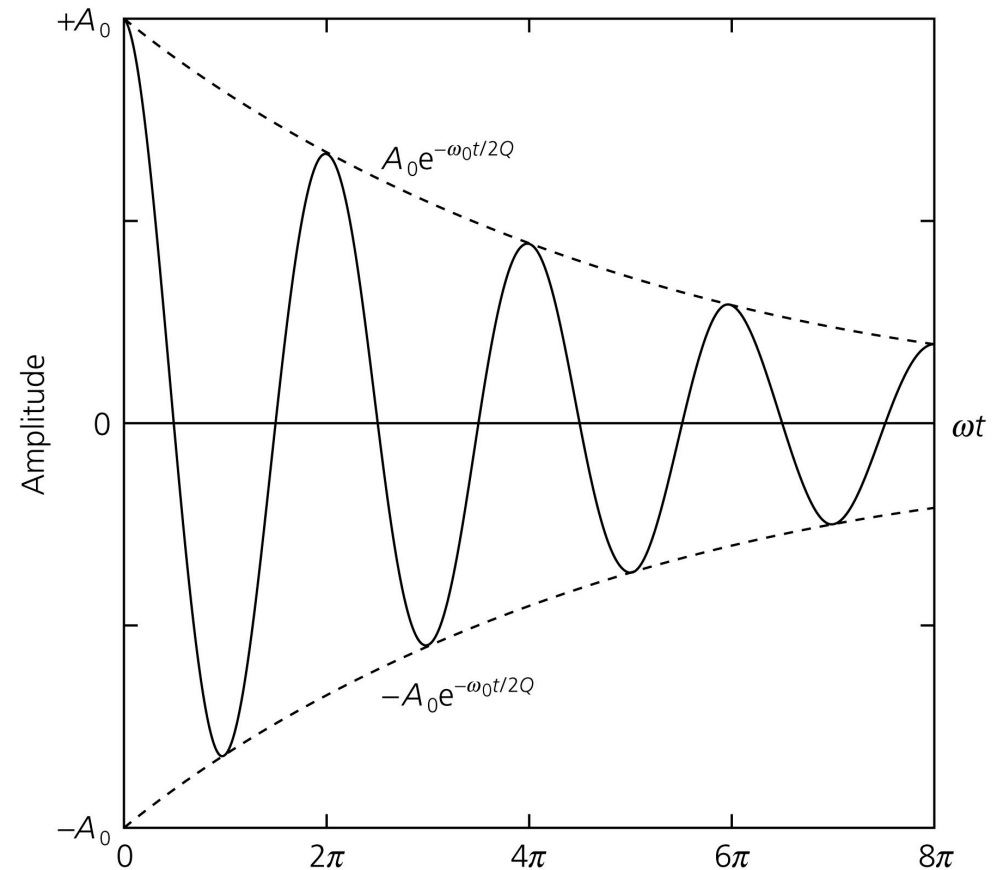
Figure 3.7-11: Wave amplitude for a damped harmonic oscillator.



Intrinsic attenuation - Anelasticity

Quality factor (or its inverse, Q^{-1} - seismic attenuation) can be determined by observing the decay of the seismic signal

Figure 3.7-11: Wave amplitude for a damped harmonic oscillator.



Measure Q from the decay of an oscillation.

Take the natural logarithm of

$$A(t) = A_0 e^{-\omega_0 t/2Q}$$

to get

$$\ln A(t) = \ln A_0 - \omega_0 t/2Q$$

so Q can be found from the slope of the logarithmic decay.

Intrinsic attenuation - Anelasticity

Quality factor (or its inverse, Q^{-1} - seismic attenuation) can be determined by observing the decay of the seismic signal

Alternatively, look at successive peaks one full period $T = 2\pi/\omega_0$ apart:

$$A_1(t_1) = A_0 \exp(-\omega_0 t_1/2Q)$$

$$A_2(t_1 + T) = A_0 \exp(-\omega_0(t_1 + T)/2Q)$$

Their ratio is:

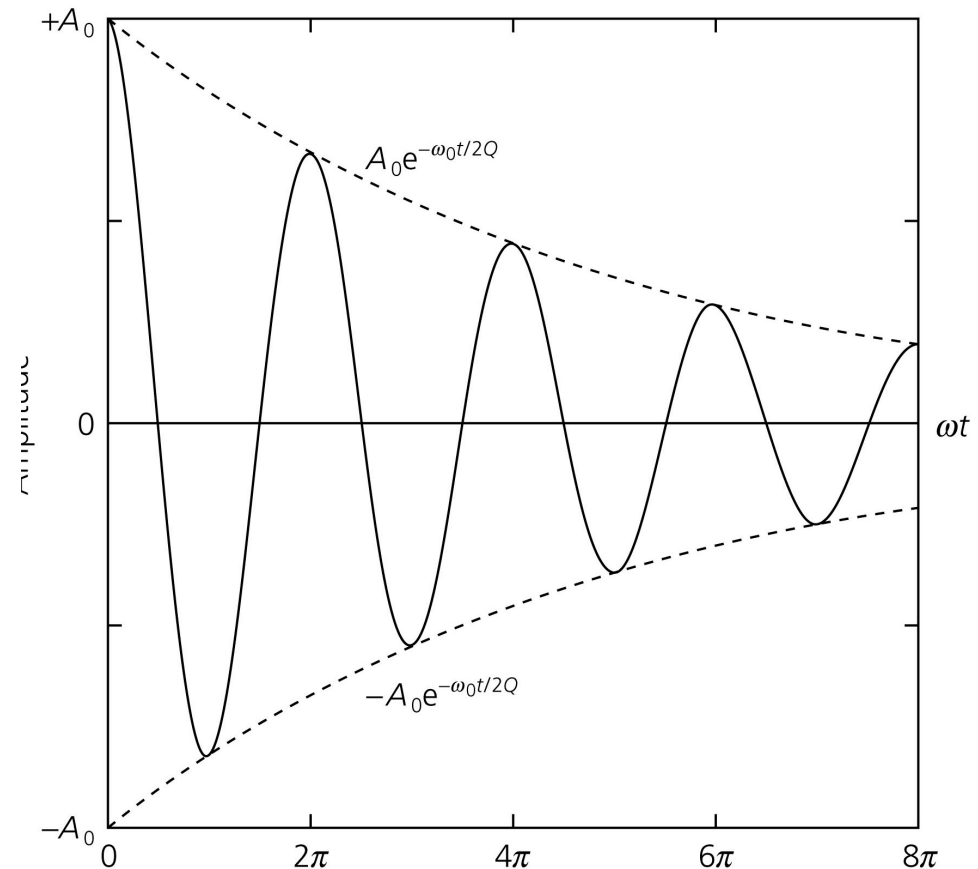
$$A_1/A_2 = \exp\left[-\omega_0 t_1/2Q - \omega_0(t_1 + T)/2Q\right] = e^{\pi/Q}$$

This gives $Q = \pi / \ln(A_1/A_2)$

In Figure 11 the second peak, at $\omega t = 2\pi$, is about 2/3 of the first peak, at $\omega t = 0$.

Therefore, $Q \approx \pi / \ln(3/2) \approx 8$.

Figure 3.7-11: Wave amplitude for a damped harmonic oscillator.



Intrinsic attenuation - Anelasticity

Quality factor (or its inverse, Q^{-1} - seismic attenuation) can be determined by observing the decay of the seismic signal

Another way to measure Q is as the number of cycles the oscillation takes to decay to a certain level.

The number of cycles n , is

$$n = t/T = \omega t/2\pi \approx \omega_0 t/2\pi,$$

The amplitude at time t_n , after n cycles is

$$A(t_n) \approx A_0 e^{\frac{-n\pi}{Q}}$$

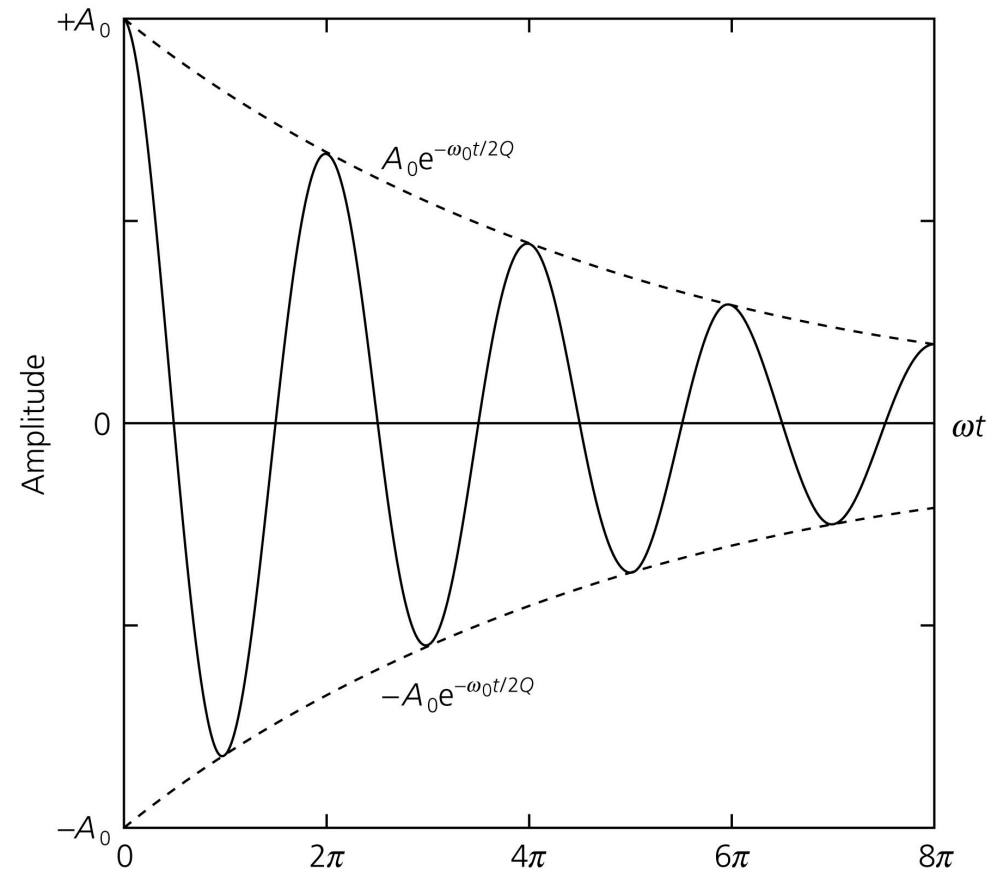
so if we define n as equal to Q ,

$$A(t_n) \approx A_0 e^{-\pi} \approx 0.04 A_0$$

Thus after Q cycles the amplitude drops to a level of $e^{-\pi}$ or 4% of the original amplitude.

In Figure 11, more than 95% of the amplitude is lost after $Q \approx 8$ cycles.

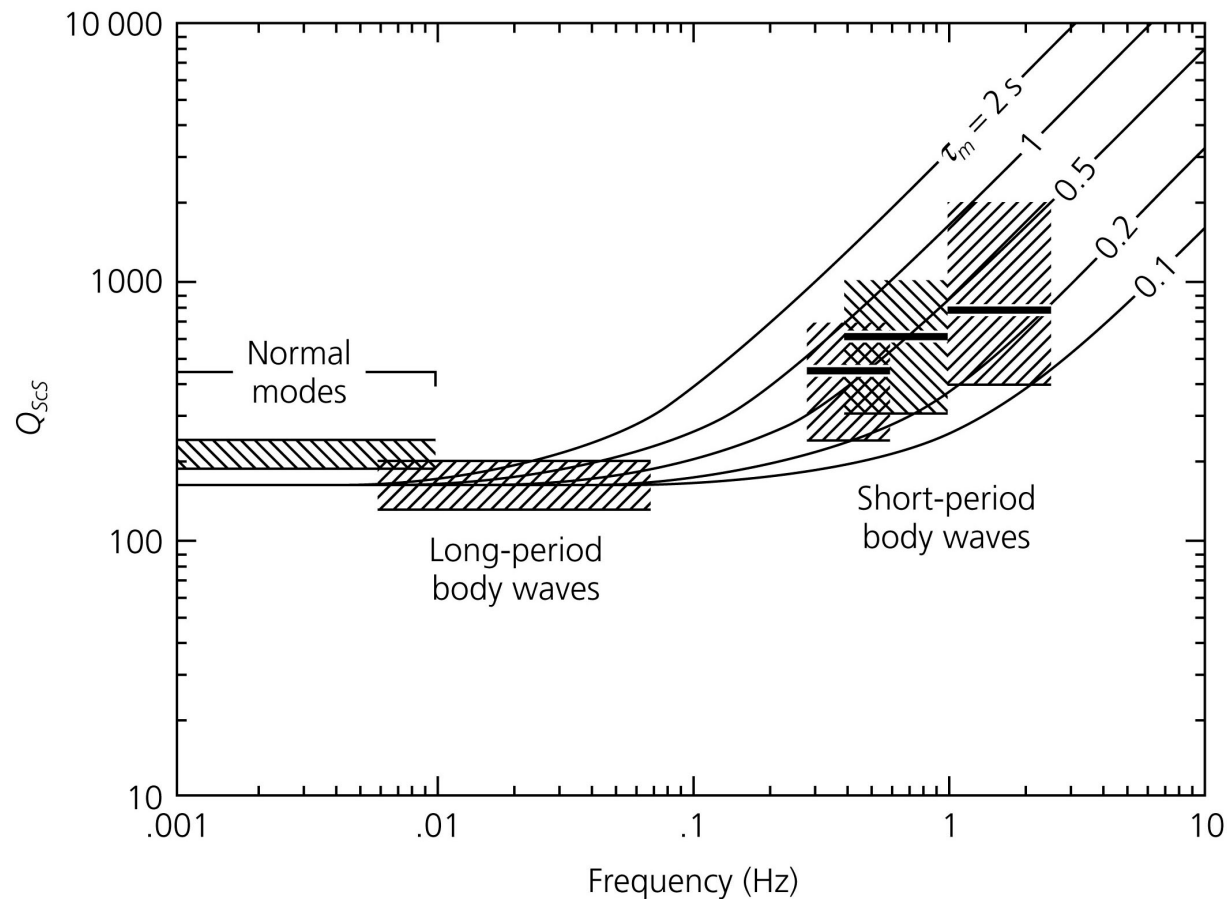
Figure 3.7-11: Wave amplitude for a damped harmonic oscillator.



Intrinsic attenuation - Anelasticity

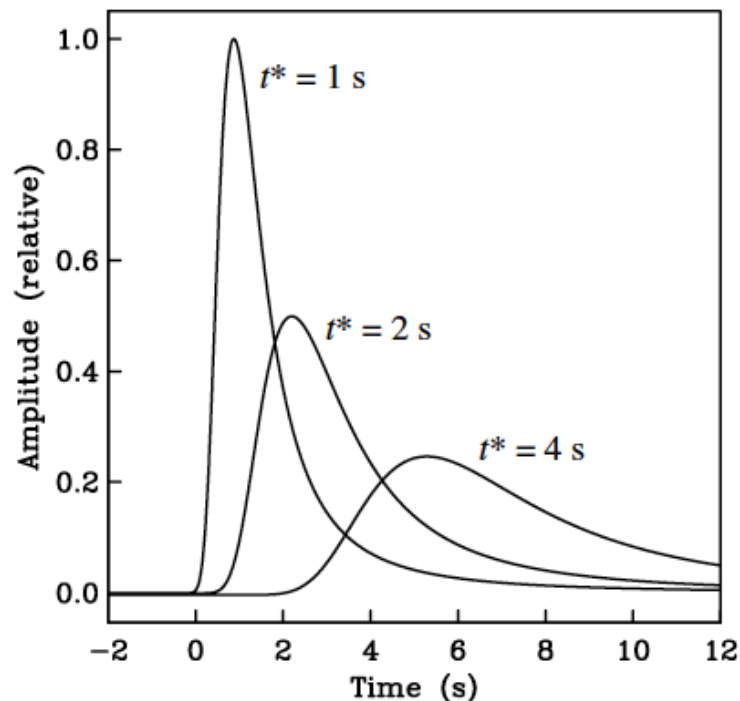
Q stay almost constant at low frequencies, but then increases with frequency

Figure 3.7-12: Frequency dependence of mantle attenuation.



Dispersion due to attenuation

$$A(x) = A_0 e^{-\omega x / 2cQ}$$



- Because they have more oscillations per unit distance, higher frequencies are more attenuated
- If all frequencies travelled at the same speed, then causality would be violated
- Low frequency waves are slowed down more than high frequency waves

figures from Shearer, 2009

Intrinsic attenuation - Anelasticity

Physical dispersion is caused by viscoelastic relaxation (at seismic frequencies) (do not confuse this with surface-wave dispersion)

Higher frequency are not only attenuated more rapidly than low frequencies, but they travel also faster

Intrinsic attenuation - Anelasticity

Physical dispersion is caused by viscoelastic relaxation (at seismic frequencies) (do not confuse this with surface-wave dispersion)

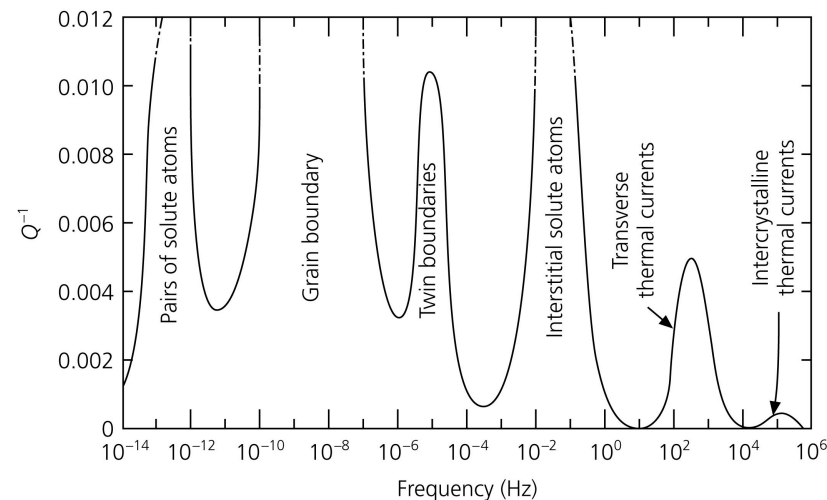
Higher frequency are not only attenuated more rapidly than low frequencies, but they travel also faster

... we cannot compare directly V_S structure of the upper mantle obtained using seismic waves at different period (correction for physical dispersion is usually done to compare, for example, surface-wave based models with S-wave one)

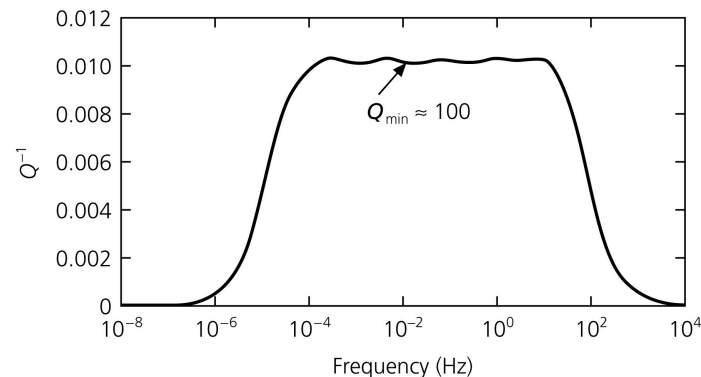
Intrinsic attenuation - Anelasticity

Physical (microscopic) mechanisms can be several, each one at a typical frequency => the total response of the Earth is typically represented by an **absorption band**

Figure 3.7-16: Relaxation spectrum for a polycrystalline material.



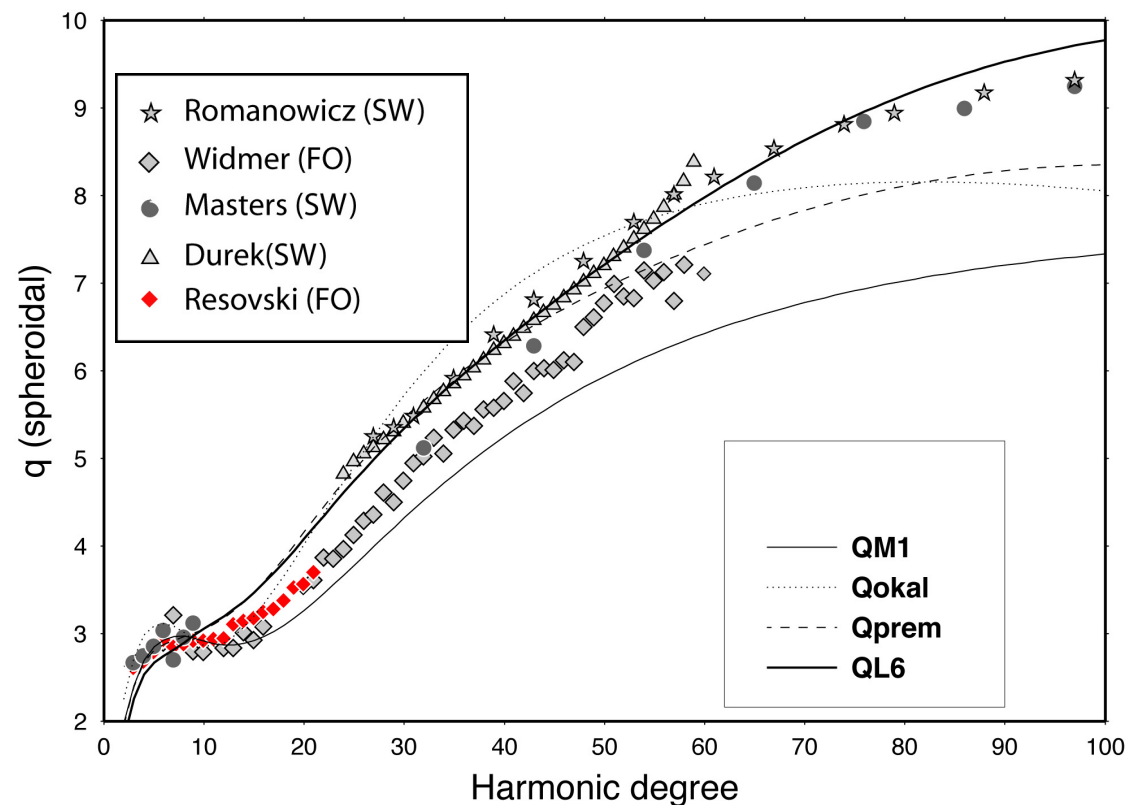
Q stays constant for a large range of frequencies, except at some boundaries



Intrinsic attenuation – Anelasticity – Seismic constraints

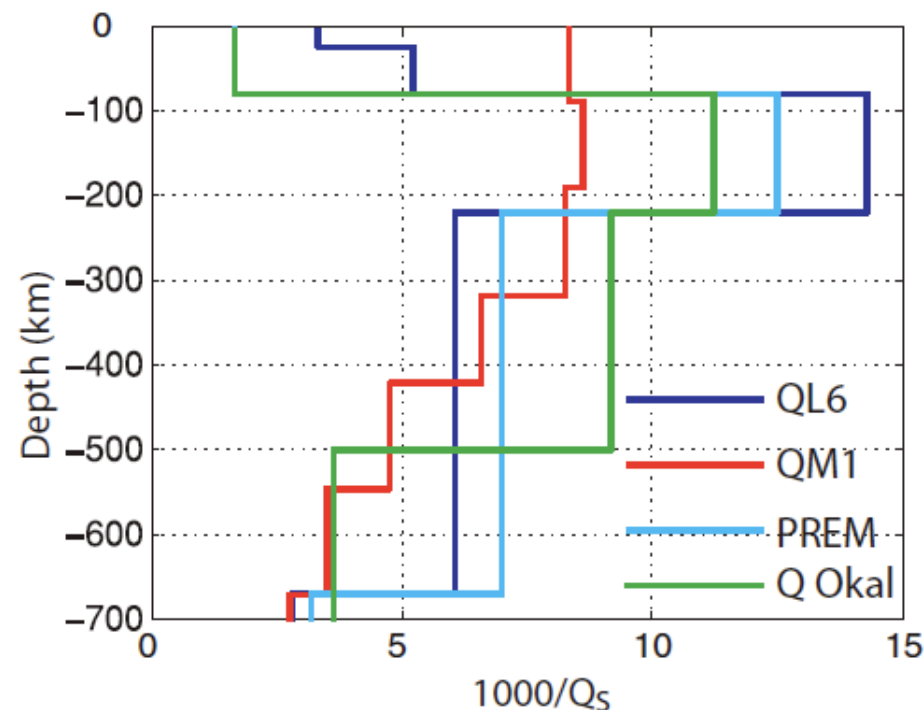
- ✓ Generally difficult to extract information on intrinsic attenuation from seismic data
- ✓ Radial Q_s ($q=1000/Q_s$) profiles defined by surface waves and free oscillations attenuation

fundamental spheroidal modes



Intrinsic attenuation – Anelasticity – Seismic constraints

- ✓ Generally difficult to extract information on intrinsic attenuation from seismic data
- ✓ Radial Q_s ($q=1000/Q_s$) profiles defined by surface waves and free oscillations attenuation



Cammarano and Romanowicz, 2008

Figure 1. Seismic attenuation 1-D profiles for the upper mantle. QL6 (Durek & Ekström 1996), QM1 (Widmer *et al.* 1991), PREM (Dziewonski & Anderson 1981) and Q Okal (Okal & Jo 1990).

Intrinsic attenuation – Anelasticity

Mineral physics constraints

- **Few measurements at seismic frequencies (Jackson, Gribb and Cooper) on polycrystalline minerals**
 - **Analogy with rheology**
-

Theoretically inferred:

- ✓ **Mechanisms are thermally activated**
- ✓ **Can be grain-size dependent**
- ✓ **frequency dependent**
- ✓ **V^* should reduce with depth**
- ✓ **Water content and partial melting should have strong effect**
(see reviews Karato, 2007 and Kolhstedt 2007 for rheology effects on water)
- ✓ **Negligible effect from dry composition variations**

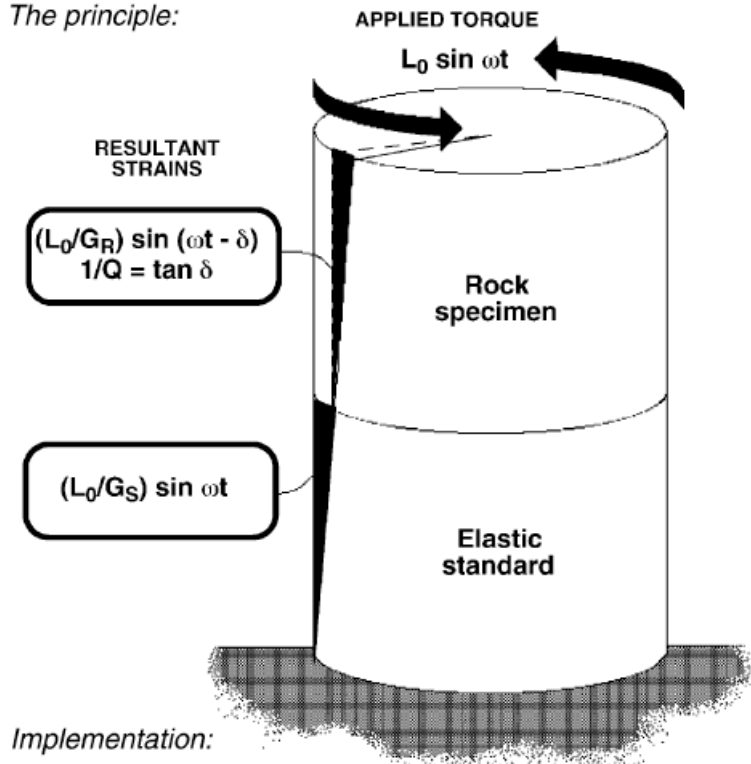
Intrinsic attenuation – Anelasticity

Mineral physics constraints

- Few measurements at seismic frequencies (Jackson, Gribb and Cooper) on polycrystalline minerals
- Analogy with rheology

Viscoelasticity via torsional forced oscillation

The principle:



Implementation:

*oscill'n periods 1-1000 s, shear strains $< 10^{-5}$
temperature to 1300C, pressure: 200 MPa*

Intrinsic attenuation – Anelasticity

Mineral physics constraints

- **Few measurements at seismic frequencies (Jackson, Gribb and Cooper) on polycrystalline minerals**
 - **Analogy with rheology**
-

What we do not know

- ✓ **Pressure dependence (V^*) not well known**
- ✓ **Few data on coarse GS**
- ✓ **Effects of water and dry composition not investigated**
- ✓ **Q_s decreases when phase transitions occur?**
- ✓ **No data on true rock material (various sizes and minerals)**

Amplitudes - absolute

- To get at absolute amplitudes, we have to consider the seismic source

$$\rho \frac{\partial^2 u_i}{\partial t^2} = \partial_j \tau_{ij} + f_i,$$

Earthquake source

✓ Studies of San Andreas fault lead to **elastic rebound model**: relative opposite motion accumulates strain and eventually breaks the material

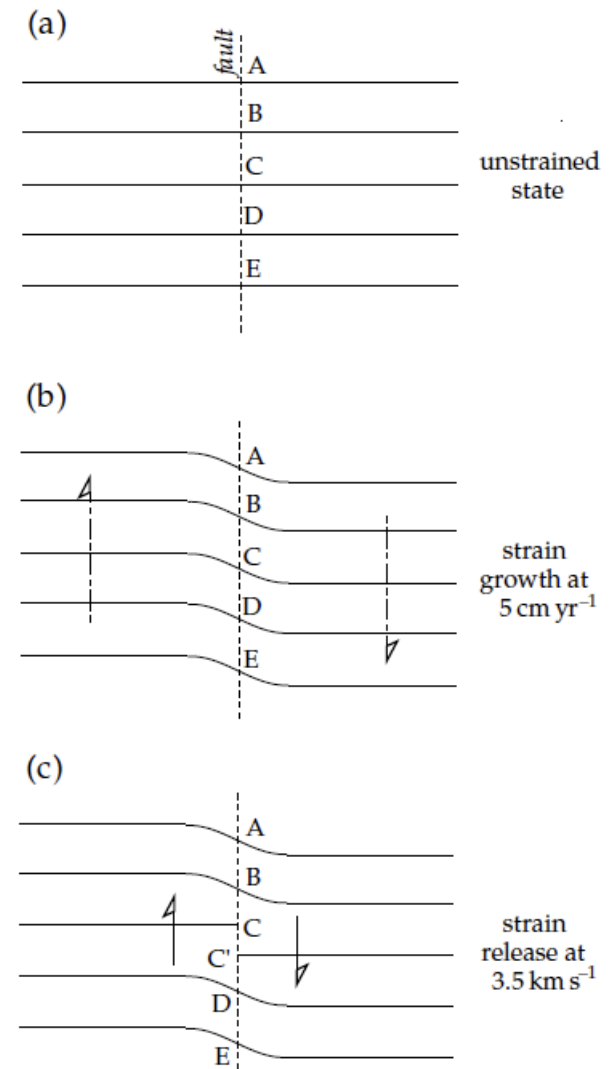
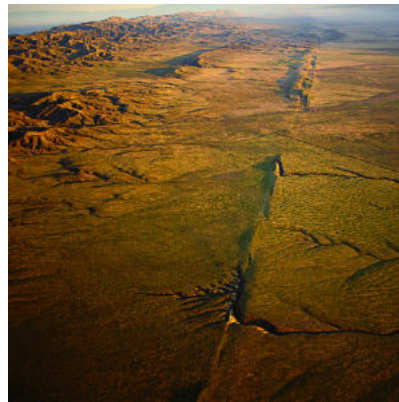
➔ The violent elastic rebound causes the Earthquake (release of seismic energy)

➔ The Earthquake intensity is directly proportional with the length of fault broken

➔ **foreshocks** (small Earthquake previous big one) can occur, but not in all cases

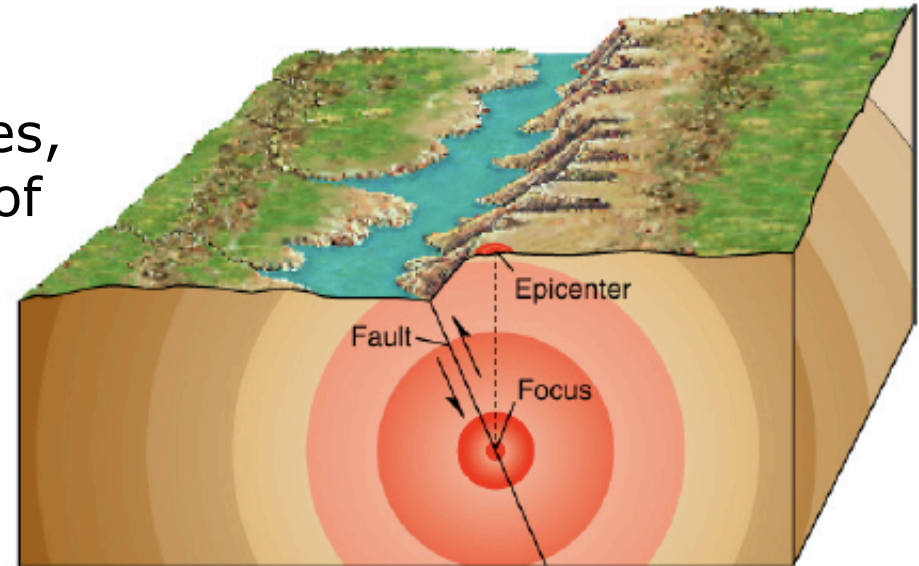
➔ **Aftershocks** typically follow the main shock

NOTE: works for brittle material, this mechanism should not work for deep Earthquakes in Subduction zones



Earthquake source

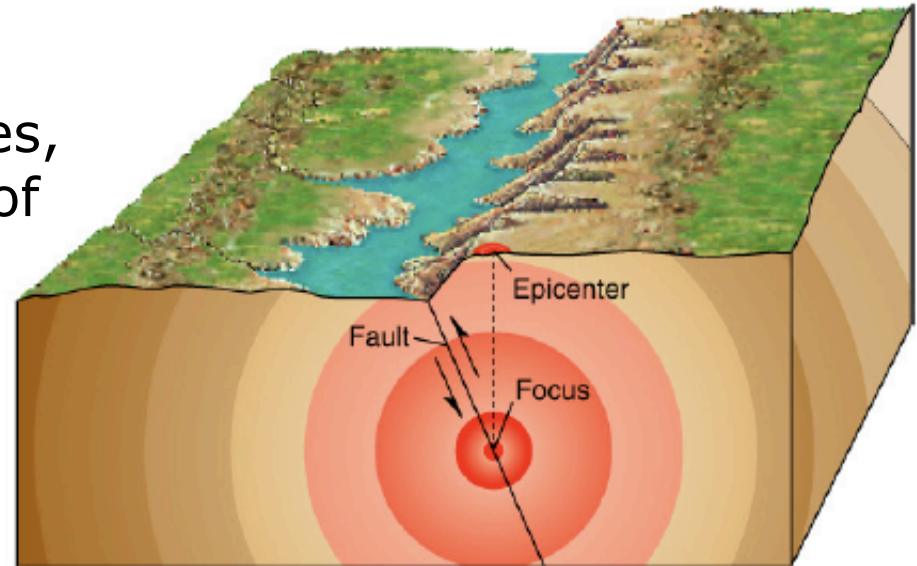
- ✓ Earthquakes occur on fault planes, energy is released from a volume of rock as it slips.
- ✓ We consider an Earthquake be a point source from far-away => latitude, longitude, depth



Earthquake source

✓ Earthquakes occur on fault planes, energy is released from a volume of rock as it slips.

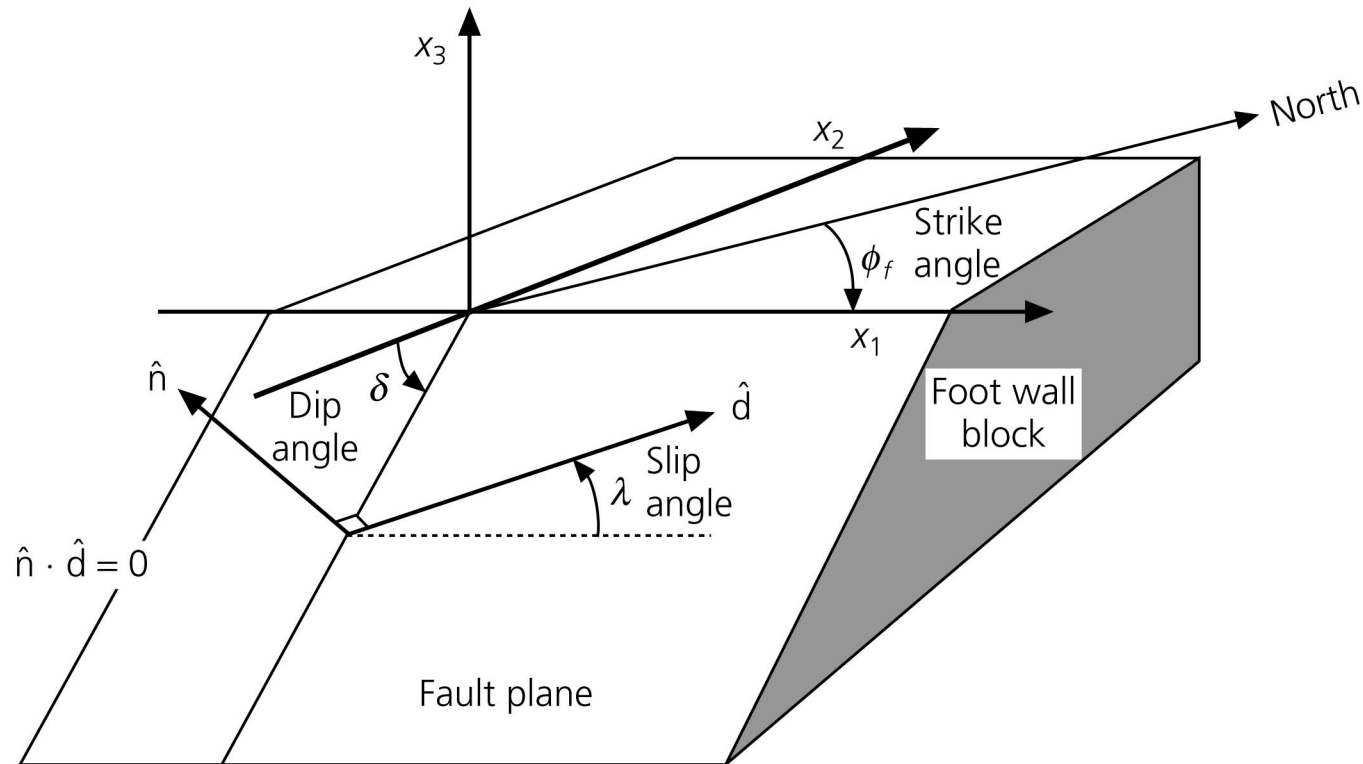
✓ We consider an Earthquake be a point source from far-away => latitude, longitude, depth



✓ Position and origin time can be determined by solving an overdetermined (more equations than unknowns) inverse problem (next week)

Earthquake source

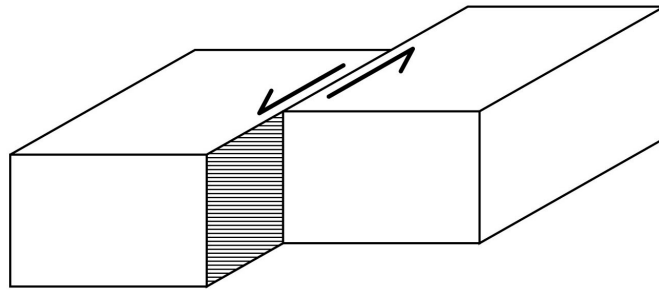
Figure 4.2-2: Fault geometry used in earthquake studies.



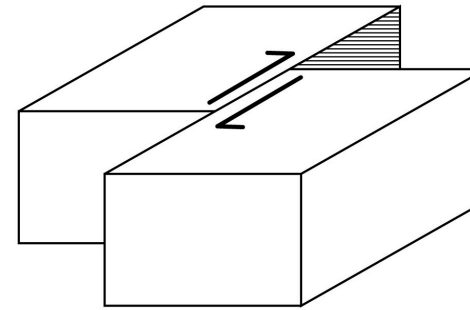
✓ Basic fault geometry (assuming them planar) are characterized by **strike** => interaction of fault plane with surface (angle with North), **dip** angle => orientation of fault plane with surface, **slip** angle => direction of motion

Earthquake source

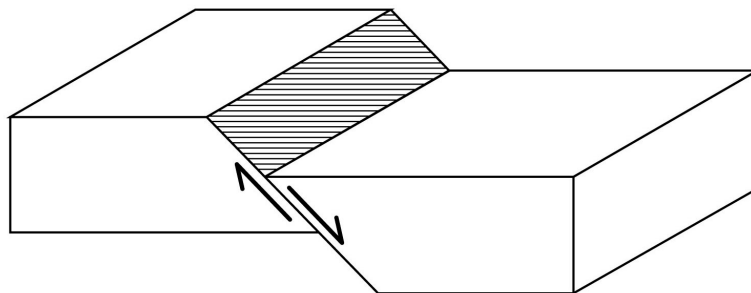
Figure 4.2-3: Basic types of faulting.



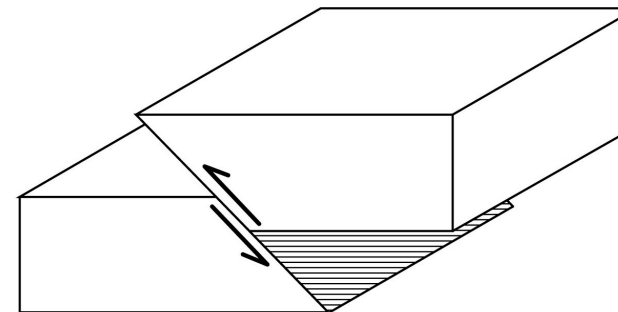
Left-lateral strike-slip fault
($\lambda = 0^\circ$)



Right-lateral strike-slip fault
($\lambda = 180^\circ$)



Normal dip-slip fault
($\lambda = -90^\circ$)

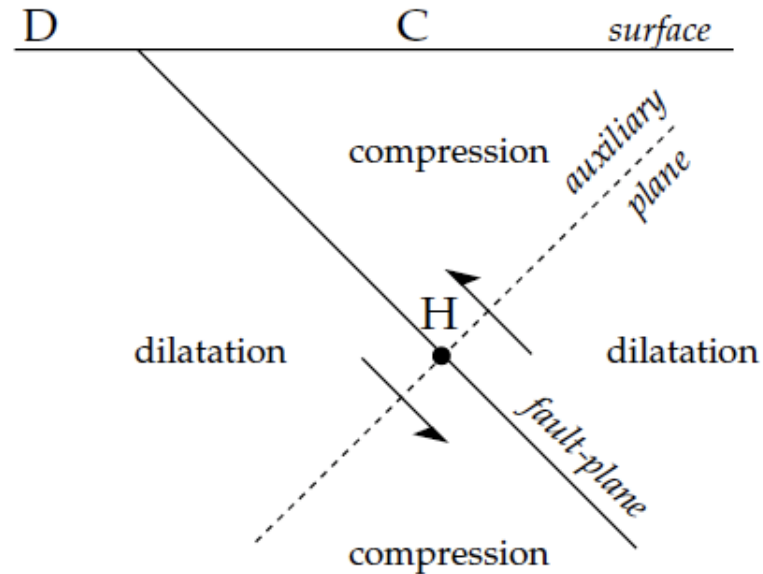


Reverse dip-slip fault
($\lambda = 90^\circ$)

✓ Basic fault geometry (assuming them planar) **define strike-slip, normal and reverse (thrust) faults**

Focal mechanisms

First Motion

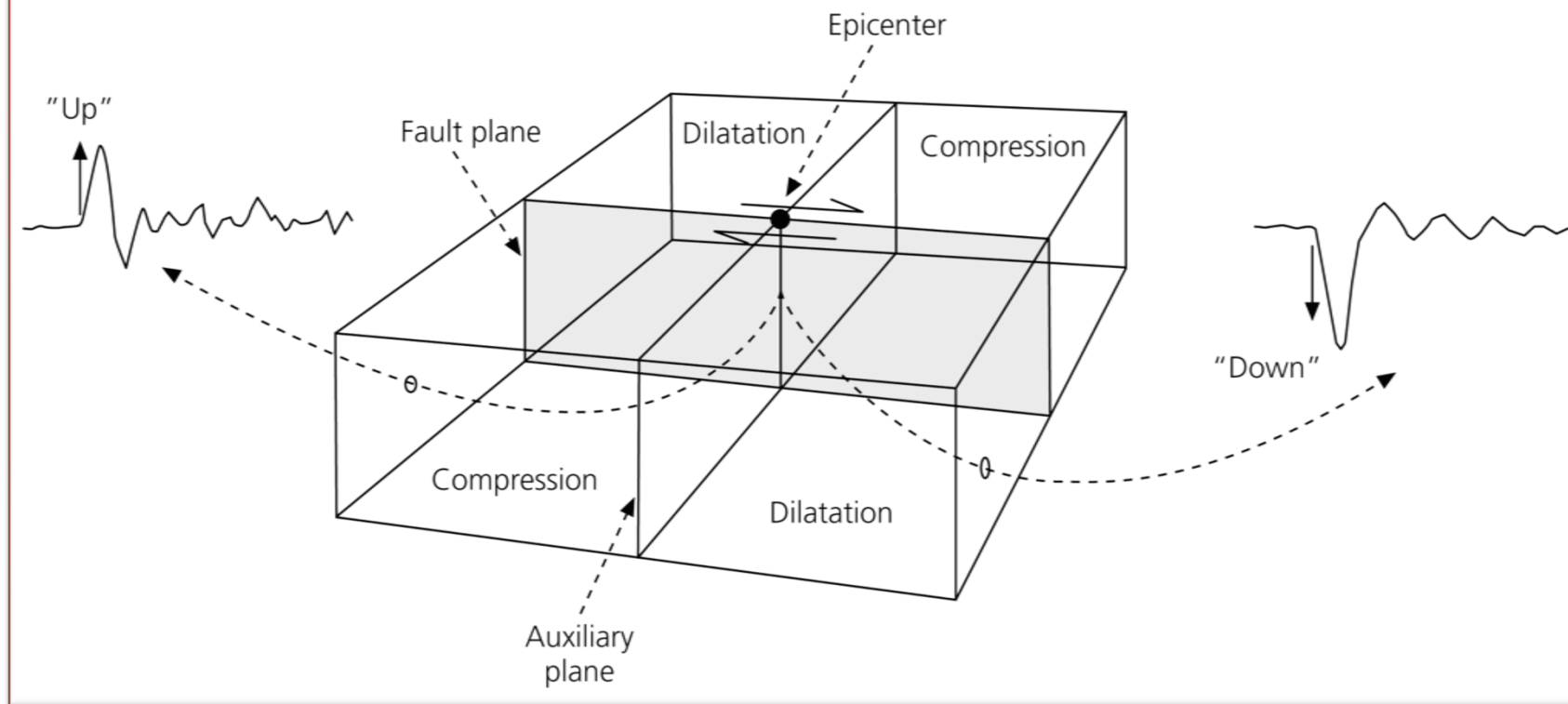


✓ The motion of a fault plane creates compression in two quadrants and dilatation in other two

Focal mechanisms

First Motion

Figure 4.2-4: First motions in relation to fault orientation.

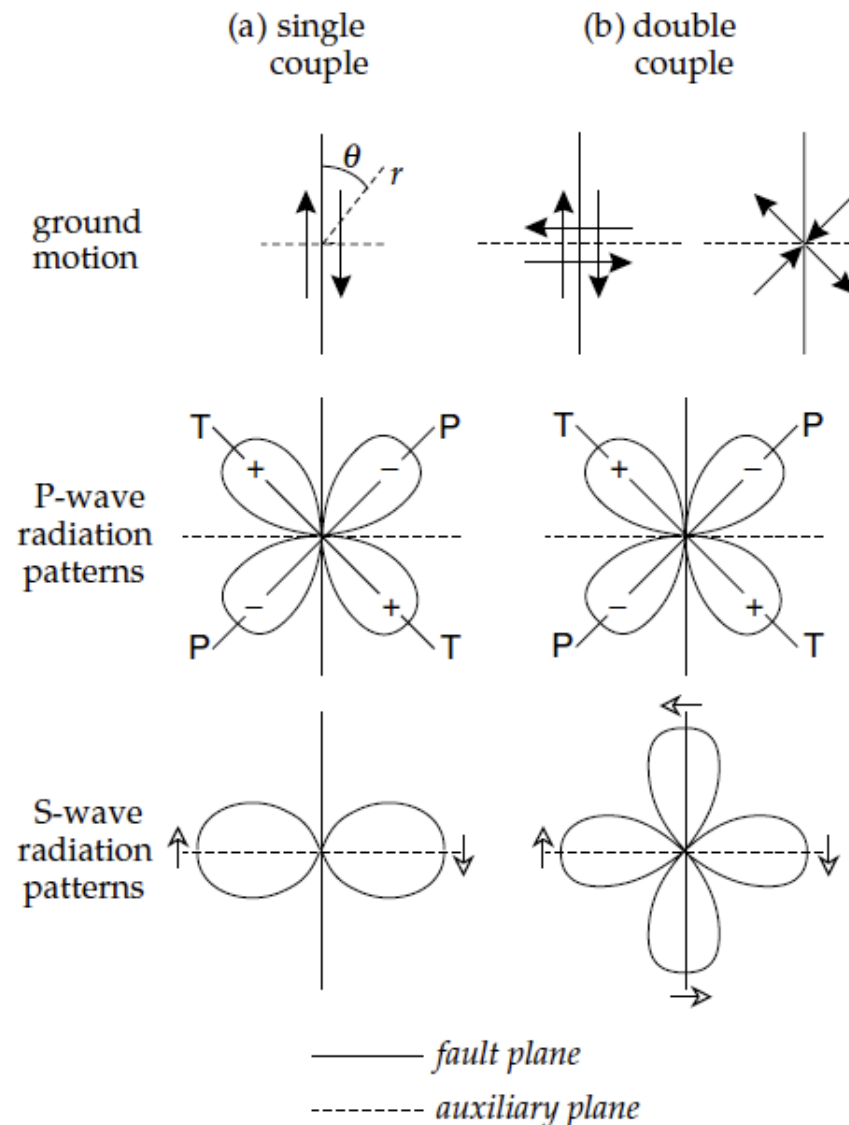


- ✓ The motion of a fault plane creates compression in two quadrants and dilatation in other two

compression → first motion up
dilatation → first motion down

Focal mechanisms

Radiation pattern



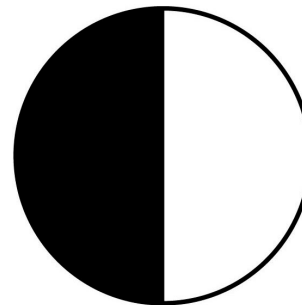
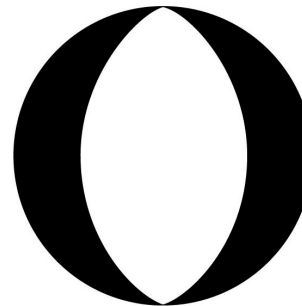
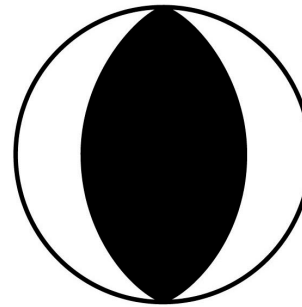
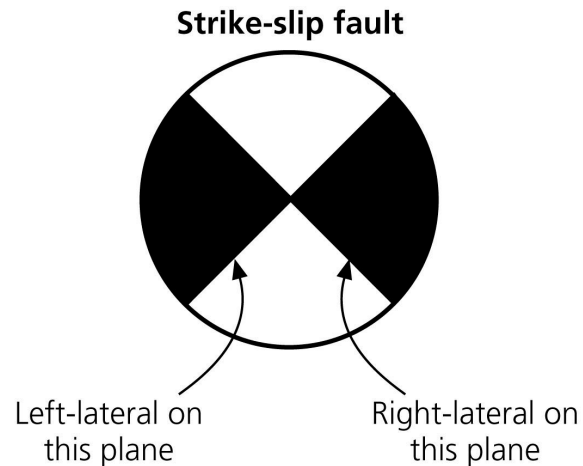
✓ The relative movement of the ground has an effect, not only on the first motion, but also on the amplitudes

✓ The analysis of seismograms show that the source mechanisms of Earthquake can be well described by a **double-couple** → so they conserve both linear and angular momentum (no net acceleration, no net torque)

Focal mechanisms

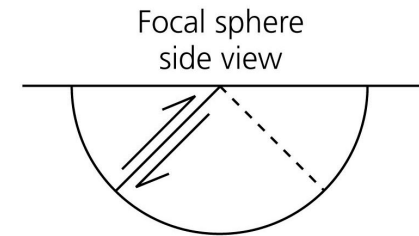
- ✓ From first motions and radiation pattern of seismograms, we determine the fault mechanism (on a sphere) and show on a stereographic projection.

Figure 4.2-14: Focal mechanisms for various fault mechanisms.

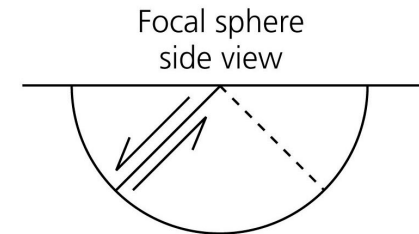


Dip-slip faults

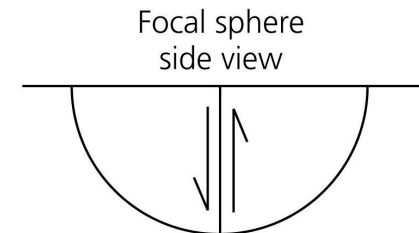
Thrust fault



Normal fault



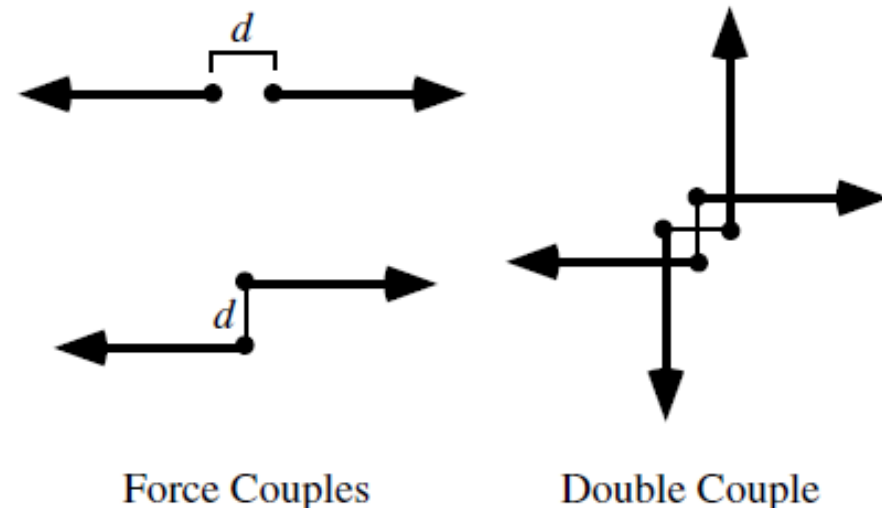
Vertical dip-slip



Amplitudes - absolute

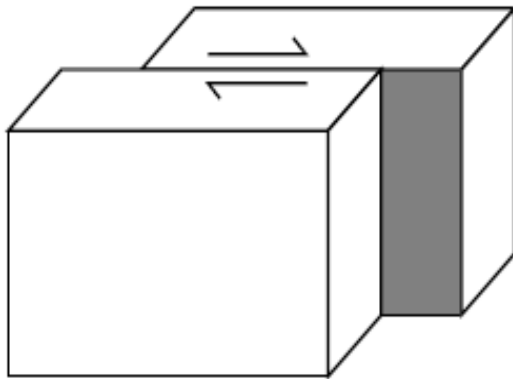
- To get at absolute amplitudes, we have to consider the seismic source
- Can an earthquake be represented by a single body force?
- To conserve both linear and angular momentum (no net acceleration, no net torque), body forces representing earthquake sources must appear in pairs of force couples (a.k.a. double couples)

$$\rho \frac{\partial^2 u_i}{\partial t^2} = \partial_j \tau_{ij} + \underbrace{f_i}_{\text{body force}}$$

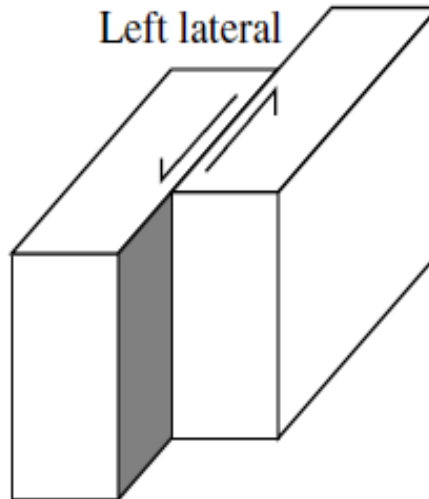


Double-couple mechanisms

Right lateral



Left lateral



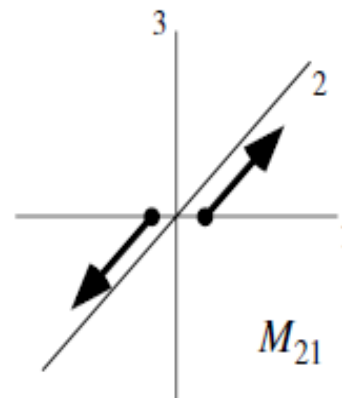
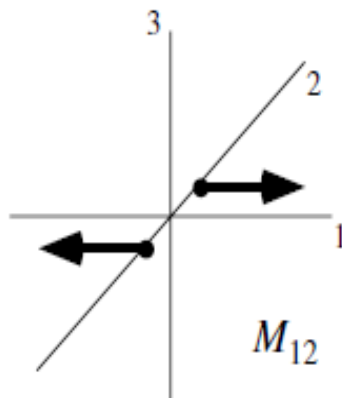
$$\mathbf{M} = \begin{bmatrix} 0 & M_0 & 0 \\ M_0 & 0 & 0 \\ 0 & 0 & 0 \end{bmatrix}$$

$$M_0 = \mu \bar{D} A$$

μ – rigidity of rock

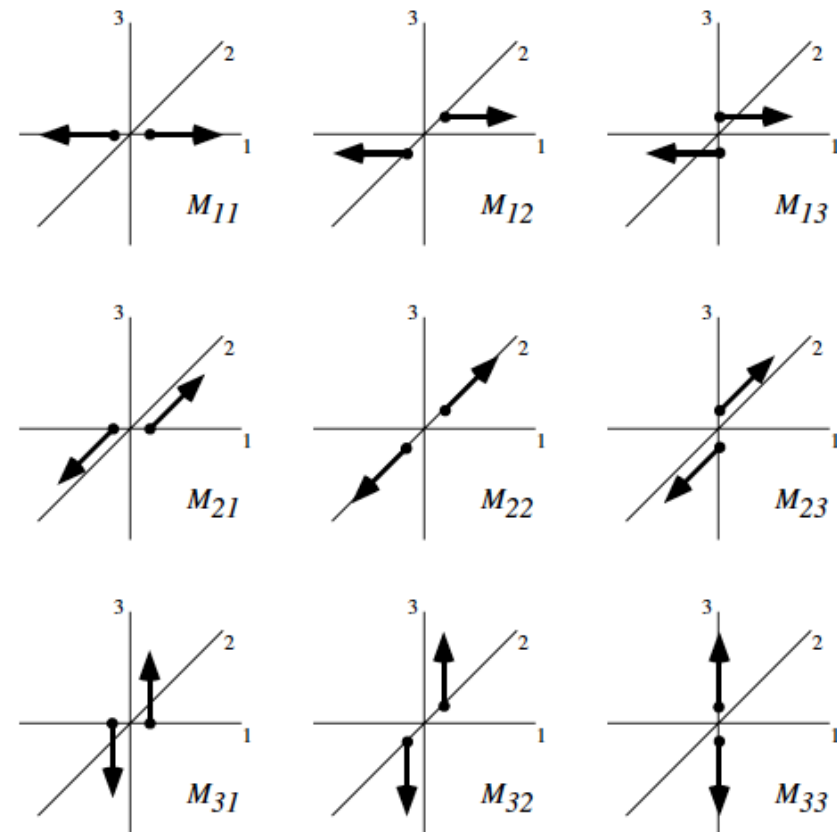
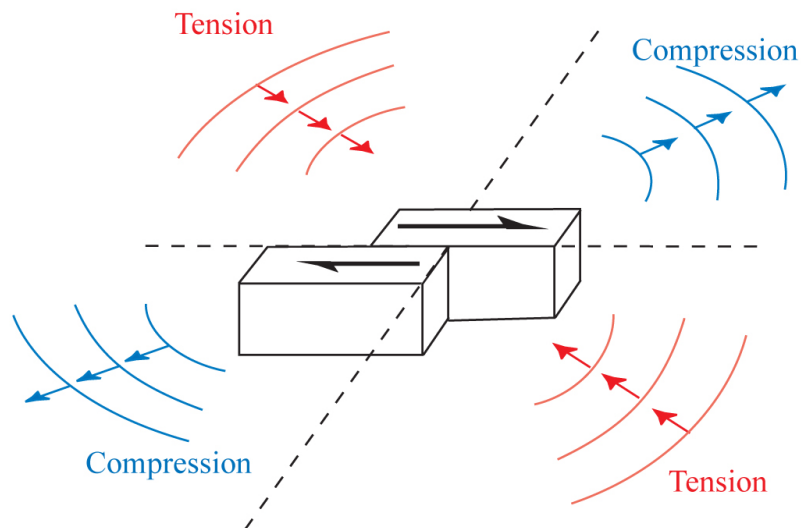
D – average slip on fault

A – area of that slipped



$$M_0 = \frac{1}{\sqrt{2}} \left(\sum_{ij} M_{ij}^2 \right)^{1/2}$$

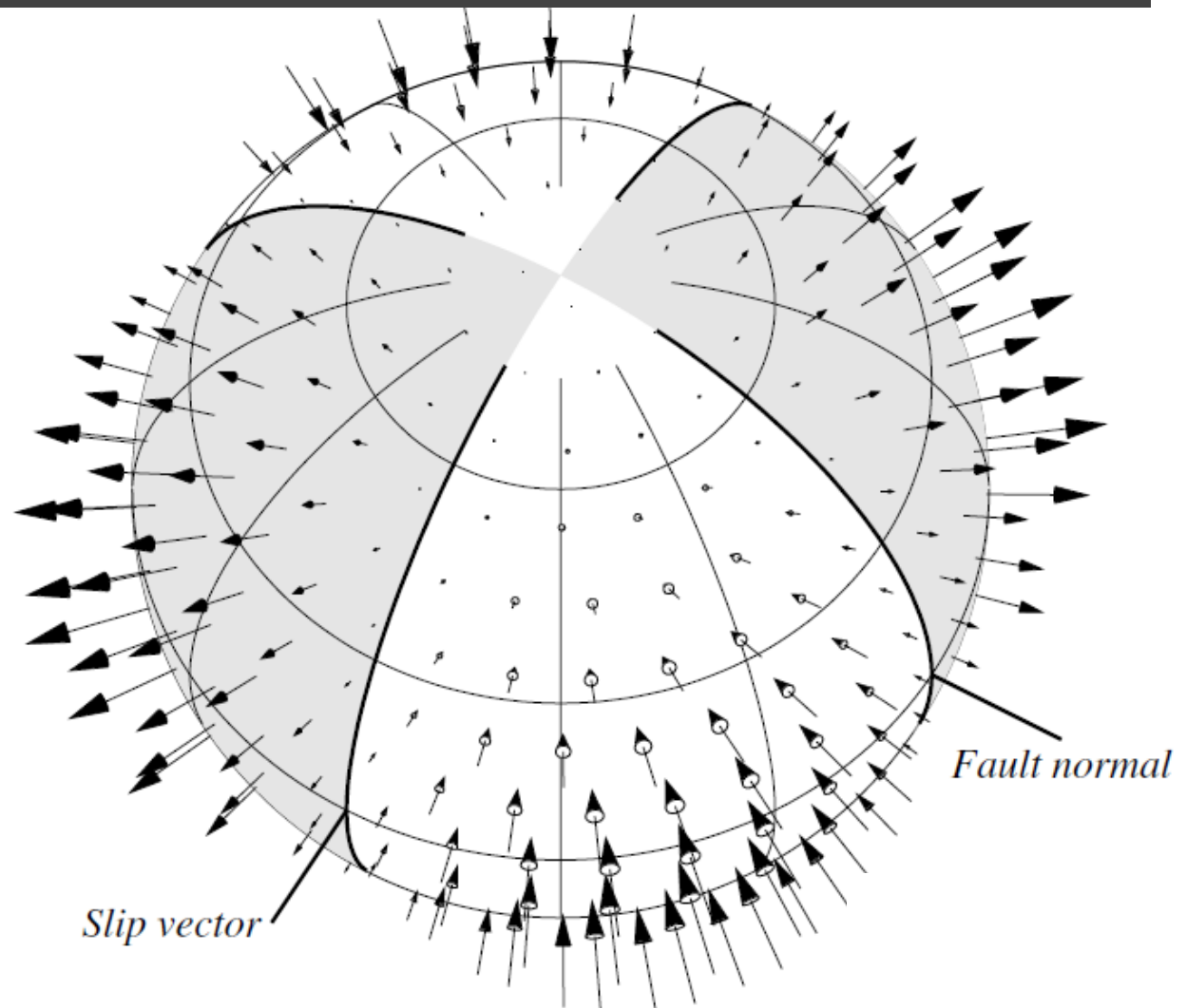
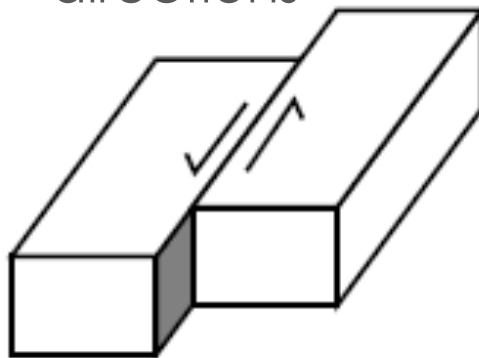
Radiation from moment tensors



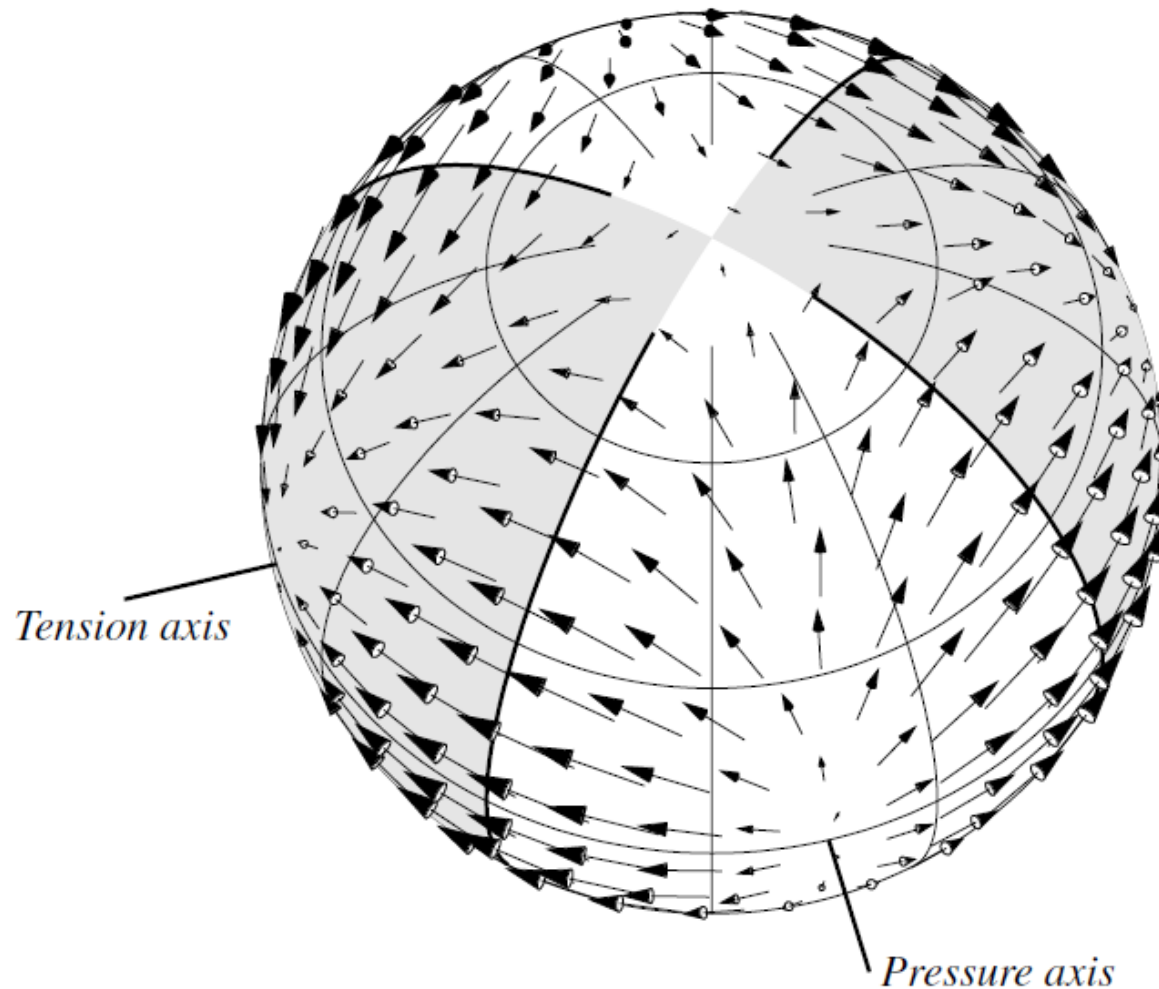
P-wave radiation pattern

P-wave amplitude is:

- Most positive in the direction of the tension axis
- Most negative along compression axis
- Zero along primary and auxiliary plane directions

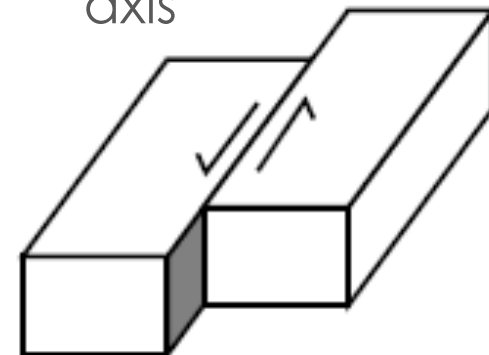


S-wave radiation pattern



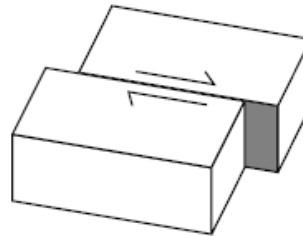
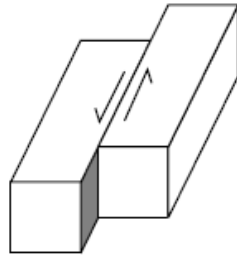
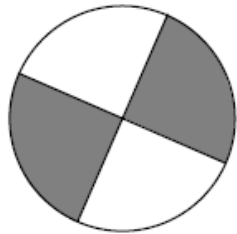
S-wave amplitude is:

- Greatest along primary and auxiliary plane directions
- Particle motions are away from P-axis and toward T-axis

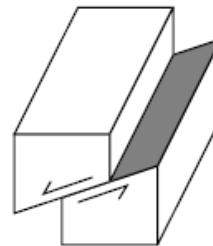
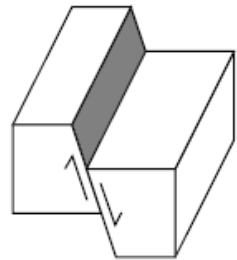
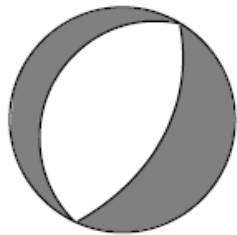


Beach-Balls

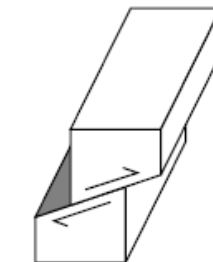
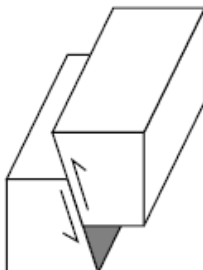
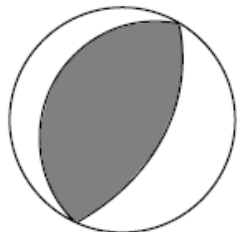
Strike Slip



Normal



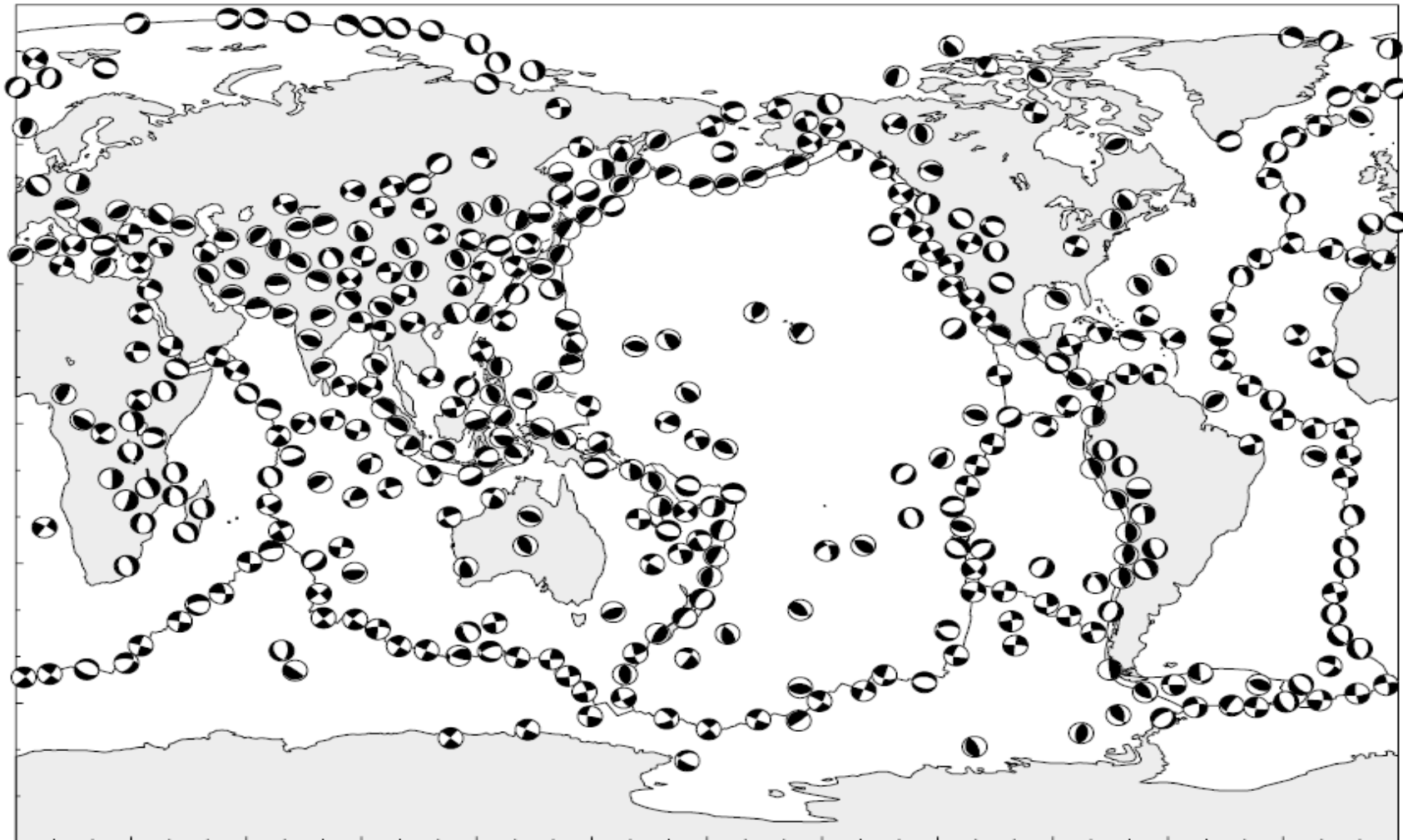
Reverse

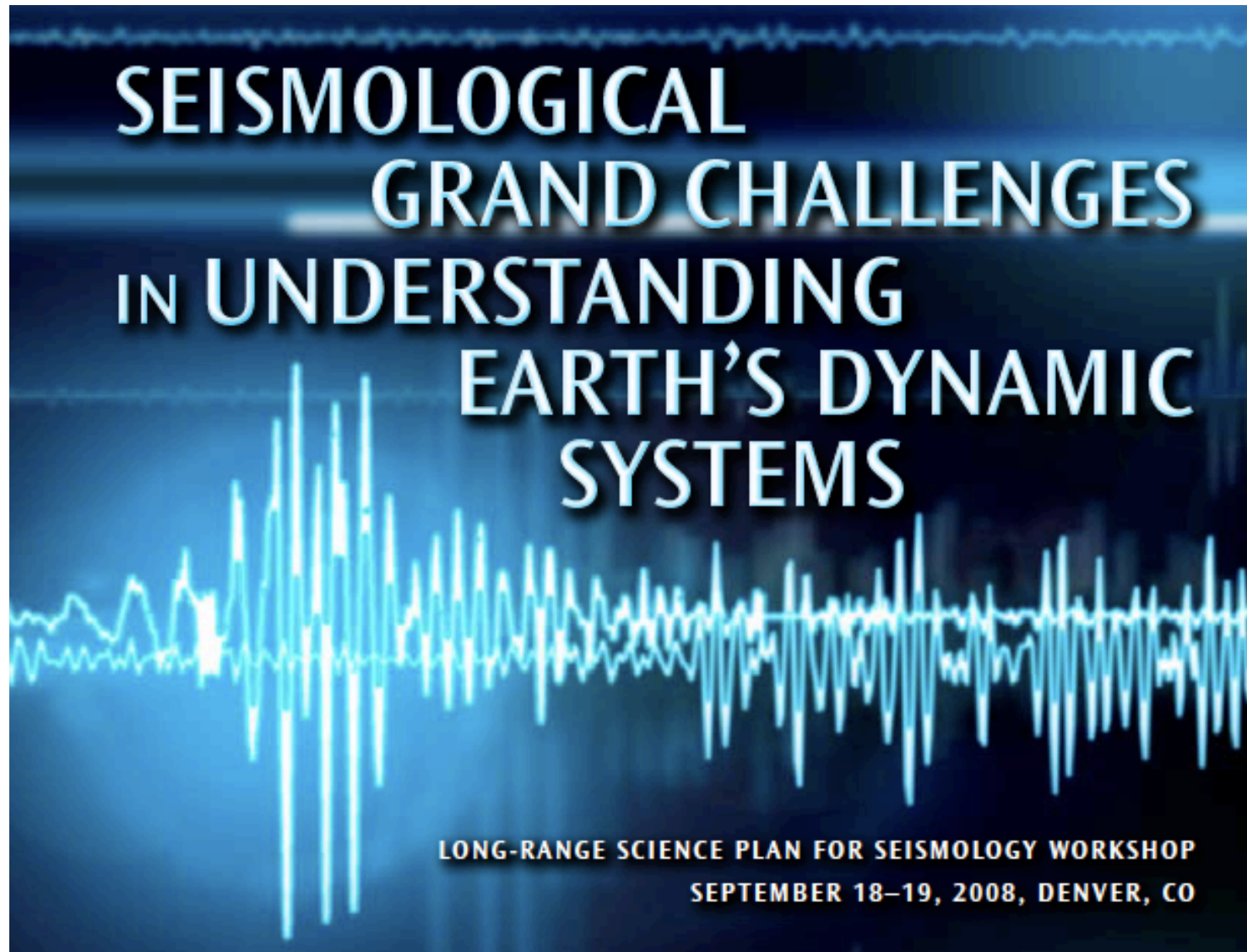


- We can graphically represent a moment tensor by shading areas where first-arriving P wave would be positive → “beach-ball” representation
- Extend along shaded portions, compress along unshaded

Centroid Moment Tensors

“Harvard” CMT (Dziewonski & Woodhouse, 1983): www.globalcmt.org





<http://www.iris.edu/hq/lrsps/>